Universitat Autònoma de Barcelona

TARGETING MITOSIS IN HORMONE-REFRACTORY PROSTATE CANCER

Nuria Masiá Fandos

TARGETING MITOSIS IN HORMONE-REFRACTORY PROSTATE CANCER

PhD thesis presented by

Nuria Masiá Fandos

To obtain the degree of

PhD for the *Universitat Autònoma de Barcelona* (UAB)

PhD thesis carried out at the Cell Cycle and Cancer Laboratory within the Biomedical Research Groups of Urology and Gynecology, at Vall d'Hebron Research Institute (VHIR)

Thesis affiliated to the Department of Biochemistry and Molecular Biology from the UAB, in the PhD program of Biochemistry, Molecular Biology and Biomedicine

Universitat Autònoma de Barcelona, September 2020

Dr. Anna Santamaria Margalef
(Director)

Dr. Ana Meseguer Navarro
(Tutor)

Nuria Masiá Fandos
(Doctorate)

Dedicatòria

Agraïments

INDEX

ABBREVIATIONS

ADT	Androgen Deprivation Therapy	**A**
AFS	Anterior Fibromuscular Stroma	
AGC	Auto Gain Control	
AI	Androgen Independent	
AJCC	American Joint Committee on Cancer	
AML	Acute Myeloid Leukemia	
APC/C	Anaphase-Promoting Complex	
AR	Androgen Receptor	
ARE	Androgen Responsive Elements	
AR-Vs	Androgen Receptor Splice Variants	
AS	Active Surveillance	
ATCC	American Type Culture Collection	
AURKA	Aurora A Kinase	
BCR	Biochemical Recurrence	**B**
BPE	Bovine Pituitary Extract	
BPH	Benign Prostatic Hyperplasia	
CDK	Cyclin-Dependent Kinase	**C**
CEEA	Comité Ètic d'Experimentació Animal	
CIN	Chromosomal Instability	
CIPF	Centro de Investigación Príncipe Felipe	
CK8	Cytokeratin 8	
CRPC	Castration-Resistant Prostate Cancer	
CZ	Central Zone	
DAB	Diaminobenzidine	**D**
DAVID	Database for Annotation, Visualization and Integrated Discovery	
DBD	DNA-Binding Domain	
DDR	DNA Damage Repair	
DEGs	Differentially Expressed Genes	
DHT	Dihydrotestosterone	
DRE	Digital Dectal Examination	
DTT	Dithiothreitol	
EBRT	External Beam Radiation Therapy	**E**
EGF	Epidermal Growth Factor	
EMT	Epithelial-to-Mesenchymal Transition	
ER	Estrogen Receptor	

ER+	Estrogen Receptor-positive	
FACS	Fluorescence-Activated Cell Sorting	**F**
FBS	Fetal Bovine Serum	
FC	Fold Change	
FDA	U.S. Food and Drug Administration	
FDR	False Discovery Rate	
FFPE	Formalin-Fixed Paraffin-Embedded	
G-CSF	Granulocyte Colony-Stimulating Factor	**G**
GEM	Genetically Engineered Mouse	
GM-CSF	Granulocyte-Macrophage Colony-Stimulating Factor	
GO	Gene Ontology	
GR	Glucocorticoid Receptor	
H&E	Hematoxylin and Eosin	**H**
HGPIN	High Grade Prostate Intraepithelial Neoplasia	
HRD	Homologous Recombinant Deficiency	
HRP	Horseradish Peroxidase	
HRR	Homologous Recombination Repair	
IC50	Half-maximal Inhibitory Concentration	**I**
ICAM1	Intercellular Adhesion Molecule 1	
ICIs	Immune-Checkpoint Inhibitors	
IDIBELL	Institut d'Investigació Biomèdica de Bellvitge	
ISUP	International Society of Urological Pathology	
ITS-G	Insulin-Transferrin-Selenium	
KLK3	Kallikrein-related peptidase 3	**K**
K-SFM	Keratinocyte Serum Free Medium	
KSP	Kinesin Spindle Protein	
LBD	Ligand-Binding Domain	**L**
LC	Liquid Chromatography	
LFA3	Lymphocyte Function-Associated molecule 3	
LGPIN	Low Grade Prostate Intraepithelial Neoplasia	
LHRH	Luteinizing Hormone Releasing Hormone	
LUTS	Lower Urinary Tract Symptoms	
MAB	Maximal Androgen Blockade	**M**
MAPK	Mitogen-Activated Protein Kinase	
mCRPC	metastatic Castration-Resistant Prostate Cancer	

MDS	Myelodysplastic Syndromes	
mp-MRI	multiparametric-Magnetic Resonance Imaging	
MS	Mass Spectrometry	
MSI-H	Microsatellite Instability-High	
NEPC	Neuroendocrine Prostate Cancer	**N**
NGS	Next-Generation Sequencing	
NHL	Non-Hodgkin Lymphoma	
NSCLC	Non-Small Cell Lung Cancer	
NTD	N-terminal Transactivation Domain	
OS	Overall Survival	**O**
PAP	Phosphatase	**P**
PB	Prostate Biopsy	
PBMCs	Peripheral Blood Mononuclear Cells	
PCa	Prostate Cancer	
PCA3	Prostate Cancer Antigen 3	
PFS	Progression-Free Survival	
PGR	Progesterone Receptor	
PI	Propidium Iodide	
PI3K	Phosphatidylinositol 3-Kinase	
PIN	Prostate Intraepithelial Neoplasia	
PLK1	Polo-Like Kinase 1	
PPIs	Protein-Protein Interactions	
PR	Partial Response	
PRC1	Phosphorylation of protein Regulator of Cytokinesis 1	
PSA	Prostate-Specific Antigen	
PSAD	Prostate-Specific Antigen Density	
PSADT	Prostate-Specific Antigen Doubling Time	
PSAV	Prostate-Specific Antigen Velocity	
PTMs	Post-Translational Modifications	
PVDF	Polyvinylidene Difluoride	
PZ	Peripheral Zone	
QoL	Quality of Life	**Q**
RB	Retinoblastoma	**R**
RECIST	Response Evaluation Criteria In Solid Tumors	
ROS	Reactive Oxygen Species	

RP	Radical Prostatectomy	
RT	Raditation Therapy	
SAC	Spindle Assembly Checkpoint	**S**
SDS-PAGE	Sodium Dodecyl Sulfate Polyacrylamide Electrophoresis Gels	
SILAC	Stable Isotope Labeling with Amino acids in Cell culture	
STLC	S-Trityl-L-Cysteine	
TBS-T	Tris Buffered Solution	**T**
TCGA	The Cancer Genome Atlas	
TiO2	Titanium dioxide	
TMAs	Tissue Microarrays	
TMB	Tumor Mutational Burden	
TNF-α	Tumor Necrosis Factor α	
TNM	Tumor Node Metastasis	
TRUS	Transrectal Ultrasound	
TURP	Transurethral Resection of the Prostate	
TZ	Transition Zone	
UAB	Universitat Autònoma de Barcelona	**U**
UICC	Union for International Cancer Control	
UNIVPM	Marche Polytechnic University	
VHIR	Vall d'Hebron Research Institute	**V**
WGS	Whole-Genome Sequencing	**W**

INTRODUCTION

1. THE PROSTATE

1.1. Function, morphology and anatomy

The prostate is an exocrine gland that belongs to the male reproductive system. Classically described as 'walnut-shaped', it surrounds the first part of the urethra and is located within the pelvic region, in front of the rectum and just below the urinary bladder (Fig. 1)[1].

The main function of this fibromuscular gland is to secrete a slightly alkaline fluid and proteins that provide nutritional support to the seminal fluid. Prostate secretions make up around 20-30% of the total volume of semen, together with spermatozoa and the seminal vesicle fluid, and are believed to enhance sperm motility and survival[2]. Moreover, the prostate plays a role in controlling the urine flow and has an important hormonal control to metabolize testosterone into its biologically active form dihydrotestosterone (DHT)[3].

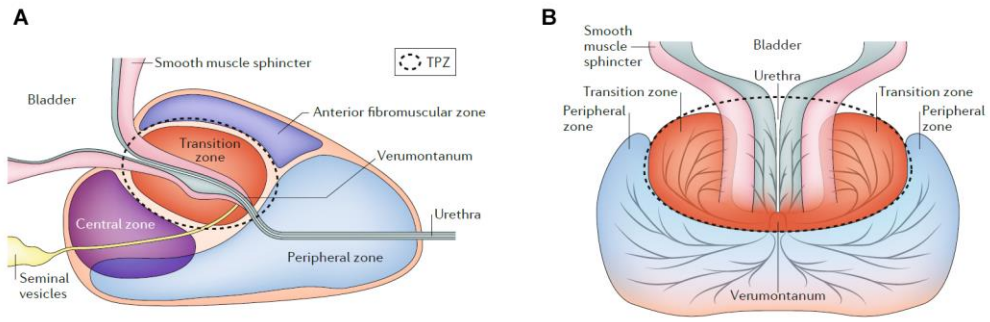

Figure 1. Schematic representation of the human prostate anatomy. Zonal distribution of the prostate proposed by McNeal is shown in **A)** the prone position and in **B)** the upright position. Adapted from Stabile A *et al.*[1].

At the histological level, the structure of the human prostate is that of a branched duct gland (Fig. 2A). It contains a pseudostratified epithelium that consists of tubuloalveolar glands, which are embedded in a dense fibromuscular stroma[4]. Cells forming this epithelium are arranged in two layers: a luminal secretory cell layer and an underlying basal cell layer (Fig. 2B)[5]. Within the prostatic epithelium, there are three different

types of cells that can be distinguished by their morphological and functional characteristics.

Secretory epithelial cells, which represent the major cell type in the gland, produce a variety of components that are released into the seminal fluid, such as the prostatic acid phosphatase (PAP) and the prostate-specific antigen (PSA)[6]. These differentiated cells are tall and columnar in shape, androgen-dependent for growth and also express high levels of characteristic markers such as androgen receptor (AR) or cytokeratin 8 and 18[7].

The second major epithelial cell type consists of basal cells, which are localized between the luminal cells and the underlying basement membrane, thus allowing the separation of the lumen and the stroma. Basal cells are flat or cuboidal, express low levels of the AR and, unlike epithelial cells, are not directly controlled by androgen signalling[8]. These non-secretory cells conform the proliferative compartment of the epithelium and are suspected to function as stem cells involved in the renewal process[9].

Finally, the third cell type that can be found within the prostatic epithelium is known as neuroendocrine cells, a minor population of uncertain embryological origin that is scattered throughout the gland, mostly in or just above the basal cell layer. They are independent of androgens and believed to support the growth and differentiation of luminal cells in a paracrine fashion[10-12].

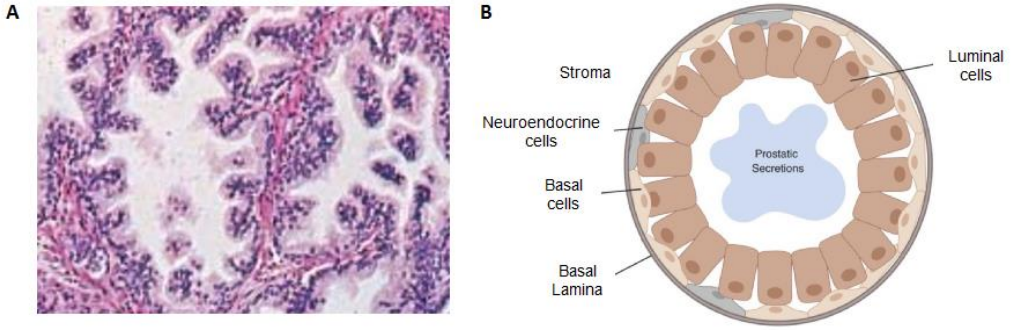

Figure 2. Structure of the human prostatic duct. A) Haematoxylin-eosin staining (80x) of a normal prostatic tissue. Adapted from Kuehnel W.[13] **B)** Representation of the cell types within the prostate epithelium. Adapted from Salem O *et al.*[5].

To date, the most widely used anatomical model of the prostate was established by McNeal in the early 1980s[14]. McNeal conceptualized the prostate as divided into 4 distinct morphological zones: the peripheral zone (PZ) and the central zone (CZ), which together comprise >95% of the normal prostate glandular tissue, the transition zone (TZ) and the non-glandular anterior fibromuscular stroma (AFS) [15,16] (Fig. 1). The importance of the described model is based upon the relationship of these glandular zones to the different forms of prostate disease. The PZ, which extends posteriorly around the prostate gland, is the most common site for prostatitis and the development of prostate carcinomas; whereas the TZ that is located in the inner part of the prostate is the region where benign prostatic hyperplasia (BPH) mainly arises[17]. In addition, around 20% of prostate cancers (PCa) occur in this zone. Only 2.5% of PCa emerge in the CZ, which is based behind the proximal prostatic urethra, surrounding the ejaculatory ducts; however, these cancers tend to be more aggressive[18].

1.2. Benign prostate diseases

Several benign disorders can affect the prostate. Identification of these pathologies is crucial for a correct diagnosis and, if necessary, an effective therapeutic management.

Prostatitis is an inflammatory condition of the prostate gland and one of the most common urinary tract problems in men below the age of 50 years[19]. 'Chronic non-bacterial prostatitis' accounts for more than 90% of cases, with patients suffering from intermittent to regular episodes of pain in the groin or pelvic area. Because the etiological cause of this condition is generally not identified, the optimal management of the disease is unknown. Prolonged courses of antibiotics are the standard treatment of prostatitis[20], however they have so far failed to demonstrate their efficacy. It has been proposed that inflammation may contribute to carcinogenesis[21], whereby inflammatory events such as prostatitis may increase the risk of cancer development among patients. Nevertheless, the relationship between this condition and malignant transformation has not been very well established.

BPH refers to the enlargement of both the epithelial and stromal constituents of the prostate. It is a highly prevalent disorder, being aging a well-established risk factor for the development of the disease. With the progression of BPH, many patients present with lower urinary tract symptoms (LUTS) due to bladder outlet obstruction, thus

affecting their life quality[22]. The mechanisms responsible of this disorder remain unclear and the effectiveness of current inhibitors in the clinic is still limited. Although several minimal invasive treatments are emerging in order to reduce complications of open surgery, the transurethral resection of the prostate (TURP) is the gold standard for surgical treatments[23]. In the last few years, a possible link between BPH and PCa has been hypothesized, since both conditions are hormone-dependent and inflammation seems to play an important role in the pathogenesis of both cases[24,25]. However, it is still not proven. Moreover, the luminal-to-basal cell relationship is retained in the BPH, and therefore is not considered to be a pre-malignant condition.

Finally, prostate intraepithelial neoplasia (PIN) is described as an intraluminal proliferation of secretory cells in the prostate gland. It is characterized by abnormalities in the nuclei and chromatin content of the cells. This disorder is traditionally classified in two different grades, based on architectural and cytological characteristics: low-grade PIN (LGPIN) and high-grade PIN (HGPIN)[26]. While intact or rarely disrupted in LGPIN, the basal layer may have frequent interruptions in high-grade lesions. HGPIN is considered most likely to represent a precursor lesion to PCa[27], even though the relationship between both conditions has not been conclusively demonstrated. It has been estimated that about 30% of patients diagnosed with HGPIN will present PCa in the following years[28], and therefore the recognition of the disease becomes clinically important.

2. PROSTATE CANCER

2.1. Epidemiology and risk factors

PCa is the second most frequently diagnosed invasive malignancy and the fifth leading cause of cancer-related deaths among men in world population, with an estimated 1,276,106 total new cases and 358,989 deaths in 2018 (Fig. 3)[29]. Incidence rates have increased over the last decades and vary worldwide, with the highest rates recorded primarily in industrialized countries such as North America, Oceania and Europe. The primary reason for this trend is the introduction of the prostate-specific antigen (PSA) test in the late 1980s[30,31], which has led to a dramatic increase not only in the earlier detection of the disease, but also in the detection of slow-growing tumors that might otherwise escape diagnosis. It has been estimated that around 90% of total new cases are diagnosed at local stage, where the 5-year survival rate is nearly 100%[32]. Moreover, PCa is viewed as an ageing-related malignancy and it is, therefore, a major public health burden and a greater concern for developed countries, which posses a larger proportion of elderly men in their population.

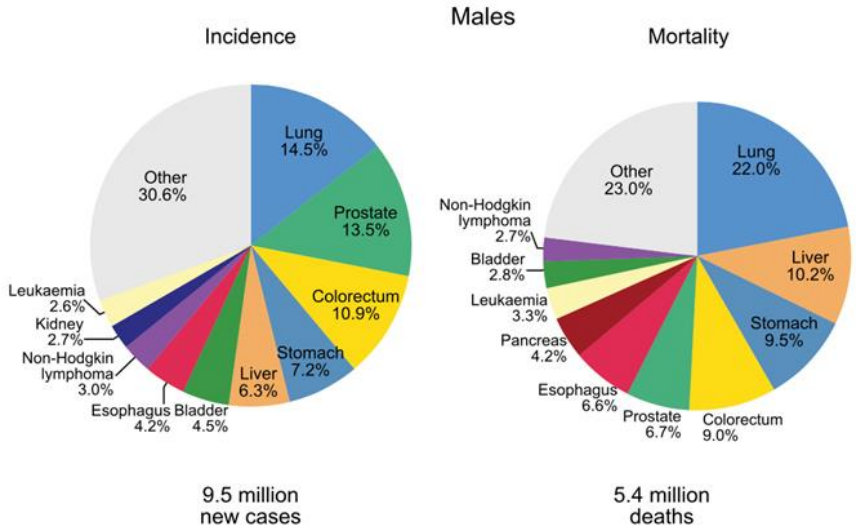

Figure 3. Distribution of incidence and mortality for the 10 most common cancers in 2018. The area of the pie chart reflects the proportion of the total number of new cases or deaths. Non-melanoma skin cancers are included in the 'other' category. Adapted from Bray F *et al.*[29].

Like many other cancers, PCa likely represents the accumulation of many genetic and epigenetic aberrations that have developed over the course of decades. Although the etiology of the disease remains debated, a few factors that are associated with elevated risk of PCa have been identified to date. Increasing age is clearly the most consistent risk factor, but there are other well-established factors that may have a role in the development of PCa, such as ethnic origin and familial inheritance[33]. Diet and lifestyle are also gaining recognition as potential risk factors[34], although their true impact remains unclear.

Several studies have shown that age is the strongest predisposing factor for PCa development. This disorder is extremely rare in men younger than 40 years, but the chances of having PCa rises rapidly after the age of 50, with 85% of all diagnoses occurring in men older than 65 years of age[29,35].

Ethnicity has also an important effect on the development of PCa. African Americans show the highest number of new cases and are more likely to present with advanced disease compared to men of any other racial background[36,37]. Asian population, meanwhile, have particularly lower incidence rates[29].

Another well-known risk factor for the development of prostate malignancies is familial inheritance. It has been estimated that 5-10% of prostate tumors are linked to hereditary predisposition, while the other 90-95% are considered sporadic. Mutations in genes associated with normal prostate development (HOXB13) and several tumor suppressor genes such as BRCA1 and BRCA2 have been linked to hereditary PCa[38]. Moreover, men with an affected first-degree relative have a two-fold higher risk of developing the disease and even an increased risk of suffering PCa at an earlier age[39,40].

2.2. Current methods for diagnosis

PCa is generally a slow growing tumor, however, it is still a lethal disease. In order to reduce the overall disease-specific mortality, it is important to detect the malignancy at early stages and monitor its progress accurately. Early PCa is commonly asymptomatic, while patients with advanced disease may present with specific LUTS or metastasis-related complains. Nevertheless, many urinary symptoms can also occur

as the result of benign prostatic disorders and, usually, mot cases of PCa are diagnosed before these symptoms appear[41].

To date, the primary tools used to diagnose PCa are based on the measurement of serum PSA levels and digital rectal examination (DRE), whereas the definite diagnosis can only be made following histopathological examination of a prostate biopsy (PB) as described in Figure 4.

2.2.1. PSA blood test

Human kallikrein-related peptidase 3 (KLK3) is commonly referred to as PSA. It is a serine protease predominantly produced by the luminal epithelial cells of the prostate gland, thus forming a major component of the seminal fluid. During prostatic disorders, it is released into the blood stream as a consequence of the disruption of the normal glandular architecture within the prostate, resulting in elevated concentrations of serum PSA. This glycoprotein was first described as a cancer marker in 1979[42], when its prostate tissue specificity was identified. In 1986, the PSA blood test was approved by the U.S. Food and Drug Administration (FDA) for monitoring tumor recurrence in patients after treatment[43]. Nowadays, it is used as the gold standard for the initial screening of the disease.

The introduction of PSA testing has resulted in a huge increase in the documented incidence of prostate adenocarcinoma, the most common type of PCa, especially in early stages[44-46]. Although some PCa will not lead to elevated PSA levels, it is used for risk stratification in patients with localized disease and as a prognostic tool in metastatic PCa. PSA serum levels above 4 ng/mL indicate an increased risk of having PCa, and hence it is the established cutoff for recommending biopsy[47]. Furthermore, higher levels are frequently observed in advanced stages.

However, the role of PSA blood test as a screening tool presents some drawbacks. It is organ-specific but not strictly a tumor-specific marker, not being able to distinguish between aggressive PCa, indolent tumors and other benign disorders (e.g., prostatitis or BPH), which also cause increased leakage of PSA into the blood[48,49]. This lack of specificity is associated with a high risk of false positives and consequently an increased number of negative PB[50]. Moreover, over-diagnosing indolent PCa is linked to over-treatment of many cases that would remain latent and never cause symptoms or death (Fig. 4)[51].

Several attempts have been made to enhance the diagnostic and prognostic potential of PSA, including measurements of PSA density (PSAD), PSA velocity (PSAV), PSA doubling time (PSADT) and ratio of free:total PSA. But they all present their own limitations and further research needs to be done[52,53].

2.2.2. Digital Rectal Examination (DRE)

Physical examination is performed on all patients suspected of having PCa due to elevated serum PSA levels. Until the popularization of the PSA blood test in the 1990s, DRE used to be the classic way of PCa diagnosis. It consists in the palpation of the prostate with a gloved finger through the rectum in order to assess the physical features of the gland. Abnormalities in size, texture and prostate symmetry are considered suspicious DREs and, combined with the PSA screening result, are currently important indicators for further testing[54].

Nevertheless, this technique is limited to bigger palpable tumors and has not proven to be sensitive enough; while it produces a large percentage of false-positive results since benign conditions generate most of the prostate enlargements (Fig. 4)[51]. In addition to the poor sensitivity and specificity, it has low accuracy in localizing PCa and is a highly subjective test, even among experienced urologists[55].

2.2.3. Prostate biopsy

Upon increased PSA values and abnormal DRE, prostatic biopsy is regarded as the gold standard for the final diagnosis of PCa[56]. Transrectal ultrasound (TRUS)-guided PB, a technique based on the use of sound waves and echoes that enable the visualization of the gland, is particularly considered the preferred technique. The current recommendation for initial biopsies is a 10-12-core systematic biopsy of the prostatic tissue, especially directed towards the PZ[57]. Local anesthesia is recommended, and additional cores can be taken from suspicious areas, thus improving PCa detection rates[58]. Positive biopsies are further examined to determine tumor stage.

Unfortunately, a great part of prostate malignancies is missed at systematic biopsies (Fig. 4)[51]. TRUS-guided biopsy is also affected by sampling errors, leading to imprecise risk stratification, over-diagnosis and over-treatment of low-volumen and indolent PCa. Men with a negative initial biopsy but persistently high or rising PSA

levels are likely to undergo another set of biopsies with a higher core sample size[59]. Nonetheless, biopsies are not without complications – adverse effects include bleeding and patient discomfort, among others.

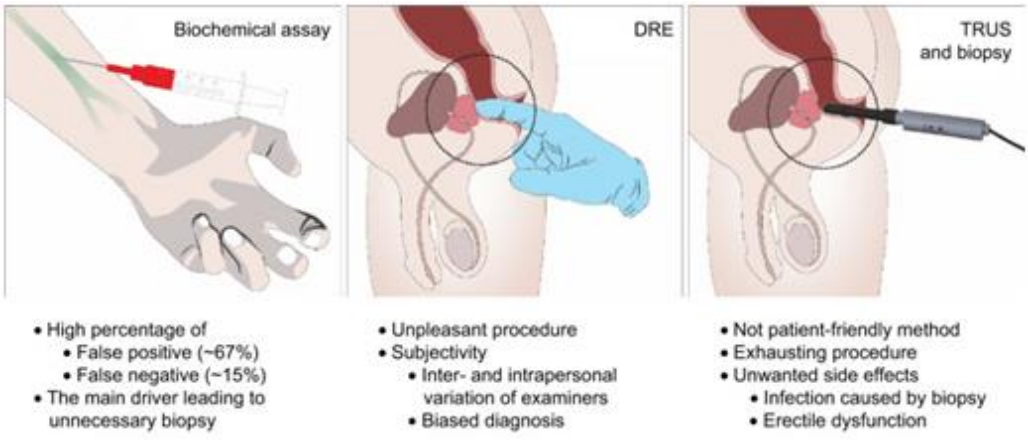

Figure 4. Current scheme for PCa diagnosis. Adapted from Kang BJ *et al.*[51].

The limitations of the above-mentioned screening methods and the invasive nature of the prostate biopsy procedure have highlighted an urgent need for novel and more clinically reliable biomarkers.

In the last few years, multiparametric-magnetic resonance imaging (mp-MRI) has emerged as a useful tool for patients with persistent suspicion of PCa despite repeated negative biopsies[60]. It has the ability to detect tumors located in the anterior part of the organ and may play a role in reducing the number of negative biopsies and their associated risks[61], thus preventing over-diagnosis and over-treatment. Moreover, it is positively associated with increased tumor volume and high tumor grade. Because assessment on mp-MRI can be subjective, education of radiologists and standardized scoring systems are assential for accurate interpretation.

In addition, PCa antigen 3 (PCA3) or TMPRSS2-ERG gene fusions have attracted much attention[49], but their clinical application for the detection and management of PCa is still being proven. Quantitative levels of urine TMPRSS2-ERG seem to be associated with clinically significant PCa, and the combination of post-DRE urine TMPRSS2-ERG gene fusion and PCA3 enhanced the utility of serum PSA levels for

predicting PCa risk[62]. However, none of these new biomarkers are suitable to replace PSA and DRE PCa screening yet. Improvement of the diagnosis accuracy will contribute not only to best therapy selection but also to maximize the efficacy of subsequent therapies for the diagnosed patients.

2.3. Classification of prostate cancer

2.3.1. Gleason grading system

If a tumor is detected in the biopsy, histopathological grading of the prostatic tissue is performed using Gleason score, one the most important prognostic predictors in PCa. Named after Donald F. Gleason, the pathologist who introduced it in 1966, this grading system characterizes the glandular architecture of the prostate according to the degree of cellular differentiation[63]. It stratifies prostate adenocarcinomas into five different histological grade patterns, where 1 represents the most differentiated and 5 the least differentiated tumor pattern (Fig. 5)[64]. Due to the heterogeneity of the disease[65], the Gleason score is calculated by adding the grade of the most common and the second most prevalent patterns, being 2 the lowest and 10 the highest Gleason score. When just one pattern is identified, the primary grade is doubled.

Nevertheless, the original Gleason grading system has suffered significant modifications over the years[66]. Most recently, in 2014, the International Society of Urological Pathology (ISUP) made further recommendations that are supposed to allow more accurate risk stratification and reduce overtreatment of indolent PCa[63,67]. The need for modifications was based on the lack of consensus of certain grading issues, leading to several refinements in the definition and interpretation of Gleason patterns 3, 4 and 5.

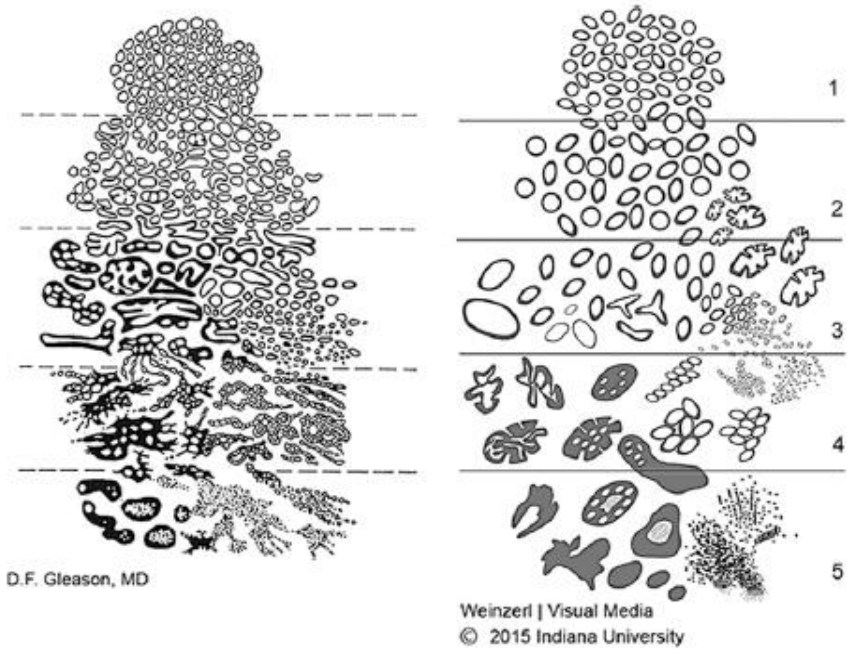

Figure 5. Gleason grading system. Original (left) and 2015 Modified ISUP (right) histologic patterns of prostatic adenocarcinoma. Adapted from Epstein JI *et al.*[64].

Notably, Gleason grade has been associated with tumor progression, aggressiveness, and disease outcome, thus strongly influencing treatment decisions.

2.3.2. TNM staging system

Following histological confirmation of the malignancy, clinical staging should be completed. The tumor node metastasis (TNM) system is the most widely used staging system for PCa. It evaluates the extent of the primary tumor (T), the affection of regional lymph nodes (N), and the presence of distant metastasis (M) (Table 1)[68]. The American Joint Committee on Cancer (AJCC) and the Union for International Cancer Control (UICC), the organizations responsible for this staging system, update it regularly. The most recent revision is the 8th edition, published in 2016[69].

Table 1. Tumor Node Metastasis (TNM) staging of PCa. Adapted from Brierley A *et al.*[68].

T - Primary Tumour		
TX	Primary tumour cannot be assessed	
T0	No evidence of primary tumour	
T1	Clinically inapparent tumour that is not palpable	
	T1a	Tumour incidental histological finding in 5% or less of tissue resected
	T1b	Tumour incidental histological finding in more than 5% of tissue resected
	T1c	Tumour identified by needle biopsy (e.g. because of elevated prostate-specific antigen (PSA) level)
T2	Tumour that is palpable and confined within the prostate	
	T2a	Tumour involves one half of one lobe or less
	T2b	Tumour involves more than half of one lobe, but not both lobes
	T2c	Tumour involves both lobes
T3	Tumour extends through the prostatic capsule[1]	
	T3a	Extracapsular extension (unilateral or bilateral) including microscopic bladder neck involvement
	T3b	Tumour invades seminal vesicle(s)
T4	Tumour is fixed or invades adjacent structures other than seminal vesicles: external sphincter, rectum, levator muscles, and/or pelvic wall	
N - Regional Lymph Nodes[2]		
NX	Regional lymph nodes cannot be assessed	
N0	No regional lymph node metastasis	
N1	Regional lymph node metastasis	
M - Distant Metastasis[3]		
M0	No distant metastasis	
M1	Distant metastasis	
	M1a	Non-regional lymph node(s)
	M1b	Bone(s)
	M1c	Other site(s)

[1]Invasion into the prostate apex or into (but not beyond) the prostate capsule is not classified as T3, but as T2.
[2]Metastasis no larger than 0.2 cm can be designated pNmi.
[2]T2a to c only exist for clinical T2 (cT2). For pathological T2 they are no longer present in the 2017 TNM. Only pT2 exists.
[3]When more than one site of metastasis is present, the most advanced category is used. (p)M1c is the most advanced category.

Since this classification provides a basis for survival prediction, tumor behaviour and initial treatment selection[70], it has important implications for the management of patients with PCa.

Once the TNM classification has been determined, this information is used in conjunction with the Gleason score and PSA levels in order to establish an overall stage[71]. This stage is expressed in Roman numerals from I (the least advanced) to IV (the most advanced) and is essential for final correct prognosis and treatment[70]. Moreover, these criteria are also effectively utilized in the stratification of men with localized PCa into different risk categories[72], which help clinicians for treatment decision-making (Table 2).

Table 2. Risk stratification guidelines for patients with localized disease. PCa is classified as low, intermediate or high risk. Adapted from EAU Guidelines[72].

Risk category	Serum PSA		Gleason Score		Clinical stage
Low	<10 ng/mL	and	≤ 6	and	T1-T2a
Intermediate	10-20 ng/mL	or	7	or	T2b
High	>20 ng/mL	or	8-10	or	≥ T2c

2.4. Initiation and progression

PCa is a heterogeneous and multifocal disease. The molecular pathways that contribute to prostatic carcinogenesis remain largely unknown, but certain molecular factors have been associated in the overall process of disease progression. For instance, aberrations in some specific signaling molecules have been indicated, such as intracellular anti-apoptotic or transcription factors, factors involved in telomerase activity, extracellular growth factors and cell cycle regulators[73].

Next-generation sequencing (NGS) has allowed the identification of several genomic lesions in prostate tumors, providing great information about tumorigenesis[74]. From initiation of hormone-naïve PCa to its progression towards androgen resistance and death, different genetic changes occur in a multi-step process (Fig. 6)[75]. Perturbations in phosphatidylinositol 3-kinase (PI3K) and retinoblastoma (RB) signaling pathways are proposed as PCa driving alterations[76]. Both tumor suppressors RB and PTEN (phosphatase and tensin homolog), a well-established negative regulator of the PI3K pathway, are frequently lost in castrated-resistant prostate tumors[77-79]. Dysregulation of PTEN is further associated with poor prognosis. On the contrary, the proto-oncogene MYC is often overexpressed in advanced PCa as well as in HGPIN lesions[80]. Other common genetic changes in PCa progression include deletions of NKX3.1 (prostate-specific NK3 homeobox 1) tumor suppressor genes and chromosomal rearrangements of ERG and ETS-like transcription factors. Downregulation of NKX3.1 is usually observed in the earliest phases of PCa carcinogenesis[81], although it has also been shown in high-grade PCa[82]. Among the *ETS* family, as mentioned before, *TMPRSS2*-

ERG fusion is most common rearrangement, being the predominant variant in approximately 40-80% of PCas, and is associated with highly aggressive tumors[83,84]. Moreover, loss of p53 occurs preferentially in the advanced stages of PCa and is linked to metastatic progression[85].

Inflammatory gene markers are also associated with poor prognosis in many cancers, including PCa. As men age, circulating levels of inflammatory cytokines such as IL-6, tumor necrosis factor α (TNF-α) and IL-1ß increase along with PCa incidence. IL-6 has been shown to enhance AR function and higher circulating levels have been observed in patients with CRPC and metastatic disease. Likewise, elevated levels of NF-κB, one of the pivotal mediators of inflammatory responses, are associated poor prognosis in primary PCa and reduced time to biochemical recurrence[75].

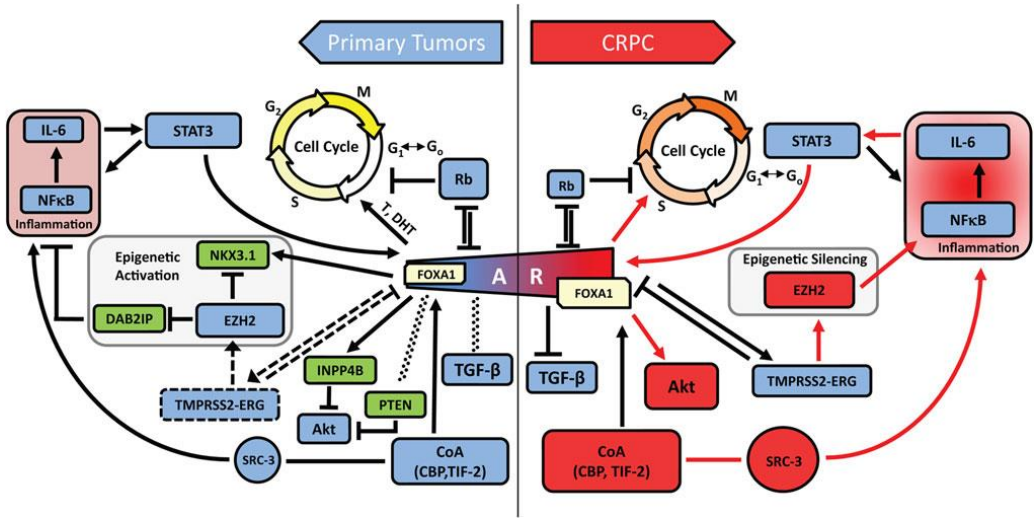

Figure 6. Signaling pathways altered in primary PCa and development of CRPC. Red arrows indicate increased levels and/or activation of signaling pathways. Green boxes denote factors that are lost during the progression of PCa. Dotted lines indicate croos talk with the AR. Adapted from Hodgson MC *et al.*[75]

2.4.1. Castration-resistant prostate cancer (CRPC)

The prostate gland depends on androgens for normal growth, maintenance and function. Likewise, during PCa development, most of the cancer cells are initially dependent on androgens. Androgens, through the androgen receptor (AR)[86], are

crucial for the initiation and progression of PCa and thus, androgen withdrawal results in tumor regression. Following androgen deprivation, rapid cellular apoptosis and AR signaling downregulation manifest the androgen dependence of prostate tissues. However, remissions are temporary and the disease invariably progresses to an androgen independent late stage, also termed castration-resistant PCa (CRPC), which is refractory to current therapies[87]. Upon progression to CRPC, the median survival of those patients is less than 2 years and the disease remains essentially untreatable[88]. Understanding the mechanisms that drive the transition to an androgen independent state becomes therefore of utmost importance in drug development for CRPC patients.

There are two models, not mutually exclusive, that have been proposed in order to explain the development of CRPC: the adaptation model and the selection model (Fig. 7). The adaptation model proposes that CRPC arise through genetic or epigenetic changes in androgen dependent cells under conditions of androgen deprivation. On the contrary, the selection model suggests that there is a small pre-existing quiescent population of castration-resistant cells, which will expand under the pressure of androgen ablation therapies leading to CRPC[89].

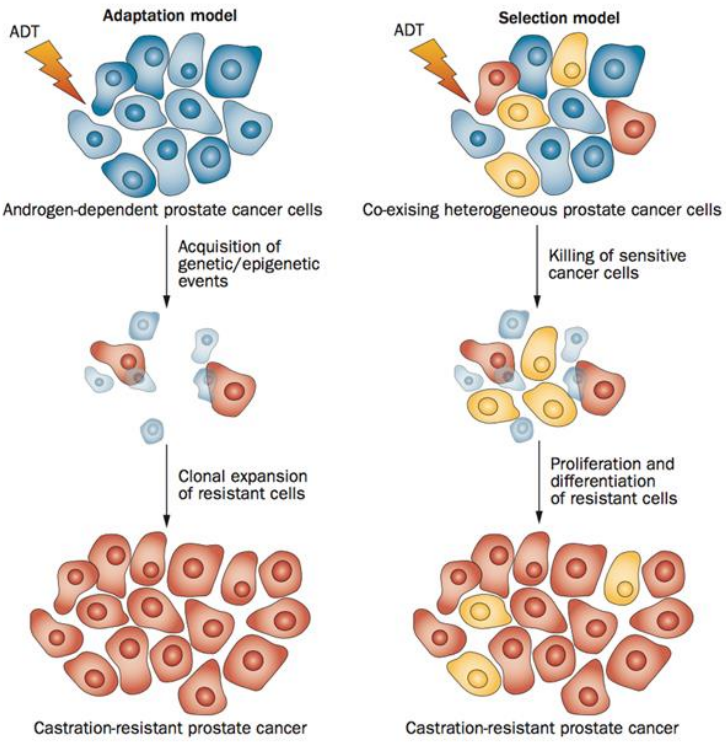

Figure 7. Adaptation *versus* selection model in CRPC development. The adaptation model proposes that a subset of androgen dependent cells acquire genetic or epigenetic changes conferring resistance to androgen deprivation therapy (ADT), whereas the selection model supports the outgrowth of pre-existing androgen independent cells in the tumor. Adapted from Zong Y *et al.*[89]

2.4.1.1. Androgen receptor (AR)

While the key molecular alterations that govern androgen independence remain to be elucidated, it is clear that AR is a major player involved in this process.

The AR is a nuclear receptor that is able to bind to androgens and act as a transcription factor to regulate a variety of genes. DHT within the prostate cell binds to cytosolic AR, which undergoes a conformational change and translocates into the nucleus. Once in the nucleus, AR acts as a transcription factor, binding to specific DNA sequences, also known as androgen responsive elements (ARE), and leading to the expression of different genes such as PSA. This ligand-dependent transcription factor contains four primary functional domains: a large N-terminal transactivation domain (NTD), a C-terminal ligand-binding domain (LBD), a central DNA-binding domain

(DBD), and a hinge region that contributes to nuclear localization and degradation[90]. The ligand-binding domain plays a role the binding of DHT to AR, whereas the DNA-binding domain is responsible for the interaction of AR with specific ARE in the nucleus.

AR signaling plays a key role in both normal prostate development and PCa, and is by far the most commonly studied pathway in the context of androgen independent PCa[91]. Although CRPC tumors continue growing in the presence of sub-optimal levels of androgens, it has been shown that the AR machinery remains active and cells continue expressing AR as well as AR targets such as PSA[92].

2.4.1.2. Mechanisms of resistance in PCa

Several mechanisms have been described for the ability of AR to retain its signaling activity in CRPC. Amplification of the AR gene copy number is a primary mechanism driving prostate tumor growth under androgen-depleted conditions, which occurs in approximately one-third of castration-resistant carcinomas[93]. Another 10-30% of prostate tumors have AR mutations that may confer increased protein stability, greater sensitivity to androgens or novel responses to other steroid hormones[94,95]. Additionally mechanisms that have been associated with altered AR signaling are changes in AR co-regulator levels, alterations in steroidogenic pathways and expression of alternative AR splice variants, as well as ligand-independent activation of AR via outlaw pathways (Fig. 8)[73].

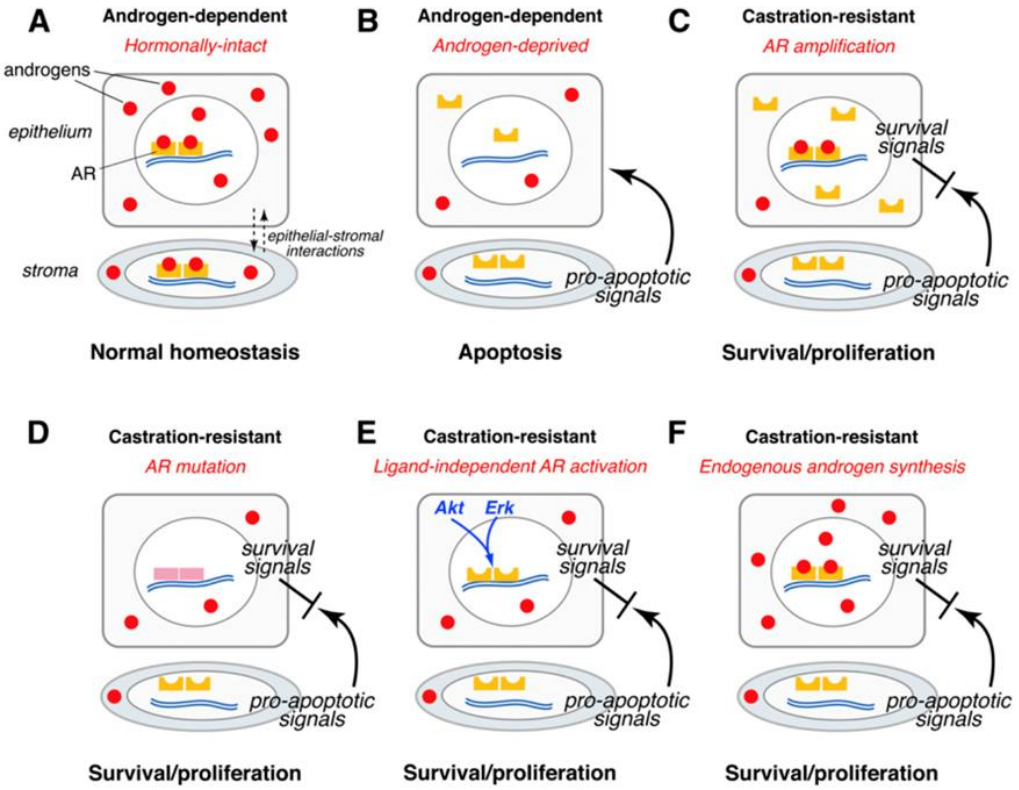

Figure 8. The role of AR in CRPC. A) AR maintains homeostasis of the epithelium and stroma in the normal prostate tissue. **B)** Following androgen ablation, stromal cells produce proapoptotic signals that promote regression of androgen dependent PCa. **C-F)** Castration resistance can occur through a variety of molecular mechanisms, including **C)** AR amplification, **D)** AR mutation, **E)** ligand-independent AR activation via upregulation of other signaling pathways such as the AKT/mTOR and MAPK, and **F)** endogenous biosynthesis of androgens. Adapted from Shen MM *et al.*[73]

AR amplification, promiscuity, and splice variant isoforms are rarely or not observed in treatment-naïve primary PCa, indicating that these changes occur as an adaptive response to androgen deprivation therapy[92].

Exposure to androgen ablation therapies with resulting castrate levels of circulating androgens selects for AR amplification in order allow continued AR signaling and castration resistance. One possible mechanism by which PCa circumvents the effect of ADT is by increasing its sensitivity to reduced levels of androgens. Some AR-amplified tumors that seem clinically to be androgen independent retain a high degree of

dependency on residual androgens, but they have a lowered threshold for these hormones[87].

The frequency of mutations in the AR is significantly increased in CRPC tumors after androgen ablation therapy. However, untreated aggressive tumors that have metastasized also harbor a great number of AR mutations[86], suggesting that hormonal therapy does not drive mutagenesis of AR itself, but contributes to the selection of specific mutations after therapy initiation. Many cases of androgen independent PCa develop from the acquisition of genetic changes that lead to aberrant activation of the androgen-signaling axis. These changes are usually missense mutations in the AR gene that occur in the LBD, resulting in either decreased specificity of the ligand binding or constitutive protein activity[87]. ARs become more promiscuous allowing inappropriate activation by different non-androgen steroids and androgen antagonists. The most common point mutation identified during CRPC is T877A[92].

In addition to mutations, AR splice variants (AR-Vs) that lack the LBD have been recently discovered and provide a novel mechanism for the resistance to androgen suppression. These variants often truncate the C-terminal domain of the AR protein and, thus, make it constitutively active and hormone insensitive[80]. Seven AR-Vs have been described, being AR-V7 the most commonly expressed splice variant in PCa[87]. Via nuclear localization, it is able to bind DNA independently, without androgen activation, regulating a unique set of target genes that facilitate mitosis and promoting disease progression. Since AR-Vs are active transcription factors independent of ligand stimulation, they are resistant to androgen ADT; moreover, AR antagonists, which target the LBD, have no effect on splice variants that lack this domain[92].

Besides endogenous androgen ligands, the AR can be also activated in ligand-independent mechanisms, also known as outlaw pathways. Upregulation of the PI3K pathway through PTEN deletion appears to be particularly effective. Alterations in the PI3K-AKT-mTOR pathway occur in the vast majority of metastatic PCa tumors and are lnown as potential drivers of CRPC[96]. In addition, various growth factors, cytokines, kinases and other proteins have been shown to upregulate AR transcriptional activity through increased tyrosine phosphorylation or elevated AR ubiquitination[73].

Another mechanism for castration resistance is the autocrine activation of androgen synthesis by tumor cells. Recent studies have demonstrated that recurrent PCa can

generate their own androgens via de novo synthesis, leading to persistent intraprostatic androgen levels despite androgen deprivation[90]. Under these conditions, drugs that effectively block hormone synthesis would be most beneficial[80].

Nevertheless, some CRPC tumors develop and progress via AR-independent mechanisms, termed 'bypass' mechanisms (Fig. 9)[96]. These mechanisms include, but are not limited to activation of kinase pathways, epithelial-to-mesenchymal transition (EMT), lineage plasticity, apoptosis inhibition and upregulation of steroid receptors[97,98]. Interestingly, the glucocorticoid receptor (GR) is a steroid hormone nuclear receptor that is closely related to the AR. Recent work has indicated that GR and AR possess the same chromatin binding sites and regulate the expression of many AR-specific genes, thus promoting CRPC development. Moreover, the progesterone receptor (PGR) may have the ability to transcriptionally regulate a subset of AR target genes in PCa and thereby bypass AR signaling pathways[99]. Both steroid hormone nuclear receptors have been proposed as important therapeutic targets the in treatment of PCa.

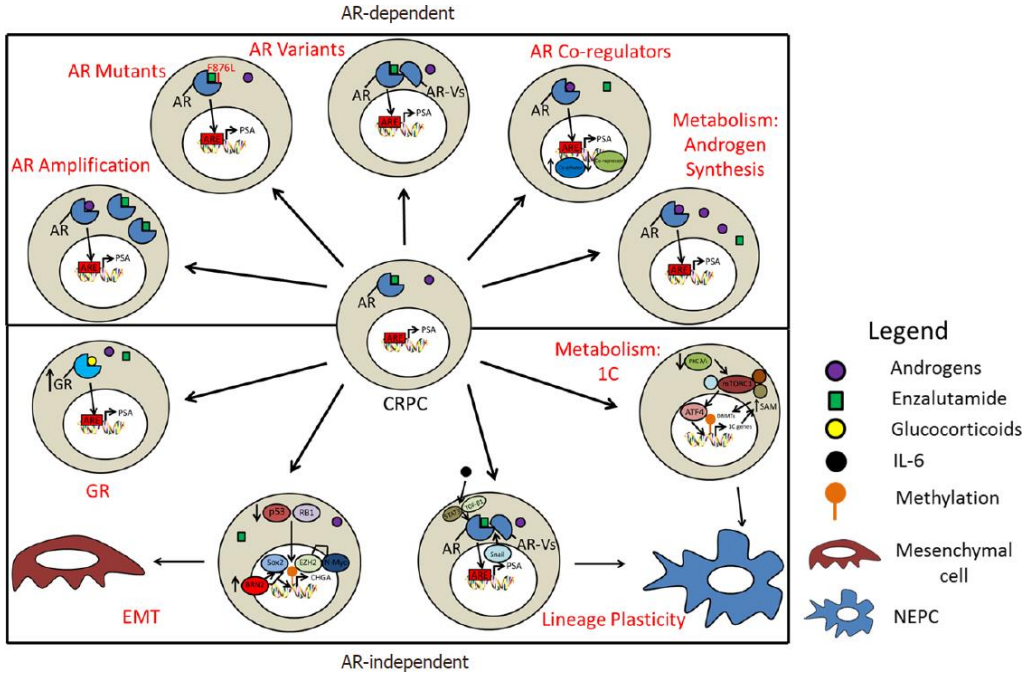

Figure 9. Molecular mechanisms of resistance in PCa. AR-dependent and AR-independent mechanisms for the development of CRPC. Adapted from Blatt EB *et al.*[96]

All together, the above-mentioned processes are supposed to confer survival and growth advantage to PCa cells in low androgen environments. Increased knowledge of the molecular alterations that occur during all theses processes may be important in anticipating resistance to available hormonal therapies and will allow for improved therapeutic strategies in CRPC patients.

2.4.2. Neuroendocrine prostate cancer (NEPC)

Neuroendocrine PCa (NEPC) encompasses various clinical contexts, ranging from de novo presentation of small cell prostatic carcinoma to a more common transformed phenotype that arises from typical adenocarcinoma of the prostate after hormonal therapy[100]. This aggressive subtype of PCa is enriched in the advanced setting of the disease and results in poor clinical outcome[101].

Histologically, NEPC differs from PCa by high mitotic count and the presence of small round cells that do not express AR or secrete PSA, but usually express neuroendocrine markers such as synaptophysin, chromogranin, CD56 and neuron-specific enolase[102]. These tumors are often characterized by loss of RB1, activation of PI3K pathway and amplification of Aurora A kinase (AURKA) and MYCN[103-105]. Upregulation of UBE2C and cyclin D1, as well as other mitotic kinases, also occur in this high-risk, lethal subset of PCa[106], thus demonstrating that progression of NEPC may require a unique cellular reprograming. Moreover, despite largely similar genomic profiles, genome-wide DNA methylation analysis revealed marked epigenetic differences between NEPC and CRPC tumors, suggesting a key role of epigenetic modifiers in modulation NEPC phenotype[98,107].

Ongoing studies have been focused on improving the molecular characterization of the disease and efforts are underway to develop novel targeted therapeutic approaches for this aggressive, AR-independent PCa subtype.

2.5. Therapeutic approaches in PCa

Because there are several current therapeutic options available for the treatment of PCa, the clinical management of the disease has become increasingly complex. Initial treatment decision in greatly influenced by tumor stage, patient age and estimated life expectancy, as well as competing co-morbidities and personal preferences[56]. The main

treatment choices for PCa include active surveillance (AS), surgery, radiation, hormonal therapy and chemotherapy.

2.5.1. Treatment modalities for early, localized PCa

The detection of PCa at early stages of the disease allows for a curative treatment of PCa patients, where the 5-year survival is nearly 100%[29]. When it is still confined to the prostate, PCa can be cured by radiation therapy or radical surgery. Active surveillance is employed in men with low-risk disease[108].

2.5.1.1. Active surveillance (AS)

For small low-risk tumors, AS is the most common approach, especially in elder men with limited life expectancy. It is an observational treatment strategy that consists in close monitoring of patients using PSA tests, DRE and prostate biopsies[109]. Any sign of disease progression would lead to radical intervention. The purpose of this non-invasive option is to avoid side effects of unnecessary treatments, thus optimizing life quality. However, a significant disadvantage of this treatment is the risk of tumor progressing in a short space of time.

2.5.1.2. Radical prostatectomy (RP)

Surgery is an accepted therapeutic choice for treating localized PCa. In particular, RP is a major surgical procedure that involves excision of the entire prostate gland and seminal vesicles, along with sufficient surrounding malignant tissue[110]. This process can be performed as open surgery or by laparoscopy, with or without robotic assistance. RP is mainly recommended for men with localized low-grade PCa and high life expectancy, or for patients with intermediate-risk disease without co-morbidities. Following effective RP, PSA levels should no be detectable, and any rise in PSA would indicate biochemical disease recurrence[111]. Adverse effects associated with this procedure include urinary incontinence and erectile dysfunction.

2.5.1.3. Raditation therapy (RT)

External Beam Radiation Therapy (EBRT) or brachytherapy are commonly used radiological approaches offered to patients with low- to intermediate-risk localized PCa. Recently, the benefit of combining local therapies, such as EBRT, with neoadjuvant hormone therapy has also been demonstrated for the treatment of locally advanced disease[112,113]. Radiation causes DNA damage and genetic instability, resulting in

destruction of the targeted cells. In EBRT, patients receive radiation treatment from an external photon source (x-rays); whereas brachytherapy involves implantation of radioactive 'seeds' directly into the prostate gland[114]. Overall, RT is a less invasive option compared to surgical therapy. Risks associated with RT include incontinence, impotence, bladder or bowel disturbances and urinary problems[115].

2.5.2. Treatment modalities for advanced PCa

Despite the effective treatment of PCa when it is localized to the prostate, ~30% of men treated with RP or RT will relapse. Yet, the 5-year survival of patients with metastatic disease drops below 31%[29]. For patients that present advanced disease, immediate treatment options, such hormonal therapy and ultimately chemotherapy, are required. The overall sequential treatment for advanced PCa is detailed in Figure 10[116].

2.5.2.1. Androgen deprivation therapy (ADT)

Hormonal therapy, also known as ADT, is the mainstay of treatment for locally advanced, metastatic and recurring PCa[87]. As AR signaling is implicated in the disease progression, therapies reducing circulating levels of androgens or blocking androgen actions have become a very efficient treatment for PCa. The beneficial effects of ADT were first described in 1941 by Huggins and Hodges, who demonstrated that removal of testicular androgens inhibited prostate tumor growth[117]. This can be accomplished by surgical or chemical castration, both leading to a decrease in testosterone production.

Bilateral orchiectomy, or surgical castration, implies the removal of the testicles, which are the main source of androgen production in the body. While surgical castration is a permanent and irreversible procedure, it is a very effective castration method[118]. Once the testicles removed, 90-95% of serum testosterone is eliminated, thus achieving a shrinking of the tumor. Although this procedure is associated with good quality of life (QoL), it has been largely replaced by medical castration because of improved patient and physician acceptance[118].

Chemical castration requires the administration of agents that manipulate the hypothalamic-pituitary-gonadal axis in order to block endogenous production of testosterone[119]. This can be achieved by blocking the androgen production pathways or inhibiting androgen affinity towards the AR. Luteinizing hormone releasing hormone

(LHRH) agonists and antagonists have been developed and become the standard of care in hormonal therapy. LHRH agonists overstimulate LHRH receptors in the pituitary gland, causing their downregulation; whereas LHRH antagonists bind directly to those receptors, blocking the release of LH[120]. These drugs avoid the physical and psychological discomfort associated with orchiectomy and, unlike surgical castration, the effect on androgen production is reversible. Another method for hormonal therapy is the use of antiandrogens that bind to AR, leading to a competition with the circulating androgens and therefore preventing testosterone production. Orally administered antiandrogens, such as flutamide and bicalutamide, may be given as monotherapy or in combination with LHRH agonists for maximal androgen blockade (MAB)[121]. Nevertheless, like other treatment options, ADT has also side effects including erectile dysfunction, fatigue, depression and osteoporosis[122]. Yet the most critical limitation is the emergence of castration-resistant PCa.

Androgen-ablation therapies can initially (18-36 months) achieve a biochemical response in the majority of patients by suppressing PSA levels and tumor size before most of them become resistant.

Recent work has focused on the development of new antiandrogens to overcome the resistance mechanisms observed within the previous agents. Since most CRPC tumors remain AR-driven, highly potent drugs that block AR signaling through inhibition of hormone production or AR receptor binding are under clinical development. By further targeting the AR signaling axis, the next-generation antiandrogens abiraterone acetate[123] and enzalutamide[124] have shown significant benefit regarding overall survival of patients with metastatic CRPC (mCRPC). Both of them have been already approved by the FDA for treating advanced PCa. Abiraterone acetate is an effective oral inhibitor of CYP17A1, a key enzyme in the androgen biosynthesis, which significantly reduces testosterone production below castration levels[125,126]. Enzalutamide (MDV3100) is another recently developed AR antagonist that has shown promising results with increased potency. It prevents the translocation of AR towards the nucleus, inhibiting DNA binding and avoiding the recruitment of co-activators[127,1128]. Moreover, MVD3100 has demonstrated *in vitro* and *in vivo* activity in bicalutamide-resistant models of PCa with overexpressed or mutant AR. Several new drugs and combinations addressing the AR pathway are currently being tested in clinical studies (Table 3)[129].

As intensive research continued to evolve rapidly, darolutamide (ODM-21) obtained last year an FDA label for the treatment of patients with non-metastatic CRPC based on the results of the ARAMIS (NCT02200614) clinical trial[130]. It is a synthetic nonsteroidal AR inhibitor with a distint molecular structure that offers potential for less severe adverse effects compared to other next-generation antagonists because of its low penetration of the blood-brain barrier. However, current available data have not clearly demonstrated improved clinical outcomes in comparison with enzalutamide[131].

Overall, these agents are ineffective in a large percentage of patients and extend the survival of those who respond by only a few months on average. Furthermore, most responding patients relapse within the first years with evidence of renewed AR activity. At this point, available treatments are essentially palliative, and hence, there is an increasing interest in the development of new and more potent agents for the molecular intervention of CRPC patients. Understanding the mechanisms driving therapeutic resistance would provide a new platform for exploring new targeted strategies, restoring sensitivity and prolonging patient survival.

Table 3. Phase III clinical studies in PCa targeting the AR pathway. Adapted from Nevedomskaya E *et al.*[129]

Agents	Population	Status	Identifier
ADT +/- abiraterone acetate + prednisolone + enzalutamide	Advancing or metastatic castration-resistant prostate cancer (mCRPC)	Completed	NCT00268476
Abiraterone acetate + prednIsone/prednisolone	mCRPC post-chemotherapy	Completed	NCT00638690
Abiraterone acetate + predInsone	Asymptomatic or mildly symptomatic patients with mCRPC	Completed	NCT00887198
ADT +/- abiraterone acetate + prednisone	Metastatic hormone-naive prostate cancer	Active, not recruiting	NCT01715285
ADT + docetaxel +/- local radiation therapy +/- abiraterone acetate +	Metastatic hormone-naive prostate cancer	Recruiting	NCT01957436
EnzalutaMide +/- abiraterone acetate + prednisone	mCRPR	Active, not recruiting	NCT01949337
Enzalutamide	nmCRPR*	Active, not recruiting	NCT02003924
Enzalutamide +/- radium-223	Castration-resistant prostate cancer (CPRC)	Recruiting	NCT02194842
Enzalutamide + ADT	Metastatic prostate cancer	Active, not recruiting	NCT02446405
Enzalutamide + ADT + radiation therapy	High-risk localized prostate cancer	Recruiting	NCT02446444

* non-metastatic CRPC

2.5.2.2. Chemotherapy

Once androgen ablation therapies have failed, the main treatment for CRPC patients relies on chemotherapeutical agents, such as microtubule-targeting taxanes. Until recently, docetaxel-based chemotherapy was the only drug that exhibited a modest survival benefit for the treatment of CRPC patients[132]. Docetaxel plus prednisone is the recommended treatment for metastatic PCa men with good performance status, demonstrating improved survival rates and enhanced quality of life[133]. However, most patients develop resistance within the first year of treatment. Mutations in tubulin may be responsible for persistent translocation of AR into the nucleus and therefore constitutive transcriptional activity[93].

Cabazitaxel is a second-generation taxane that has been approved over the past few years for the treatment of docetaxel-resistant hormone-refractory PCa[134,135]. Compared with docetaxel, it has poor affinity for P-glycoprotein, thus reducing the chances of resistance. Both chemotherapy drugs bind the beta subunit of tubulin and stabilize microtubules, blocking cell division and thereby inducing cell death[135]; but benefits are on average minimal and tumor resistance inevitably develops. Despite intense research, resistance to current therapies remains a critical point in the clinical management of CRPC patients, as evidenced by the moderate survival benefits offered by each of the above-mentioned treatments. Yet, the addition of some AR targets in combination with taxanes has shown an increased patient survival benefit. Enzalutamide compared to placebo has revealed a reduction in risk of death in CRPC patients who have been previously treated with docetaxel-based chemotherapy[136,137].

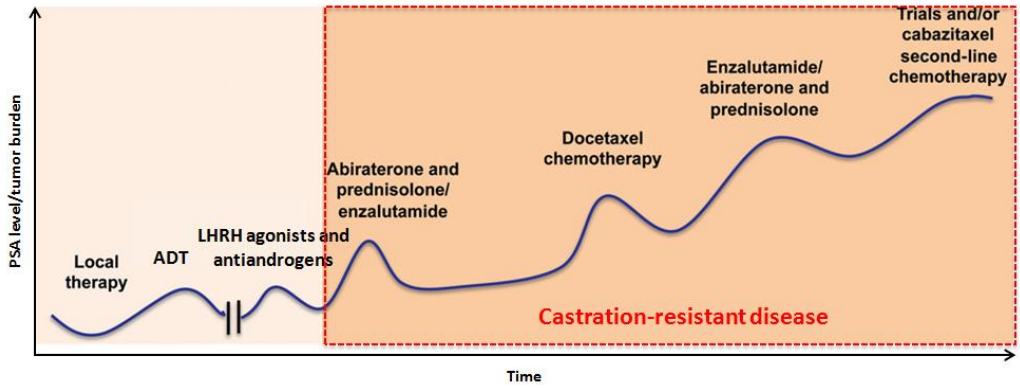

Figure 10. Natural history of PCa. Sequential treatment. Adapted from Carreira S *et al.*[116]

2.5.2.3. Immunotherapy

Immune checkpoint-targeting drugs are indicated for cancers with DNA repair defects, high tumor mutational burden (TMB) and microsatellite-high (MSI-H) tumors. Several evidence supports a role for immunotherapy in PCa disease[88]. Its has been shown that PCa can evade the immune system by downregulating antigen presentation, recruiting regulatory T cells, producing immunosuppressive cytokines and escaping cytotoxic T cells. Thus, activating the immune system against PCa tumor-associated antigens, such as PSA and PAP, may help this defense system in overcoming these evasive processes[138].

For instance, one example of a novel immunotherapy that is FDA-approved for advanced PCa, and in particular CRPC patients, is sipuleucel-T, a vaccine that is well tolerated and improves overall survival by 4 months compared to placebo[139]. It is a dendritic cell-based approach in which peripheral blood mononuclear cells (PBMCs) are extracted from a patient, enriched and incubated with PAP fusion protein PA2024 plus granulocyte-macrophage colony-stimulating factor (GM-CSF) for approximately 40 h, and then infused back to the patient[140].

Immune-checkpoint inhibitors (ICIs) have revolutionized the therapeutic landscape in patients with melanoma and non-small cell lung cancer (NSCLC)[141]. Some of these approaches are currently being evaluated in CRPC patients, including ipilimumab and the PD-1 inhibitor prembrolizumab. Ipilimumab is a human immunoglobulin G1 monoclonal antibody that binds to and blocks CTLA4. Early-phase studies in CRPC showed a >50% decline in PSA levels in a number of patients and one complete response. Nevertheless, in a phase III clinical trial against placebo, there was no significant effect of this antibody in the overall survival primary endpoint[142,143].

PROSTVAC-VF immunotherapy comprises two recombinant viral vectors encoding PSA transgenes and three immune co-stimulatory molecules: CD80, intercellular adhesion molecule 1 (ICAM1) and lymphocyte function-associated molecule 3 (LFA3). The interaction of infected antigen-presenting cells with T cells initiates a targeted immune response that mediates tumor cell destruction. A phase II study comparing this PCa vaccine to control emtpty vectors showed a significant improvement in overall survival in men with minimally symptomatic CRPC[144]. Optimal patient selection,

combination strategies and treatment timing remain under investigation in all these immunotherapy approaches.

2.5.2.4. Targeted therapies

Although improvements have been made in the past decade, the therapeutic benefits of standard chemotherapy regimens in castration-resistant patients are still limited. Molecular characterization of PCa using high-throughput sequencing technologies has led to the development of precision medicine, thus providing clinically actionable information that could guide treatment decisions in men with advanced PCa.

Recent strategies have been aimed at targeting signaling pathways that seem to be activated in CRPC, including the AKT/mTOR and MAPK pathways. PTEN loss and PI3K and AKT alterations provide potential targets for the management of PCa (Fig. 11)[102]. Rapamycin and related compounds, which target mTOR signaling, have been evaluated in different clinical trials without evidence for efficacy as single agents[145]; however, combination therapy using AKT/mTOR inhibitors plus first-line chemotherapy or agents targeting MAPK pathway may be highly effective, as has been suggested in a preclinical mouse model in which combination therapy led to hormone-refractory PCa inhibition[146]. Ipatasertib, an AKT inhibitor, was assessed in a phase II study that randomized mCRPC patients to treatment with abiraterone with or without ipatasertib after progression on docetaxel[147]. Accordingly, men with loss of PTEN showed improved clinical outcomes from ipatasertib *versus* placebo than patients without this alteration.

Selecting patients predicted to respond might reduce drug development failures in clinical trials. An example of such an approach is the phase II TOPARP study. In this trial, the PARP inhibitor olaparib was used in mCRPC-preselected patients harbouring putatively pathogenic DNA damage repair (DDR) alterations, showing high response rates[148]. Multiple clinical trials are being performed using PARP inhibitors in preselected populations of PCa men with DNA repair pathway defects (Fig. 11)[102]. The PROfound trial is a phase III multicentre study (NCT02987543) that randomizes mCRPC patients with specific DNA repair defect mutations to olaparib *versus* enzalutamide or abiraterone[149]. Further, TRITON3 is a randomized phase III trial (NCT02952534) evaluating the efficacy of rucaparib in mCRPC men harbouring select DDR gene aberrations who have progressed after AR-directed theray ad taxane-based

chemotherapy[150]. Both olaparib and rucaparib received FDA breakthrough therapy designation for patients with BRCA-mutated mCRPC. Alterations in the WNT pathway have also been observed in CRPC individuals and therefore represent potential targets for therapeutic decision-making in those patients (Fig. 11)[102].

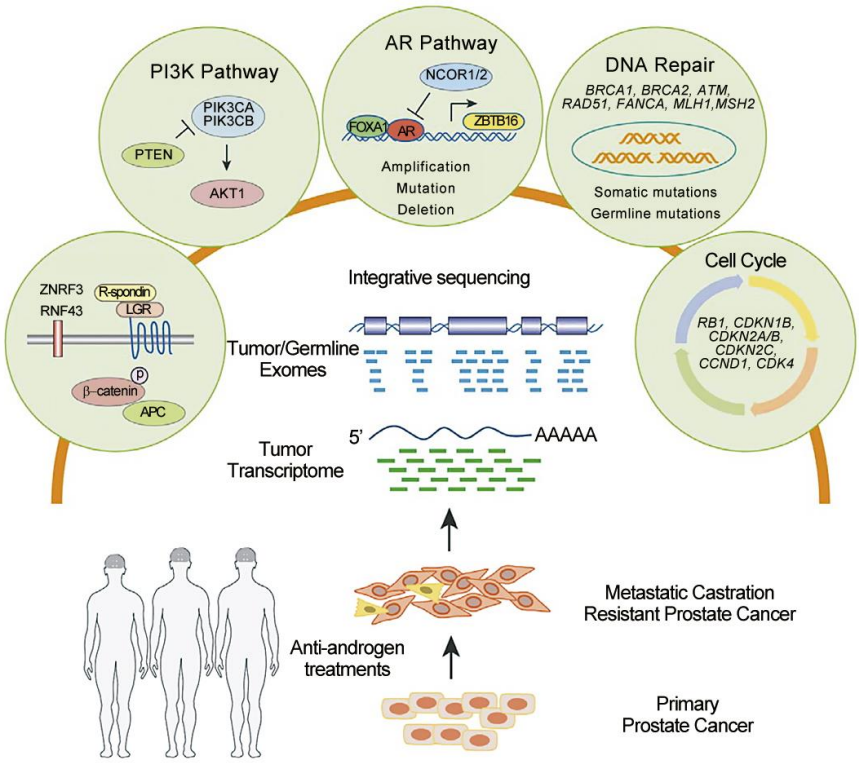

Figure 11. Pathway-guided treatment in CRPC. Five signaling pathways harbour clinically actionable genomic alterations for targeted therapies in CRPC. Adapted from Shevrin DH *et al.*[102]

Given the key role of the cyclin/cyclin-dependent kinase (CDK)/retinoblastoma (RB)-*axis in controlling cell cycle entry in multiple cancers, including PCa, a prime* therapeutic candidate has been CDK activity[151,152] (Fig. 11). Recently, the antitumor properties and mechanistic functions of palbociclib (PD-0332991), a potent and selective CDK4/6 inhibitor, has been studied in preclinical PCa models and primary tumors[153,154]. This kinase inhibitor has been already approved for the treatment of advanced or metastatic estrogen receptor (ER)-positive breast cancer[155]; and considering the similar role of estrogens and androgens in driving cell proliferation, it is

not surprising that palbociclib was also found to be effective in PCa models. An ongoing phase II single arm study (NCT02905318) is actively recruiting participants to better ascentain the clinical benefit of palbociclib in mCRPC[156]. Interestingly, cyclin D1 amplification and RB1 status will be assessed in this study and correlated with disease response, since they are critical prognostic factors for therapeutic efficacy. Ribociclib is another FDA-approved CDK4/6 inhibitor that have entered the treatment landscape for several solid tumors[157]. In particular, its efficacy is being evaluated in combination with hormonal depletion (NCT02555189)[158] and cytotoxic chemotherapy (NCT02494921)[159] in mCRPC patients.

Overall, progress continues to be made in the management of the disease and precision medicine will certainly expand therapeutic options and create combination strategies to enhance treatment response in CRPC patients.

3. MITOTIC REGULATORS IN PROSTATE CANCER

Alterations in the expression of several mitotic regulators have been associated with tumor formation in many cancers[160]. Recent genomic studies have shown that AR activity in hormone-refractory PCa is not identical to that displayed in androgen dependent cells. Interestingly, increasing evidence in the last years suggest that CRPC cells have undergone a genetic reprogramming to upregulate the expression of M-phase cell cycle genes. Wang *et al.*[161] reported that AR selectively and directly upregulates a set of mitotic regulators to promote androgen independent PCa. Enrichment of M-phase proteins and pathways has been found in CRPC chemotherapy-resistant tumors compared with their chemotherapy-naïve counterparts[162]. Moreover, Horning and colleagues[163] identified a subpopulation of PCa cells with enhanced cell cycle-related genes and decreased dependence on AR signaling that had the potential to develop androgen independence.

3.1. Cell cycle: a special focus on mitosis

The cell cycle is a sequence of strictly ordered events that lead to duplication and subsequent division of cells into two viable daughter cells. While it is divided into four different phases, there are two major parts: interphase and M-phase. Interphase is then further subdivided into (i) G_0 phase in which cells are in a resting state (quiescent), (ii) G_1 where cells are prepared for DNA synthesis, (iii) S phase in which DNA replication takes place, and (iv) G_2 phase where cells prepare to enter mitosis. On the other hand, M-phase consists of two main divisions: the nuclear division known as mitosis and the cytoplasmic division or cytokinesis[164]. At this point, the genetic material is equally distributed into the daughter cells and the process of cell division is completed.

Different cellular proteins tightly regulate the transition from one cell cycle phase to another. Major regulatory proteins are cyclin-dependent kinases (CDKs), a set of serine/threonine kinases that are activated at specific points of the cell cycle and phosphorylate selected proteins to induce downstream signaling[165]. While CDK levels remain stable, cyclin protein levels rise and fall during the cell cycle, leading to the activation and inactivation of the CDK kinases. Thus, specific CDK/cyclin complexes are characteristic of each cell cycle phase[166].

CDK1 monitors M-phase entry and exit and binds either cyclin A or cyclin B orchestrating different processes. Notably, activation of CDK1 is essential to govern mitosis, a crucial step of the cell cycle that must be carefully coordinated to ensure a faithful distribution of chromosomes into newly forming daughter cells (Fig. 12)[167].

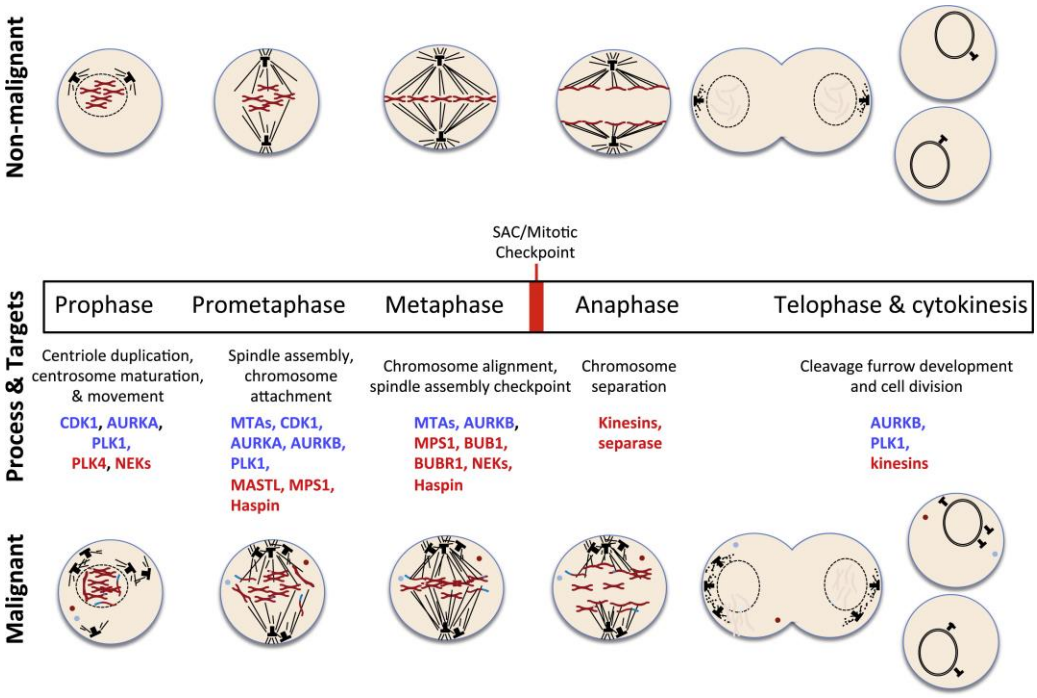

Figure 12. Mitotic regulators targeted for cancer therapy. Stages of mitosis include prophase, prometaphase, metaphase, anaphases and telophase. Finally, the cleavage furrow causes the division of the cell cytoplasm in a process called cytokinesis. After all these changes, the genetic content of one cell has been equally divided and two genetically identical daughter cells are produced. Numerous compounds have been developed to target various aspects of mitosis, including spindle micorutubles (microtubule targeting agents, MTAs), cyclin-dependent kinases, mitotic kinases, motor proteins and muti-protein complexes. Classic anti-mitotic therapeutic targets that have been already evaluated are highlighted in blue, whereas emerging targets are indicated in red. Adapted from Dominguez-Brauer C *et al.*[167]

The temporal and spatial control of mitotic events has to be precisely regulated in order to assure a proper cell division. Almost all eukaryotic proteins are subjected to post-translational modifications during mitosis and cell cycle, being reversible phosphorylation a key event[168]. Dynamic changes in the phosphorylation status of many cell cycle-mediated proteins are coordinated by a network of kinases and their counterbalancing phosphatases, thus controlling molecular and cellular fates.

However, errors in these processes can occur and are the underlying cause of a faulty cell division. To ensure that only healthy cells proliferate, many checkpoints have evolved to induce cell cycle arrest in response to the detection of defects that may have arisen during the different phases of the cell cycle[165]. Thus, it permits defects to be repaired, so that only intact genomes can be transferred to each daughter cell. Processes that prevent the propagation of severely damaged or high-risk cells, such as mitotic catastrophe, senescence or apoptosis, can also be triggered by these checkpoints. The spindle assembly checkpoint (SAC), in particular, is the major cell cycle control mechanism in mitosis. It is responsible for ensuring fidelity of chromosome segregation, via detecting improper chromosome alignment and stopping cell cycle in metaphase. MAD and BUB proteins are activated when defects in microtubule attachment are detected, resulting in Cdc20 (subunit of the anaphase-promoting complex (APC/C)) inhibition and, consequently, prevention of metaphase-anaphase transition[167].

This entire precise network is essential to avoid chaotic cell division and reduce aneuploidy and genomic instability (CIN)[169], which are well-known hallmarks of human cancer and therefore central subjects of cancer research. CIN, defined as a defect that involves loss or rearrangement of chromosomes during cell division, is a common feature of solid tumors. It has been recognized as a source of genetic variation, favoring tumor adaptation to stressful environments as well as cytotoxic anticancer drugs. In cancer research, both numerical (gain or loss of whole chromosomes) and structural (gain or loss of chromosomal fragments) CIN have demonstrated to impact cancer development and therapeutic responses[170].

Because mitosis is a highly regulated process, aberrantly expressed proteins and phosphoproteins can contribute to many pathological conditions and diseases. Specially, M-phase proteins seem to confer an advantage for PCa cells to grow in androgen-depleted conditions[161-163] and, as a consequence, are potential targets for the molecular intervention of CRPC patients. Among the key genes for mitotic progression, kinases appeared to have an important regulatory role. Thus, mitotic kinases have emerged as an attractive therapeutic modality for the treatment of hormone-refractory PCa[171,172].

3.2. Antimitotic agents in clinical practice

Once tumors have progressed to a castration-resistant state, PCa remains a lethal disease. A wide variety of compounds have been tested in the clinic, however, only two groups are currently being used for the treatment of CRPC patients: hormonal therapy, which targets AR signaling, and antimitotic chemotherapeutic agents.

The development of antimitotic drugs for PCa treatment started several years ago when patients with advanced disease were treated with estramustine or vincristine[173]. Anti-microtubules were the first antimitotic agents to be tested and approved for clinical use, since they showed significant survival benefit in certain types of cancer[174,175]. In particular, the microtubule inhibitors docetaxel[133] and cabazitaxel[134] are the only FDA-approved chemotherapeutic agents for the treatment of CRPC patients. Both taxanes act by targeting and stabilizing microtubules, leading to mitotic arrest and finally triggering cell death[176]. Nevertheless, even if they have shown great success in the clinic, resistance and specially toxicity substantially limit their effectiveness. These drugs also disrupt microtubule dynamics in non-dividing cells, where microtubules have structural and transportational functions, resulting in considerable side effects such as neurotoxicity[177]. Therefore, efforts have been focused on the development of inhibitors of alternative mitotic-specific proteins with improved specificity for tumor cells, including kinases (e.g. Polo-like and Aurora kinases) and motor proteins[178].

3.2.1. Targeting motor proteins

Kinesins are a family of motor proteins that carry two major roles in eukaryotic cells: they are crucial for intracellular vesicle and organelle transport, and they are implicated in coordinating different processes in cell division, such as mitosis and cytokinesis. To fulfill their many roles, kinesins use ATP energy to move unidirectionally along microtubule tracks[179].

Targeting the mitotic spindle apparatus leading to disruption of mitosis is a validated approach in cancer treatment. Kinesin spindle protein (KSP) inhibitors specifically target mitotic cells by inhibiting the mitotic kinesin KIF11, a motor protein involved in the assembly and maintenance of the mitotic spindle. Inhibition of KIF11 leads to activation of the spindle checkpoint, mitotic arrest characterized by the monoastral spindle phenotype and subsequent cell death[179].

Unlike microtubules, the spindle proteins targeted by these agents mainly function in mitosis, thus leaving unaffected the majority of non-proliferative cells in the body and avoiding microtubule poisons-related neuropathies. Conceptually, this rationale should render a better therapeutic index[180]. However, healthy rapidly dividing cells are inhibited by these agents too, and major side effects of this treatment modality include neutropenia and thrombocytopenia. But stimulating the bone marrow with the addition of granulocyte colony-stimulating factor (G-CSF) may decrease the severity of these hematological adverse effects. In this context, multiple KSP inhibitors based on distinct chemical scaffolds have been identified (Table 4)[179], but only ispinesib has been tested specifically in PCa patients. Importantly, these inhibitors are highly specific for KIF11, and their specificity is based on a particular long loop L5 region in the motor domain.

Table 4. Kinesin inhibitors in clinical development. Different KSP inhibitors are shown together with the phase and status of the clinical trials in which they are enrolled. Adapted from Rath O *et al.*[179]

Inhibitor	Company	Clinical phase	Status	Number of trials
Ispinesib	Cytokinetics	II	Ongoing	Ongoing: 2. Completed: 14
AZD4877	AstraZeneca	II	Discontinued	Ongoing: 0. Completed: 6
ARRY-520	Array BioPharma	II	Ongoing	Ongoing: 2. Completed: 2
SB-743921	Cytokinetics	I/II	Ongoing	Ongoing: 0. Completed: 2
ARQ 621	ArQule	I	Ongoing	Ongoing: 0. Completed: 1
LY2523355	Kyowa Hakko Kirin/Eli Lily	I	Ongoing	Ongoing: 6. Completed: 1
MK-0731	Merck & Co.	I	Discontinued	Ongoing: 0. Completed: 1
EMD534085	Merck-KGaA	I	Discontinued	Unknown
4SC-205	4SC AG	I	Ongoing	Ongoing: 1. Completed: 0

Ispinesib, a potent inhibitor of the KSP ATPase, is one of the most advanced drugs targeting KIF11 and has entered phase II clinical trials for different cancers with attractive results. In a phase I study combining ipinesib and docetaxel in patients with diagnosed mCRPC, 43% of the mCRPC patients included in the trial showed stable disease[181]. No reponse was observed in a phase II clinical trial in which ispinesib was administered to androgen independent PCa patients who had progressed during or

after docetaxel[182]; nevertheless, immunohistochemistry analysis revealed that most tumors did not have significant KIF11 expression. PCa patients were also included in studies for MK-0731[183] and AZD-4877[184], but neither partial responses nor complete responses were achieved according to response evaluation criteria in solid tumors (RECIST).

Overall, KSP inhibitors have been moderately successful when used as monotherapy. The ability of the kinesin 15 to substitute for KIF11 and replace all its essential functions in bipolar spindle assembly may be one of the potential reasons for the limited antitumor effects observed so far[185,186]. Moreover, the optimal efficacy of KIF11-targeting inhibitors may be as part of combination treatments. Novel compounds are being evaluated and ongoing studies are focused on identifying potential synergistic effects of KSP inhibitors with other already approved agents[173,187,188].

3.2.2. Targeting kinases

Considering that mitotic kinases are mostly expressed in actively dividing cells, targeting these kinases is considered a potentially fruitful approach for cancer management. Agents that inhibit mitotic kinases such as PLK1[189] and Aurora A[190], both of which also play a role in spindle formation, have been developed. The expression of these mitotic kinases seems to be associated with androgen independent PCa growth[191,192], and therefore multiple inhibitors are being tested for the treatment of CRPC[173].

3.2.2.1. Aurora A kinase (AURKA)

Aurora A is a serine/threonine kinase involved in the G_2/M transition and centrosome maturation, thereby playing a role in establishing the bipolar mitotic spindle[193]. It is overexpressed in several tumor types, including breast, pancreatic, bladder and colorectal cancer[167]. In PCa, AURKA has been described as an androgen-regulated AR target gene, and higher expression levels have been associated with AR-positive CRPC[194]. Moreover, AURKA inhibition is a possible strategy for targeting treatment-related androgen independent NEPC. Co-amplification of Aurora A and the transcription factor NMYC has been reported in this type of PCa, thus representing potential targets for the molecular intervention of NEPC patients[103].

Currently, multiple AURKA inhibitors have been tested in clinical trials (Table 5)[173]. Unfortunately, although great promise in preclinical development, these agents have shown poor anticancer activity in the clinic, with few exceptions[195].

Table 5. Aurora A inhibitors in clinical development. Different compound targeting AURKA are shown together with the phase and status of the clinical trials in which they are enrolled. Adapted from Wissing MD *et al.*[173]

Inhibitor	Company	Clinical phase	Status	Number of trials
Danusertib (PHA-739358)	Nerviano Medical Sciences	I/II	Discontinued	Ongoing: 0. Completed: 3
MLN8054	Millennium Pharmaceuticals	I	Discontinued	Ongoing: 0. Completed: 2
Alisertib (MLN8237)	Millennium Pharmaceuticals	I/II/III	Ongoing	Ongoing: 7. Completed: 49
ENMD-2076	CASI Pharmaceuticals	I/II	Discontinued	Ongoing: 0. Completed: 8
Tozasertib (MK-0457/VX-680)	Merck & Co	I	Discontinued	Ongoing: 0. Completed: 2
AT9283	Astex Therapeutics	I/II	Completed	Ongoing: 0. Completed: 5
PF-03814735	Pfizer	I	Discontinued	Ongoing: 0. Completed: 1
AMG-900	Amgen	I	Completed	Ongoing: 0. Completed: 2

MLN8237 (alisertib), a highly specific second-generation AURKA inhibitor that is being studied in a wide range of clinical trials, demonstrated encouraging efficacy in several solid tumors. Treatment with alisertib has shown to induce mitotic arrest and polyploidy, and resulted in apoptosis or senescence[196]. A phase I study conducted with alisertib in solid tumors included mCRPC patients. However, none of them achieved a partial response[197]. The efficacy of alisertib was also assessed in a phase II trial with NEPC patients and, even if the study did not meet its primary endpoint, responders with NMYC and Aurora A overactivity were identified[198]. Nevertheless, a phase I/II trial designed to determine the effect of alisertib when given in combination with abiraterone plus prednisone in men diagnosed with mCRPC failed to show any clear benefit of adding this agent for patients progressing on abiraterone[199].

Similar to what has been observed for KSP inhibitors, new AURKA inhibitors are emerging and efforts are being focused on combination regimens.

3.2.2.2. Polo-like kinase 1 (PLK1)

Polo-like kinase 1 (PLK1), which is the most characterized PLK member, has emerged as a key regulator of essential mitotic events and therefore garnered a lot of attention. It is involved in multiple processes of cell division such as mitotic entry, spindle assembly, chromosome segregation and cytokinesis[200,201].

Likely because PLK1 is intimately involved in DNA damage repair and cell cycle progression, this kinase has been found to be overexpressed in many cancer types, including colorectal, melanoma, breast, NSCLC and bladder, as well as non-Hodgkin lymphoma (NHL) and acute myeloid leukemia (AML)[202]. Some other studies have further suggested a correlation between PLK1 overexpression and poor disease prognosis, leading to the development of anti-PLK therapies for cancer treatment[203].

Interestingly, resistance to several anticancer agents has also been linked to PLK1 overexpression, and PLK1-mediated mitotic events have been found to reduce the efficacy of chemotherapy drugs. In particular, Hou and colleagues[204] demonstrated that PLK1 phosphorylation of Clip-170 is essential for the regulation of microtubule dynamics and microtubule-kinetochore attachment, thus resulting in PCa resistance to taxol. For this reason, PLK1 seems to be a potential target to reduce taxol resistance and, hence, increase its efficacy in cancer management.

It has been shown that PLK1 is a positive regulator of the AR pathway and PLK1 overexpression results in a constitutively active AR signaling, eventually leading to androgen ablation therapies resistance. Accordingly, combining PLK1 inhibition and androgen signaling blockade might be an effective strategy to treat CRPC patients[205,206]. Moreover, PLK1 inhibition has shown promising results in rescuing androgen dependent PCa phenotype and arresting CRPC growth[207].

With all these mechanisms in mind, considerable efforts are underway and several small-molecule inhibitors targeting PLK1 have been intensively investigated and become attractive candidates for anticancer drug development, either as monotherapy or in combination therapies. To date, PLK1 inhibitors can be classified into two main groups: ATP-competitive inhibitors targeting the ATP-pocket of the N-terminal kinase domain and PBD inhibitors targeting the C-terminal polo-box domain (Table 6)[173].

Table 6. PLK1 inhibitors in clinical development. Different PLK1 inhibitors are shown together with the phase and status of the clinical trials in which they are enrolled. Adapted from Wissing MD *et al.*[173]

Inhibitor	Company	Clinical phase	Status	Number of trials
HMN-214	Nippon Shinyaku	I	Discontinued	Ongoing: 0. Completed: 2
BI 2536	Boehringer Ingelheim	I/II	Discontinued	Ongoing: 0. Completed: 11
Volasertib (BI 6727)	Boehringer Ingelheim	I/II/III	Ongoing	Ongoing: 11. Completed: 16
GSK-461364	GSK	I	Discontinued	Ongoing: 0. Completed: 1
NMS-1286937	Nerviano Medical Sciences	I	Discontinued	Ongoing: 0. Completed: 1
TKM-080301	Arbutus Biopharma Corporation	I/II	Completed	Ongoing: 0. Completed: 3
TAK-960	Millennium Pharmaceuticals	I	Discontinued	Ongoing: 0. Completed: 1
Rigosertib (ON 01910.Na)	Oncova Therapeutics	I/II/III	Ongoing	Ongoing: 5. Completed: 28

Overall, pharmacological inhibition of PLK1 results in significant reduction of cell viability, G_2/M phase arrest, mitotic catastrophe and induction of apoptosis in cancer cells[208]. However, minimal or no clinical activity has been reported so far for the majority of PLK1 inhibitors in clinical trials, despite the promising preclinical results in solid tumors and hematopoietic malignancies[209]. Volasertib and rigosertib are the PLK1 inhibitors that have shown more encouraging results, having reached phase III trials.

BI 6727 (volasertib) is an ATP-competitive PLK1 inhibitor that was developed by tailoring the dihydropteridinone structure of BI 2536[210]. In a phase I study in patients with advanced solid cancer, 26 patients (44.1%) showed stable disease[211]. Nevertheless, in a separate phase II clinical trial in patients with metastatic urothelial cancer, antitumor activity was limited as only 14% of the patients achieved a partial response (PR) with a manageable safety profile[212]. It is likely volasertib is effective in only certain cancer types, as it appears to have better outcomes in some tumors than others. Therefore, combination therapies are being actively pursued in clinical trial. In a combination phase II trial, volasertib combined with low dose of the chemotherapeutic drug cytarabine achieved an improved complete response rate (31% versus 13%), improved progression-free survival (PFS) (5.6 months versus 2.3 months) and

improved overall survival (OS) (8.0 months versus 5.2 months) compared to cytarabine monotherapy in AML patients[213]. Its clinical benefit is currently being validated in a phase III trial (POLO-AML-2). Although no PLK1 inhibitor is approved for any tumor treatment yet, volasertib received the FDA BreAKThrough Therapy designation for its activity in combination with cytarabine in AML[214]. Future clinical application will depend on identification of predictive biomarkers of clinical response.

Rigosertib (ON 01910.Na) is a non-ATP-competitive small molecule inhibitor with dual targetability affecting both PLK1 and PI3K[215]. In a phase I study, rigosertib was orally administered to patients with advanced solid malignancies, with an overall response rate of 21.7%[216]. Clinical trials with rigosertib mainly focused on pancreatic cancer and myelodysplastic syndromes (MDS). While treatment combined rigosertib and gemcitabine did not improve survival in pancreatic cancer patients, the response rates in MDS patients were more promising[217]. A phase III clinical trial (INSPIRE) is currently validating the clinical benefit of this treatment.

PBD are unique for PLKs and PBD inhibitors are therefore much more specific than inhibitors targeting the ATP-binding domain, which is found in hundreds of protein kinases and is crucial for kinase activity[218]. In 2008, Reindl and colleagues[219], developed poloxin, a PLK1 inhibitor that was shown to interfere with the function of the PBD. More recently, the optimized analog poloxin-2 was identified with significantly improved potency and selectivity[220]. However, most inhibitors that are currently being tested in clinical trials are directed towards the less specific ATP-binding domain. Combination regimens may be essential in order to combat issues observed with monotherapy and are frequently used in trials in the past years.

3.2.3. Understanding mitotic death

A key question is to learn whether these new antimitotic agents will present clinical efficacy. In order to identify which tumors are most likely to benefit from these treatment modalities, understanding the mechanism of action of these drugs becomes of utmost importance. Following treatment with antimitotic agents, most cells (85%) cannot exit mitosis and ultimately undergo apoptosis, usually in a caspase-dependent proceeding. However, some cells divide unequally to produce aneuploidy daughter cells, and other are able to escape from mitotic arrest by a process known as ‘slippage’. After a prolonged arrest in mitosis, cells can (i) activate cell death

mechanisms and die, (ii) enter a senescent state or (iii) enter a new division cycle and continue proliferating (Fig.13)[221,222]. Two competing and independent networks working in opposite directions determine the cell fate, which is dictated by different thresholds. One network involves the activation of cell death pathways, while the other controls cyclin B1 degradation and thus mitotic exit. If the death threshold is reached first, the cell dies during mitosis; whereas 'mitotic slippage' occurs when cyclin B1 levels fall below the mitotic-exit threshold in the first place[223].

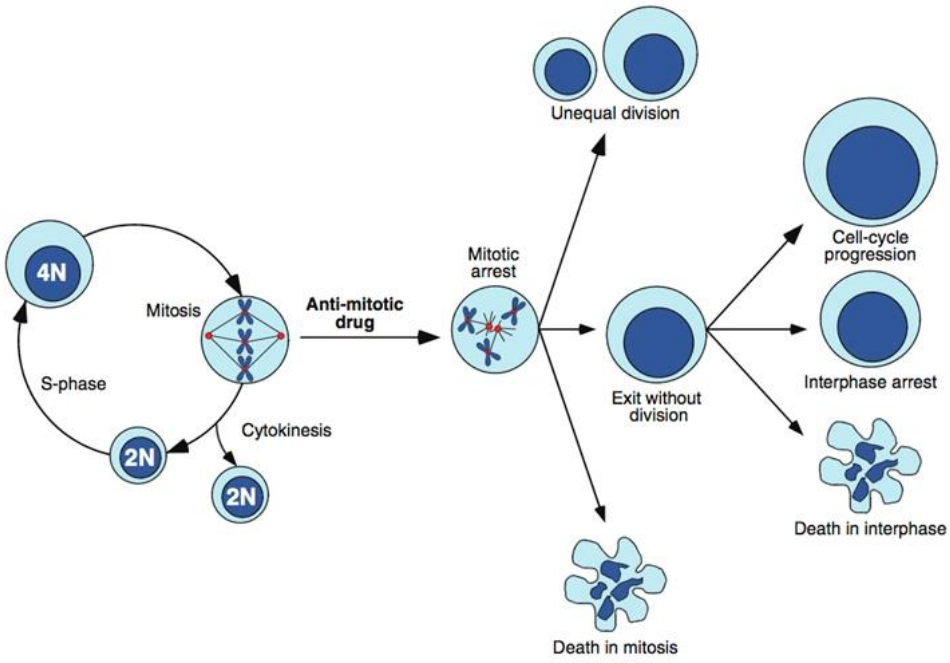

Figure 13. Cell fates in response to antimitotic agents. Adapted from Gascoigne KE *et al.*[221]

Although these findings could explain why mitotic-based therapies are not effective in some tumors, the above-mentioned mechanisms are still poorly understood[223]. Identifying markers that predict individualized tumor response, discovering novel potential targets for the treatment of CRPC patient and improving combination therapies, could also increase the efficacy of these mitotic inhibitors.

4. CLINICAL PROTEOMICS

Despite the essential and well-known functions of mitotic regulators in coordinating cell cycle, only few proteins and substrates have been assigned to specific roles during PCa progression. Understanding the processes that become deregulated during the acquisition of androgen independence is crucial in order to find novel effective therapeutic targets and more personalized treatments.

Genomics and transcriptomics, which are commonly used in the clinic, have delivered major advances in the management of cancer; however, they provide a more static image of the disease. During the last decade, proteomics has emerged as an important tool to study more dynamic molecular entities[224]. While the genome is a rather constant entity, the proteome is constantly changing and relies on cell specific, temporal and environmental specific readouts. Moreover, the proteins represent the actual functional molecules Integration of proteomic findings with other –omics technologies can be used to bridge the gap between genomic information and functional proteins[225,226].

The cellular proteome is a highly dynamic network that is subject to changes in response to various signals[227]. Altered protein expression, aberrant localization and changes in specific protein activities may affect cellular function and are frequently found during disease progression. Thus, identifying those changes can lead to a more comprehensive understanding of the disease.

Proteomics techniques are tremendously useful for measuring protein abundance, analyzing protein interactions and characterizing post-translational modifications (PTMs)[228]. Advances in the field of proteomics have provided the opportunity to study the proteome of virtually any biological specimen. In this context, mass spectrometry (MS)-based quantitative proteomics aims to investigate protein expression changes between different biological conditions, often focusing on a particular subset of proteins. The study of proteomic profiles from cancer patients are expected to identify promising molecular signatures and enable novel molecular insights in the process of carcinogenesis. Since the field of proteomics demonstrated the ability to identify and quantify a large number of proteins and their PTMs, it has been then applied for different clinical purposes, such as the discovery of biomarkers and potential therapeutic targets for drug development[229].

Significant technological advances in the field of MS and its combination with bioinformatics have allowed the introduction of proteomics into the clinic[224], but the impact of clinical proteomics on patient management is still low. Given the potential of MS-based proteomics, there are some limitations that need to be overcome. Although MS techniques are able to detect low-abundance proteins, these proteins are yet difficult to identify when high abundant proteins are present[228]. Furthermore, the disease heterogeneity (e.g. cancer)[230], the complexity of the human proteome and the quality of samples[231] represent a challenge to the proteomics community. Nonetheless, improvements are in progress and MS-based quantitative proteomics is nowadays considered a powerful tool in biomedical research.

Proteomics has been already applied for the study of many cancer types[232,233], and might have a great contribution to the understanding of PCa diagnosis and treatment outcome prediction. An example of this is the use of MS-based proteomics to identify different isoforms of SPOP, a commonly mutated gene in PCa[234]. Moreover, proteomic signature has the ability to establish promising targets for novel treatments, thus achieving a personalized management of patients with PCa. The activity and efficacy of drug candidates can be reported and lead to rational combinations to enhance the behavior of antitumor agents[235]. Eventually, deep profiling of the cellular proteome will provide new insights regarding pathways that become altered during the progression of PCa[236]. Saraon *et al.*[237] and Höti *et al.*[238] already used of state-of-art technologies for the study of mechanisms involved in the transition to androgen independence.

For all these reasons, any proteomic study with the goal of identifying and verifying novel and specific therapeutic targets for the molecular intervention of CRPC patients offers an exciting challenge.

4.1. Mass spectrometry- (MS) based quantitative proteomics

Once PCa has progressed to a castration resistant stage, the disease remains incurable despite the approval of several new treatments. Identification of new biomarkers and potential targets to provide effective stratification of patients and enable personalized medicine, with the aim of maximizing therapeutic responses and minimizing treatment-related toxicities in CRPC patients, is urgently needed.

Given superior analytical features, MS-based quantitative proteomics is well suited for basic research and clinical diagnosis of human diseases. Modern MS allows detailed functional characterization of pathogenic processes by means of accurate and sensitive quantification of proteins and their regulatory modifications[239].

Previously, two-dimensional polyacrylamide gel electrophoresis was applied in clinical practice for discovering disease-associated proteins; however, it is a laborious method, requires large quantities of proteins and is not easily converted into a routine diagnostic test[236]. The development of an MS and bioinformatics-coupled approach has proven to be a fast, cost-efficient and minimally invasive diagnostic tool, thus overcoming many of the above-mentioned limitations. Moreover, improvements in chromatography, ionization, instrumentation and data analysis enable proper quantification by direct measure of the signal produced by specific peptide ions[240].

4.1.1. Stable Isotope Labeling with Amino acids in Cell culture (SILAC)

Stable isotope labeling with amino acids in cell culture (SILAC) is a widely used technique that relies on the metabolic incorporation of isotope-labeled amino acids into growing cells, resulting in peptides of predictable mass difference[239]. It is a simple and powerful approach on MS-based quantitative proteomics, which enables the relative quantification of the proteome of different states. Here, amino acids labeled with 13C and 15N (tipìcally lysine and arginine), also called ‘heavy’ amino acids, are added to a culture media where cells with a specific biological condition are grown. At least five cell doublings are needed until cells reach an incorporation rate over 95%[241].

Due to its robustness, the relative ease of the protocols and the quality of the high data generated, SILAC is becoming increasingly popular within the proteomics community[242]. It minimizes the number of manipulations after cell culture and reduces the differences in labeling efficiency between samples, favoring its adoption for proteomic studies. For all these reasons, this technique is the common choice for accurate quantitative MS.

The most widespread application of SILAC is to characterize global changes in protein expression between two distinct biological samples. Yet, this method is being expanded with great success in other proteomic research areas. It has been applied to investigate dynamic changes of protein post-translational modifications (PTMs), to

identify specific protein-protein interactions (PPIs)[243] and to analyze protein turnover[244], thus providing new knowledge on the regulation of cellular processes, including PCa.

Saraon *et al.*[245] benefited from the expanding field of SILAC to associate the ketogenic pathway with PCa progression. Besides, one of the most comprehensive quantitative proteomic profiling on prostatic tissues was performed by Iglesias-Gato *et al.*[246], who employed SILAC MS-based approach to compare the protein expression between prostate tumors and neighboring nonmalignant tissues.

This method, though, present few disadvantages, namely that only a limited number of conditions can be compared, since the use of 'heavy' amino acids implies a limited number of labeling combinations. In addition, metabolic labeling of whole proteomes requires a population of metabolically competent cells, and therefore it cannot be employed in the analysis of tissues or body fluids. SILAC-based techniques are still under development, but some technologies have emerged to overcome these drawbacks. Spike-in SILAC[247] and super-SILAC[248] allow the comparison of multiple samples and extend the application of SILAC to tissue samples and biological fluids. The development of these techniques supports the introduction of SILAC technology in the clinic and will be very useful for the understanding of many different diseases.

4.1.2. Phosphoproteomics

PTMs play a key role in the regulation of protein function and act as regulatory switches for different signaling pathways[249]. Therefore, analysis and quantitative assessment of these modifications and their dynamic changes can provide valuable information for understanding relevant signaling networks. Protein phosphorylation, the most important and extensively studied PTM, is a central mechanism that reversibly regulates almost all processes in a living cell[250,251].

Protein kinases are major effectors of cellular functions, and deregulation of these signaling pathways has been associated with many types of cancer, including PCa[252]. For instance, hyperactivation of PI3K-AKT and MAPK pathways has been shown to drive PCa development and progression[253]. So kinases have been extensively investigated in cancer research, to explore their role in tumorigenesis and to discover novel therapeutic targets. To date, many small molecule inhibitors are in active clinical development and can be used to target aberrantly expressed kinases, thus emerging as important anticancer drugs[254,255].

Several high-throughput phosphoproteomic approaches have been developed over the last years to identify activated kinases and their downstream substrates across many signaling pathways[256]. Nevertheless, these approaches are not without limitations. More than 500,000 potential phosphorylation sites can be found in the cellular human proteome[257], however, the number of phosphosites that can de detected in a single MS-based experiment usually ranks around 10,000 and 40,000. The upstream kinase is not known for all substrates that can be identified, and only a small portion of the described phosphorylation events can be directly associated with an already characterized function[258]. Moreover, requirement of relatively large amount of samples, high cost and long duration of large-scale experiments are also some disadvantages. All these obstacles need to be overcome before its potential can be realized in routine clinical practice.

Even with these current limitations, phosphoproteomics has tremendous potential to enhance patient stratification and target selection, predict treatment outcomes, and analyze drug resistance pathways to standard therapies (Fig. 14)[259-261].

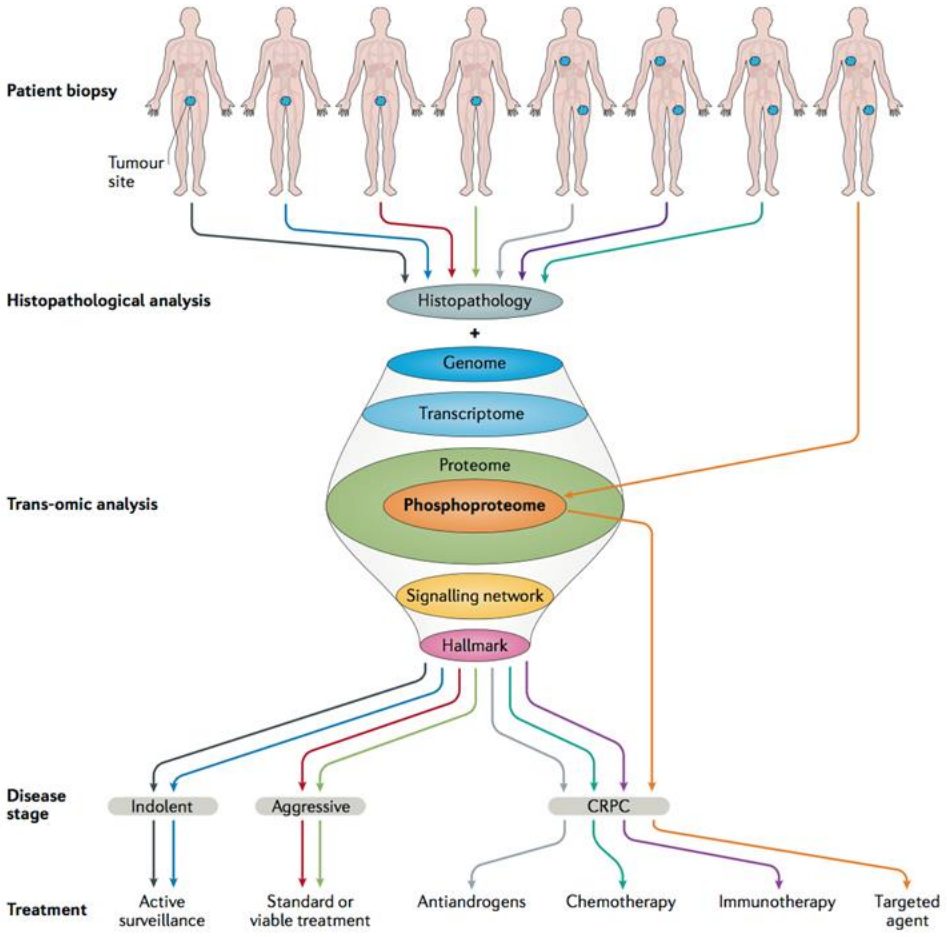

Figure 14. Illustration of phosphoproteomics-centric profiling for personalized management of PCa patients. Clinical samples from men suffering PCa are analyzed by multiple –omics technologies. This approach allows multilevel evaluation of signaling networks deregulation and aid clinicians in deciding the best treatment strategy. Adapted from Yang W *et al.*[260]

It is particularly valuable in identifying aberrantly activated protein kinases that are drivers of PCa progression. For example, Drake *et al.*[262] integrated phosphoproteomics with genomics and transcriptomics data to reveal patient-specific networks in PCa, and pinpointed promising kinases as therapeutic targets in PCa patients. This author also identified distinct tyrosine phosphorylation signature in mCRPC tissues compared to hormone-naïve primary prostate tissues, suggesting that CRPC samples are prime candidates for studying the function of activated kinases driving resistance to hormonal

therapies[263,264]. Accordingly, phosphoproteomic profiling has also been applied to investigate regulators that contribute to CRPC cancer growth[265] or to androgen independent transition[266,267].

Considering that phosphoproteomics can facilitate optimized CRPC management through improved biomarker discovery and targeted therapies, different approaches have been initiated in our laboratory to better study the role of the above-mentioned kinases in the progression of the disease.

HYPOTHESIS AND OBJECTIVES

HYPOTHESIS

PCa is the second most frequently diagnosed invasive malignancy and the 5-year survival rate of men with metastatic disease drops below 30%. Androgens, through the AR, are crucial for the initiation and progression of PCa and thus, ADT has been the mainstay of treatment for locally advanced, metastatic and recurring PCa. Androgen-ablation therapies can initially achieve a biochemical response in the majority of patients; however, remissions are temporary and the disease invariably progresses to an androgen-independent state, also termed CRPC. Upon progression to CRPC, the median survival for those patients is less than 2 years, and the disease is essentially untreatable. The molecular mechanisms that cause this transition remain largely unknown.

Increasing evidence in recent years suggest that androgen insensitive PCa cells have undergone a genetic reprogramming to selectively upregulate the expression of M-phase cell cycle genes. Microtubule-targeting taxanes are already being used in the clinical practice for patients with advanced PCa, but survival remains modest and resistance inevitably develops. Because mitotic progression is a highly regulated process, we hypothesized that aberrantly expressed M-phase proteins may confer PCa cells an advantage to growth in androgen-depleted conditions and consequently represent potential therapeutic targets for the molecular intervention of CRPC patients. Although several small molecule inhibitors of the cell cycle have failed to demonstrate benefit in the clinical setting of CRPC, there remains a keen interest in this approach and significant challenges persist to match patients with effective targeted therapies.

GENERAL OBJECTIVE

In this context, the main goal of this thesis is to gain novel molecular insights into the progression of PCa, with special emphasis on the involvement of mitotic regulators in the acquisition of prostate tumors androgen independence.

SPECIFIC OBJECTIVES

1. **To identify new potential mitotic candidates involved in the transition to androgen independent PCa.** Proteomic analysis of deregulated M-phase

proteins in androgen independent PCa and clinical validation on publically available datasets.

2. **To decipher the role of the kinase PBK in the progression of CRPC.**

   a) **To characterize PBK as a potential therapeutic target for hormone-refractory PCa.** Analysis of PBK expression levels in human PCa samples and correlation with clinical varials, prognosis and response to therapy.

   b) **To provide new insights into the role of PBK as an oncogenic driver of androgen independence in PCa.** Evaluation of the capacity of androgen dependent LNCaP cells stably overexpressing PBK to grow under androgen-depleted conditions.

   c) **To explore the effects of the pharmacological inhibition of PBK *in vitro, ex vivo* and *in vivo*.** Examination of the growth-inhibitory effect of a specific PBK inhibitor in different PCa cells and validation of its antitumor potential in a PCa preclinical mce models.

MATERIALS AND METHODS

1. MATERIALS

1.1. Cell cultures

1.1.1. PCa cell lines

The non-malignant human prostatic normal epithelial RWPE-1 and the human PCa LNCaP, DU145, PC3 and VCaP cell lines were obtained from the American Type Culture Collection (ATCC, Manassas, VA, USA). LNCaP AI cells, an androgen insensitive *in vitro* derivative of the above-mentioned LNCaP cell line, were obtained from Dr. Anna C. Ferrari's laboratory (Icahn School of Medicine at Mount Sinai, NY, USA). Another batch of VCaP cells were a generous gift from Dr. MJ Vicent (Centro de Investigación Príncipe Felipe (CIPF), Valencia, Spain) (Table 7). LNCaP, DU145 and PC3 were grown in RPMI-1640 medium (Biowest, Nuaillé, France) supplemented with 10% (v/v) heat-inactivated fetal bovine serum (FBS) (Biowest, Nuaillé, France). RWPE-1 cells were grown in Keratinocyte Serum Free Medium (K-SFM) (Thermo Fisher Scientific Inc., Walham, MA, USA) supplemented with 0.05 mg/mL bovine pituitary extract (BPE) and 5 ng/mL epidermal growth factor (EGF). LNCaP AI cells were grown in RPMI-1640 medium supplemented with 10% heat-inactivated charcoal (Sigma-Aldrich, San Luis, MO, USA) stripped FBS and 1% insulin-transferrin-selenium (ITS-G) supplement (Life Technologies, Carlsbad, CA, USA). VCaP were grown in DMEM High Glucose (Biowest, Nuaillé, France) supplemented with 10% (v/v) heat-inactivated fetal bovine serum (FBS) (Biowest, Nuaillé, France). All media were supplemented with 2 mM L-glutamine, 1% penicillin-streptomycin solution, 1% MEM non-essential amino acids and 1% sodium pyruvate (Biowest, Nuaillé, France). No penicillin/streptomycin was added in culture media when cells were transfected. All cultures were maintained at 37 ºC in a humidified saturated atmosphere of 95% air and 5% CO2. Cells were amplified and stored at -80 ºC or in liquid nitrogen.

Table 7. General features of the used PCa cell lines.

Cell Line	Site of Origin	Androgen Receptor (AR)	Androgen Sensitivity*	Culture Medium
RWPE1	Normal prostate tissue	+	AD	Keratinocite Serum Free Medim (K-SFM)
LNCaP	Lymph node metastasis	+	AD	RPMI
LNCaP AI	LNCaP subline, derived after prolonged (> 6 months) androgen withdrawal	+	AI	RPMI charcoal stripped FBS
VCaP	Spinal cord metastasis	+	AI/S	DMEM
Du145	Brain metastasis	-	AI	RPMI
PC3	Bone metastasis	-	AI	RPMI

* AD, androgen-dependent: requiered androgens for their growth; AI, androgen-independent: do not need androgen to grow nor have their growth affected by androgens; AI/S androgen-independent/androgen-responsive: androgens are not required for growth but show a growth response in their presence.

1.1.2. Patient-derived prostate primary cultures

The prostate primary culture used in this study was established from tumor cells obtained from biopsies of a PCa patient treated in the Urology Department at the Vall Hebron Hospital (Table 8), and cultured under an optimized protocol (Dr. Rosanna Paciucci's group at VHIR). All samples were obtained under the corresponding informed consent and the supervision of the ethical committee of the Vall Hebron Hospital (CEIC number PR(AG)96/2015). In summary, primary cultured cells were maintained in DMEM-F12 medium (Biowest, Nuaillé, France) supplemented with 7% FBS and containing 2 mM L-glutamine, 1% penicillin-streptomycin solution, 1% MEM non-essential amino acids, 0.6% glucose, 1 mg/mL transferrin, 1 µg/mL putrescine, 0.3 µM sodium selenite, 100 µM hydrocortisone (Sigma-Aldrich, San Luis, MO, USA), 0.25 mg/mL insulin (Life Technologies, Carlsbad, CA, USA). Culture flasks were not manipulated during the first days, since patient-derived cells take usually one week to adhere and disaggregate. After one week, culture medium was changed and adherent cells were grown until 80% confluence. 10 ng/mL FGF, 20 ng/µL EGF (ProSpec-Tany Technogene Ltd, Rejovot, Israel), 200 ng/mL vitamin A and 200 ng/mL vitamin E (Sigma-Aldrich, San Luis, MO, USA) were freshly added every time. Primary culture was maintained at 37 ºC in a saturated atmosphere of 95% air and 5% CO2, amplified

and stored in liquid nitrogen. Cells from 2-6 passages were used for the 3D culture assays.

Table 8. Characteristics of the patient-derived primary cultures used in the study.

#	PSA	Gleason	Metastasis	CRPC
VH01	1106	9 (5+4)	✔	✔

1.2. Human PCa samples

Tissue microarrays (TMAs) previously generated by our group consisted of a total of 146 samples of radical prostatectomy (RP) that were selected from patients with > 7 years of clinical follow up. Patients with and without biochemical recurrence (BCR) were included. BCR is defined as the first post-operative PSA value > 0.4 ng/mL, confirmed by at least one subsequent increasing value (persistent PSA increase) after undetectable post-operative PSA. From each PCa patient, both cancerous and benign peripheral tissues were inspected. Clinical data and outcome information of those patients are detailed in Table 9. For TMA construction, a hematoxylin and eosin (H&E)-stained section was made from each block to define representative tumor regions. Tissue cylinders with 1 mm diameter were then punched from selected tumor areas of each donor tissue block in triplicates and brought into a recipient paraffin block using a custom-made precision instrument (Advanced Tissue Arrayer; Chemicon International Inc., Temecula, CA, USA). Sections (3 µm) of the resulting TMA block were obtained with a Leica RM 2255 microtome (Finesse ME+ #A77500016 microtome; Thermo Fisher Scientific Inc., Walham, MA, USA) and transferred to glass slides. TMAs were stained with different antibodies as described below in this thesis.

Table 9. Tissue microarrays (TMAs) description.

TMAs (FFPE)			
	NO BCR	BCR	BCR-M1
No. of samples	69	56	21
Age (yr)*	64	63	64
Low Grade (GS ≤ 7(3+4))	37	7	1
High Grade (GS ≥ 7(4+3))	32	49	20

* values are represented as mean (range); GS (Gleason Score)

Samples from PCa-naïve patients were obtained from radical prostatectomies (RPs). Formalin-fixed paraffin-embedded (FFPE) tissues from the repository of the Pathology Department of Vall Hebron University Hospital (Barcelona, Spain) were used. Written informed consent was obtained from all patients and samples were coded to ensure simple tracking and confidentially on patient identity. Additionaly, the section of Pathological Anatomy of the Marche Polytechnic University (UNIVPM, Ancona, Italy) proportionated FFPE tissues from CRPC cases. Clinical features of all those patients are summarized in Table 10.

Table 10. Clinico-pathological conditions of patients included in the study.

FFPE Tissues			
	BPH	PCa-naive	CRPC
No. of samples	8	8	8
Age (yr)*	74	63	80
Low Grade (GS ≤ 7(3+4))	-	8	-
High Grade (GS ≥ 7(4+3))	-	-	7**

* values are represented as mean (range); GS (Gleason's Score)

** GS was not available for one CRPC pacient

1.3. Antibodies

The antibodies and conditions employed are listed in Table 11.

Table 11. List of antibodies used for different applications.

Antibodies	Weight (kDa)	Origin	Application	Dilution	Supplier	Reference
CDK1	34	Mouse	WB	1:1,000	Abcam, Cambridge, UK	[A17] ab18
KIF4A	60	Rabbit	WB	1:500	Abcam, Cambridge, UK	ab122227
KIF11	120	Rabbit	WB	1:1,000	Proteintech, Manchester, UK	23333-1-AP
KIF20A	100	Rabbit	WB	1:1,000	*	
ASNS	64	Rabbit	WB	1:1,000	Proteintech, Manchester, UK	14681-1-AP
PBK	40	Rabbit	WB/IHQ	1:1,000/1:50	Cell Signaling Technology, Danvers,	#4942
phospho-PBK (Thr9)	40	Rabbit	WB	1:500	Cell Signaling Technology, Danvers,	#4941
phospho-p44/42 (Erk1/2) (Thr202/Tyr204)	42-44	Rabbit	WB	1:500	Cell Signaling Technology, Danvers,	#9101
PARP	89-116	Rabbit	WB	1:3,000	Cell Signaling Technology, Danvers,	#9542
Cleaved PARP (Asp214)	89	Rabbit	WB	1:500	Cell Signaling Technology, Danvers,	#9541
Caspase 3	17-19, 35	Rabbit	WB	1:1,000	Cell Signaling Technology, Danvers,	#9665
Cleaved Caspase 3 (Asp175)	17-19	Rabbit	WB	1:500	Cell Signaling Technology, Danvers,	#9664
Cyclin B1	58	Mouse	WB	1:1,000	Merck Millipore, Burlington, MA, USA	#05-373
phospho-H3 (Ser10)	17	Rabbit	WB	1:500	Cell Signaling Technology, Danvers,	#9701
GAPDH	38	Rabbit	WB	1:1,000	Sigma-Aldrich, San Luis, MO, USA	G9545
α-Tubulin	52	Mouse	WB	1:5,000	Sigma-Aldrich, San Luis, MO, USA	T9026
Actin	42	Rabbit	WB	1:5,000	Santa Cruz Biotechnology Inc.,	sc-1616
Plk1	66	Mouse	WB	1:1,000	Abcam, Cambridge, UK	ab17057
Aurora A	48	Mouse	WB	1:1,000	BD Biosciences, Franklin Lakes, NJ, USA	610938
FOXM1	84	Rabbit	WB	1:1,000	Abcam, Cambridge, UK	ab180710
CENPF	330	Rabbit	WB	1:500	Abcam, Cambridge, UK	ab5
AR	110	Rabbit	WB	1:1,000	Santa Cruz Biotechnology Inc.,	sc-7305
Anti-rabbit IgG		Goat	WB	1:5,000	Sigma-Aldrich, San Luis, MO, USA	A0545
Anti-mouse IgG		Rabbit	WB	1:5,000	Sigma-Aldrich, San Luis, MO, USA	A9044
P-S6		Rabbit	IHQ	1:600	Cell Signaling Technology, Danvers,	#2211S
p-ERK		Rabbit	IHQ	1:500	Cell Signaling Technology, Danvers,	#4376S
AR		Rabbit	IHQ	1:100	Abcam, Cambridge, UK	ab133273
Ki-67		Rabbit	IHQ	1:100	Novus Biologicals, Centennial, CO, USA	NB600-1252
BIOTINYLATED ANTI-RABBIT IgG (H+L)		Goat	IHQ	1:300	Vector Laboratories, Burlingame, CA, USA	BA-1000

(*) kind gift from Dr. Thomas U. Mayer, Universität Konstanz, Germany

1.4. Bioinformatic tools

1.4.1. DAVID

The Database for Annotation, Visualization and Integrated Discovery (DAVID) (available online, https://david.ncifcrf.gov) was applied to identify the most significant deregulated Gene Ontology (GO) biological processes found in the quantitative proteomics approaches.

1.4.2. In Silico analysis of PCa databases

PCa patient datasets (Table 12) were used to analyze the expression of clinically relevant mitotic candidates with the R2: Genomics Analysis and Visualization Platform (available online, https://hgserver1.amc.nl/cgi-bin/r2/main.cgi) or the GEO2R platform (available online, https://www.ncbi.nlm.nih.gov/geo/geo2r/). Three different analyses were made to evaluate the potential role of M-phase proteins in different stages of the disease.

Table 12. PCa expression datasets employed in this study.

Dataset	No. of samples	Parameter	Reference
GSE35988	122	Benign lozalized Pca and CRPC samples	Grasso CS *et al.* [268]
GSE21034	300	Primary tumor and metastatic samples	Robinson D *et al*.[269]
TCGA	497	Gleason score	Weinsten W *et al.* [270]

2. METHODS

2.1. Cell proliferation assay (crystal violet)

For drug toxicity assays, cells were seeded at specific densities (LNCaP 3 x 10^3 cells/well, LNCaP AI 3.5 x 10^3 cells/well, DU145 2 x 10^3 cells/well and RWPE1 4 x 10^3 cells/well) on 96-well plates. The day after, cells were treated with the corresponding inhibitor (Table 13). At the indicated time points, cells were fixed with 4% formaldehyde (VWR International bvba, Leuven, Belgium) for 20 min at room temperature (RT) and stored in PBS at 4 ºC. At the end of the experiment, cells were stained with 0.5% crystal violet solution (AppliChem GmbH, Darmstadt, Germany) for 15 min, followed by extensive washing with H2O. Crystals were then dissolved with 15% acetic acid (Sigma-Aldrich, San Luis, MO, USA) and optical density was measured by spectrophotometry at 595 nm using an Epoch microplate reader (BioTek Instruments, Winooski, VT, USA).

Table 13. List of compounds employed *in vitro* in this study.

Product	Description	Working concentration	Supplier
HI-TOPK-032	ATP-competitive PBK inhibitor	0.25-20 µM	Sigma-Aldrich, San Luis, MO, USA
Palbociclib (PD-0332991)	CDK4/6 inhibitor	0.5-5 µM	Selleckchem, Houston, TX, USA
Abemaciclib (LY-2835219)	CDK4 and CDK6 inhibitor	0.5-5 µM	Selleckchem, Houston, TX, USA
S-Trityl-L-cysteine (STLC)	Eg5 inhibitor	10 µM	Tocirs Bioscience, Bristol, UK

2.2. Protein extraction and Western blotting

Cells were harvested with homemade 1x RIPA buffer (1.5 M Tris-HCl pH=8.8, 5 M NaCl, Triton X-100, 500 mM EDTA) supplemented with 1x EDTA-free complete protease inhibitor cocktail (Roche Diagnostics GmbH, Mannheim, Germany) and phosphatase inhibitor cocktails 2 and 3 (Sigma-Aldrich, San Luis, MO, USA). Lysis was performed on ice for 1 h incubation with a 30 sec vortex every 15 min. Lysates were

obtained after centrifugation at 12000 x g for 15 min at 4 ºC and incubated for 5 min at 95 ºC in 5x Laemmli Sample buffer (100 M Tris-HCl pH 6.8, 4% SDS, 20% glycerol) for denaturalization. Cell lysates (40-50 µg of total protein) were then resolved on 6-15% sodium dodecyl sulfate polyacrylamide electrophoresis gels (SDS-PAGE) and transferred onto polyvinylidene difluoride (PVDF) membranes (Millipore Corporation, Burlington, MA, USA). Membranes were blocked for 1 h with 5% bovine serum albumin in Tris buffered solution containing 0.1% Tween (TBS-T) and then probed overnight at 4 ºC with the indicated primary antibodies (see Table 11). After being washed three times with TBS-T at RT, membranes were incubated for 1 h with the corresponding horseradish peroxidase (HRP)-conjugated secondary antibodies. Final detection was obtained through chemiluminiscence using ECL Western Blotting System (GE Healthcare, Little Chalfont, UK) following manufacturer's instructions. The expression of α-tubulin and GAPDH was used as an internal standard.

2.3. Cell cycle assay (Fluorescence-Activated Cell Sorting (FACS))

LNCaP and LNCaP AI cells were tripsinized, resuspended in 300 µL PBS and fixed by slowly adding 700 µL of ice-cold absolute EtOH for at least 2 h on ice. Cells were then pelleted at 5000 rpm, washed twice with PBS and resuspended in 1 mL PBS containing 1.14 mM sodium citrate (Sigma-Aldrich, San Luis, MO, USA), 15 µg/mL propidium iodide (PI) (Sigma-Aldrich, San Luis, MO, USA) and 300 µg/mL RNAse A (Panreac AppliChem GmbH, Darmstadt, Germany). Samples were incubated overnight at 4 ºC and analyzed by flow cytometry using FACScalibur (BD Biosciences, Franklin Lakes, NJ, USA) and data by BS CellQuestTM Pro software. A minimum of 10,000 events was taken for each analysis. Data were represented using FCS Express by De Novo software (BD Biosciences, Franklin Lakes, NJ, USA).

2.4. High-thoughput quantitative proteomics

2.4.1. Stable isotope labeling by amino acids in cell culture (SILAC) and synchronization

The SILAC workflow comprises mainly two phases: an adaptation phase and an experimental phase. During the adaptation phase, cells are grown in the 'heavy' and

'light' media until a complete labeling with the 'heavy' amino acids has been achieved. The degree of labeling is evaluated at peptide level. As the two cell populations are harvested under the same conditions and exhibit identical biochemical properties, they are only distinguishable by MS due to their residue-specific mass difference. In the experimental phase, and after full incorporation has been confirmed, equal amounts of labeled and unlabeled cells are mixed prior to subsequent cell lysis, protein extraction and digestion. Peptides are then analyzed using liquid chromatography (LC) coupled to mass spectrometry (MS) (LC-MS), since it has emerged as the most effective method for studying complex proteomes with high sensitivity[271]. After obtaining high-quality MS raw data, database search softwares are applied for the peptide identification and quantification. Given that the corresponding isotope-labeled and unlabeled peptides from the same protein will coelute during reverse-phase chromatography, relative abundance of each protein can be quantified by the ratio between the MS signal intensity of the 'heavy' and 'light' peptides (H/L ratio)[272]. At present, MaxQuant is by far the most widely used software for the analysis of SILAC, as it is especially designed for high-resolution MS quantitative data[273,274]. The obtained protein list is finally converted into relevant results and biological insights by means of annotation databases or bioinformatics tools, such as KEGG, STRING or DAVID[275].

LNCaP and LNCaP AI cells were seeded into 150 mm-dishes and SILAC media were prepared from customized RPMI-1640 lacking two essential amino acids: L-arginine and L-lysine (Silantes GmbH, Munich, Germany). Heavy amino acids, L-Arg^{10} (HCl, 13C 15N labeled) and L-Lys^{8} (HCl, 13C 15N labeled) (Silantes, GmbH, Munich, Germany) were supplemented to the medium to obtain the 'heavy' medium, whereas L-Arginine and L-Lysine (Sigma-Aldrich, San Luis, MO, USA) were added to generate the control or 'light' medium. Both media were further supplemented with 2mM L-glutamine (Silantes, GmbH, Munich, Germany) and 1% penicillin-streptomycin. Additionally, the light medium was supplemented with dialyzed FBS (Silantes, GmbH, Munich, Germany) and the heavy medium with dialyzed charcoal-stripped FBS and insulin. LNCaP cells were metabolically labeled with light conditioned medium and LNCaP AI cells were labeled with heavy medium. Fresh medium was replaced every 2-3 days and cells were cultured for approximately 5 doublings to achieve complete labeling of cellular proteins. (Fig. 15).

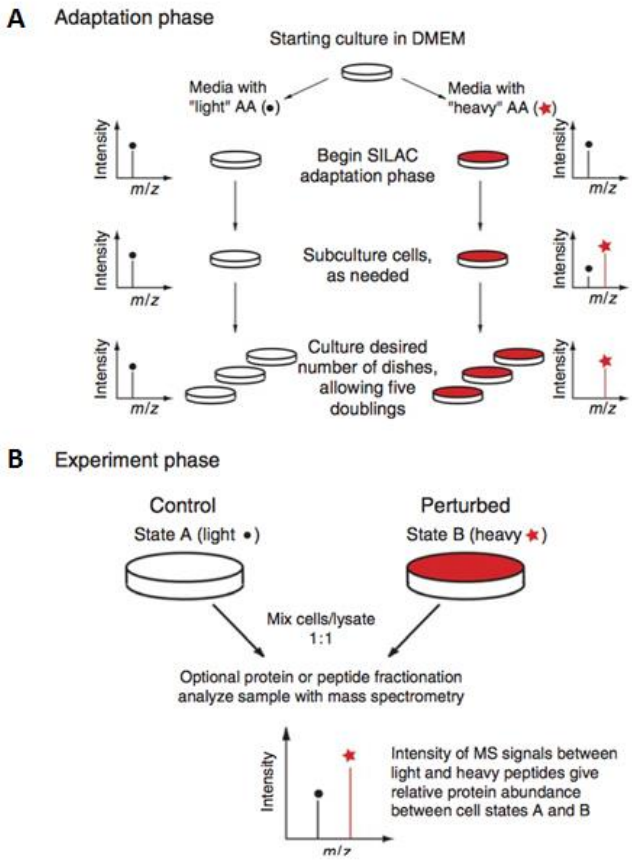

Figure 15. Overview of SILAC protocol. The SILAC technique consists of two different phases – an adaptation (A) and an experimental (B) phase. A) Cells are grown in 'light' and 'heavy' culture media until cells have fully incorporated the 'heavy' amino acids (red star). This allows the two cell pools to be distinguishable by MS due to their mass diference. B) The two cell populations are mixed in equal amounts and proteins are extracted. The sample is further digested to peptides and analyzed by MS for protein identification and quantification. Adapted from Ong SE *et al.*[271]

Once assured that cells were correctly labeled (incorporation rate >95%), both cell lines were synchronized in G1/S phase by a single 2 mM thymidine arrest (20-24 h) and then released into fresh medium to later accumulate cells in mitosis by addition of 10 μM S-trityl-L-cysteine (STLC) (Tocris Bioscience, Bristol, UK). Three independent biological replicates for both LNCaP and LNCaP AI cell lines were used. After 16 h, cells were trypsinized, washed twice with PBS and mixed in a 1:1 ratio. Cells were then centrifuged at 1200 rpm for 5 min and cell pellets were kept at -80 ºC until further processing.

2.4.2. Mass Spectrometry (LC-MS/MS)

Cells were trypsinized, lysed with 6 M Urea in 0.1 M Ammonium bicarbonate and subsequently sonicated four times for 5 s. Total protein concentration was determined by means of BSA Kit and cell lysates were mixed in a 1:1 ratio to obtain a total of 2 mg total protein in each replicate (Fig. 15).

Protein extracts were dissolved in 6 M urea, 0.2 M NH4HCO3, reduced with dithiothreitol (DTT, 10mM, 37 ºC, 60 min), alkylated with iodoacetamide (IAM, 20mM, 25 ºC, 30 min) and digested overnight with LysC 1:10 ratio (w:w; enzyme:substrate) at 37 ºC overnight followed by trypsin 1:10 ratio (w:w; enzyme:substrate) at 37 ºC for 8 h. Tryptic peptide mixtures were desalted using a C18 Hypersep columns (Thermo Fisher Scientific Inc., Walham, MA, USA).

2µg of each sample was analyzed by LCMSMS using an Orbitrap Fusion Lumos with an EASY-Spray nanosource coupled to a nano-UPLC system (EASY-nanoLC 1000 liquid chromatograph) equipped with a reverse-phase chromatography 25-cm column with an inner diameter of 75 µm, packed with 1.9 µm C18 particles (Nikkyo Technos Co., Ltd., Japan). Chromatographic gradients started at 7% buffer B with a flow rate of 250 nL/min and gradually increased to 35% in 120 minutes. After each run, the column was washed for 15 min with 90% buffer B (Buffer A: 0.1% formic acid in water. Buffer B: 0.1% formic acid in acetonitrile). The mass spectrometer was operated in data-dependent acquisition mode, with full MS scans over a mass range of m/z 350–1500 with detection in the Orbitrap (120K resolution) and with auto gain control (AGC) set to 100,000. In each cycle of data-dependent acquisition analysis, following each survey scan, the most intense ions above a threshold ion count of 10,000 were selected for fragmentation with HCD at normalized collision energy of 28%. The number of selected precursor ions for fragmentation was determined by the “Top Speed” acquisition algorithm (maximum cycle time of 3 seconds), and a dynamic exclusion of 60 s was set. Fragment ion spectra were acquired in the ion trap with an AGC of 4,000 and a maximum injection time of 300 ms.

2.4.2.1. Data analysis

Acquired data was analyzed using MaxQuant v1.6.0.16 for peptide identification and quantification. Raw data was searched with Andromeda against SwissProt Human database (as in April 2018, 20501 entries) with the most common contaminants as

defined in MaxQuant. A precursor ion mass tolerance of 4.5 ppm at the MS1 level was used, and up to three miscleavages for trypsin were allowed. The fragment ion mass tolerance was set to 0.5 Da. Oxidation of methionine, protein acetylation at the N-terminal, and heavy labels Lys^8 (13C6, 15N2-Lys; +8.014 Da) and Arg10 (13C6, 15N4-Arg; +10.008 Da) were defined as variable modifications, whereas carbamidomethylation on cysteines was set as a fix modification. The identified peptides were filtered using a false discovery rate (FDR) < 5%. Proteins relative abundances were using normalized heavy-to-light ratios at logarithmic scale (log2) with Perseus v1.6.2.1. One-way ANOVA was performed to assess for statistical significance and proteins with a q-value < 0.05 were considered differentially abundant.

The mass spectrometry proteomics data have been deposited to the ProteomeXchange Consortium via the PRIDE[276] partner repository with the dataset identifier PXD011393.

2.5. Immunohistochemistry

2.5.1. Human PCa tissues

First, slides were incubated overnight at 55 ºC, de-paraffinized with xylene and subsequently re-hydrated through graded alcohol rinses. To detect PBK protein expression, citrate buffer pH 9 was used for heat-induced antigen retrieval. Slides were then incubated with PBK primary antibody (listed in Table 11) for 1 h at RT, followed by a second incubation with the appropriate horseradish peroxidase (HRP)-conjugated secondary antibody complex (Envision+ poly-HRP system; DAKO Cytomation, Glostrup, Denmark). Color development was achieved using diaminobenzidine (DAB) chromogen, and slides were counterstained with H&E. The staining of the sections was evaluated by our reference pathologist and a histoscore was calculated based on the percentage of stained cells and the intensity of the staining.

2.5.2. Mice tissues

Slides were incubated overnight at 55 ºC, de-paraffinized with xylene and subsequently re-hydrated through graded alcohol rinses. Antigen retrieval was performed using a citrate-based Vector® Antigen Unmasking Solution (Vector Laboratories, Burlingame, CA, USA). The corresponding primary antibodies (see Table 11) were then incubated

overnight in a humid chamber at 4 ºC. The day after, slides were incubated with a biotinylated anti-rabbit IgG for 1 h at RT, and color development was achieved using Vector® NovaRED™ Peroxidase (HRP) Substrate Kit (Vector Laboratories, Burlingame, CA, USA). Slides were then counterstained with H&E and staining was finally evaluated attending the help of a pathologist. Based on the nuclear staining, Ki67 positive cells were and quantified counted using the ImageJ software.

2.6. Viability assay in 3D culture from patient-derived cells

For spheroid viability assays, primary cultured cells derived from a patient biopsy were seeded at 20 x 10^3 cells/well in triplicates in non-adherent 6-well plates (Corning Inc., Corning, NY, USA) (coated with 0.5% agar solution in non-supplemented medium) in serum-free DMEM-F12 medium (Biowest, Nuaillé, France) containing all the above-mentioned supplements plus 10 ng/mL FGF, 20 ng/µL EGF (ProSpec-Tany Technogene Ltd, Rejovot, Israel) and 0.4% B27 (Invitrogen, Carlsbad, CA, USA). Patient-derived cells of PCa were grown in anchorage independent conditions. After 24 h, spheroids were treated with increasing concentrations of HI-TOPK-032 inhibitor, and CellTiter 96® AQueous Non-Radioactive Cell Prolifetation Assay (MTS) (Promega, Madison, WI, USA) was used to evaluate surviving cells 72 h after treatment. Tumor spheres were washed with 1X PBS, disaggregated with 0.5 mL 1X StemPro® Accutase® (Thermo Fisher Scientific Inc., Walham, MA, USA) and reseeded in p96-well plates. PMS:MTS (1:20) mixture was then added 1:10 to each well, plates were incubated for 2-4 h and absorbance was measured at 490 nm.

2.7. Plasmids, lentivirus production and transduction

Four different TRIPZ inducible lentiviral shRNA constructs (Table 14) targeting PBK were purchased from Dharmacon (GE Healthcare Dharmacon Inc., Lafayette, CO, USA). Packaging vectors pMD2G and psPAX2 were obtained from Addgene (Watertwon, MA, USA). To prepare PBK viral particles, lentiviral expression vectors and packaging vectors were transfected into HEK-293T cells using Oligofectamine® 2000 (Thermo Fisher Scientific Inc., Walham, MA, USA) following the manufacturer's instructions. Medium was changed 6 h after transfection and HEK-293T cells were cultured for further 48 h. Viral particles were harvested by filtration using a 0.45 µm

syringe filter, then combined with 8 µg/mL polybrene (Millipore, Burlington, MA, USA) and infected into LNCaP and LNCaP AI cells.

PBK in pDONR221 was obtained from Harvard PlasmID Database (Table 14) and transferred into pINDUCER20 (Addgene, Watertown, MA, USA) using LR Clonase II (Invitrogen, Carlsbad, CA, USA) (Fig. 16). pINDUCER20-PBK was infected into LNCaP cells by using the protocol mentioned above, and selection was performed using 400 µg/mL. Cell culture medium was replaced with fresh growth medium after 24 h and stably transduced cells were used for functional assays.

Table 14. Plasmids and vectors used in this study.

Vectors	Function	Supplier	Sequence
pTRIPZ-PBK#4	Tet-inducible lentiviral vector for human PBK shRNA	Dharmacon, GE Healthcare ID Clone V2THS_175901	5'-TAATGTTACAGTTTACAGC-3'
pTRIPZ-PBK#2	Tet-inducible lentiviral vector for human PBK shRNA	Dharmacon, GE Healthcare ID Clone V3THS_409420	5'-AAAACTTTACAGAAAACCC-3'
pTRIPZ-PBK#3	Tet-inducible lentiviral vector for human PBK shRNA	Dharmacon, GE Healthcare ID Clone V3THS_409421	5'-AGAGTCTAATAACTACTGA-3'
pTRIPZ-PBK#1	Tet-inducible lentiviral vector for human PBK shRNA	Dharmacon, GE Healthcare ID Clone V3THS_366222	5'-CTTTTGATACACACTTCGA-3'
psPAX2	2nd generation lentiviral packaging plasmid	Addgene plasmid #12260	--
pMD2.G	2nd generation lentiviral envelope plasmid	Addgene plasmid #12259	--
pDONR221 PBK	Coding sequence of human PBK cloned	Harvard PlasmID Database	--
pINDUCER20	Tet-inducible lentiviral vector for ORF expression	Addgene plasmid #44012	--
pINDUCER20-PBK	Tet-inducible lentiviral vector for PBK expression	--	--

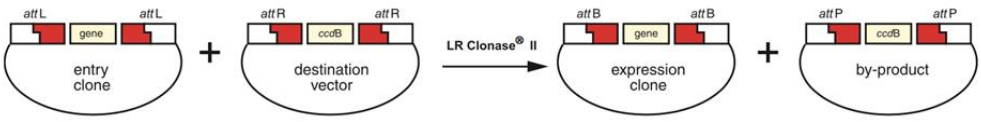

Figure 16. Gateway™ cloning system: LR Reaction. LR reaction facilitates recombination of an attL substrate (entry clone) with an attR susbtrate (destination vector) to create an attB-containing expression clone, with all the components necessary for gene expression. This reaction is catalyzed by the LR Clonase II enzyme mix.

2.8. Cell proliferation assay (cell counting)

Proliferation was analyzed by cell counting. LNCaP and LNCaP AI cell lines stably expressing PBK shRNA were seeded at 80,000 cells into 35 mm-dishes with or without 1 µg/mL doxyxycline (Sigma-Aldrich, San Luis, MO, USA). Both LNCaP cells stably expressing pINDUCER20-PBK was seeded at 100,000 cells into p6-well plates, with or without 0.5 µg/mL doxyxycline, and using RPMI-1640 medium containing 10% heat-inactivated FBS or 10% heat-inactivated charcoal stripped FBS. After trypsinization, viable cells were counted on a Neubauer chamber and reseeded at days 6, 9 and 12 into 100 mm and 150 mm-dishes, respectively.

2.9. Preclinical PCa mice models

2.9.1. Genetically Engineered Mouse (GEM) Xenograft

Animal experiments were carried out in collaboration with the group of Dr. Alvaro Aytes at the IDIBELL Animal Facility (Institut d'Investigació Biomèdica de Bellvitge, Barcelona, Spain) and projects were approved by the Comité Ètic d'Experimentació Animal (CEEA-IDIBELL).

Athymic nude mice were obtained from Envigo (ENVIGO+, Huntingdon, UK) and castrated in the animal facility. After bilateral orchiectomy, 3 M NPp53 (PTEN and TP53 null) mice cell lines (rationale described on Aytes *et al.*[277]) were subcutaneously injected into each mouse using 1X PBS and Matrigel (1:1). Once tumors became palpable, mice were randomized into four experimental groups: (i) vehicle (N = 6), (ii) enzalutamide (N = 6), (iii) HI-TOPK-032 (N = 7) or (iv) combination therapy with enzalutamide and HI-TOPK-032 (N = 7). Enzalutamide was administrated orally at a concentration of 10 mg/kg, while HI-TOPK-032 was administrated intraperitoneally at a

dose of 10 mg/kg 3 times/week. Animals were distributed in cages (5 mice/cage) and weighted every time before treatment. Tumors were measured every 2-3 days using an electronic caliper and volumes were estimated with the formula [Volume = (*Width*)^2 x *Length*/2], where *W* means the shortest and *L* the longest radius of the tumor (mm). When tumor volumes approximately exceeded 2000 mm^3, mice were euthanized and tumors were removed and weighted. After longitudinally split into smaller pieces, tumors where fixed with formalin and snap frozen in liquid nitrogen and stored for further proceeding.

2.9.2. Orthotopic mice model

Animal experiments were carried out in collaboration with the group of Dr. MJ Vicent at the CIPF Animal Facility (Centro de Investigacion Principe Felipe). VCaP cells were orthotopically injected into each mouse following MJ Vicent´s internal lab protocol. Mice were randomized into two experimental groups: (i) vehicle (N = 6) and (ii) HI-TOPK-032 (N = 6). HI-TOPK-032 was administered intraperitoneally at a dose of 10 mg/kg 3 times/week during 5 weeks. Tumor measurements were determined by luminescence. After 37 days, mice were euthanized and tumors were removed and weighted.

2.10. Statistical analysis

Experimental sample size for *in vivo* experiments was chosen following the criteria of the Institut d'Investigació Biomèdica de Bellvitge (IDIBELL). Unless otherwise stated, mean ± SEM values are representative of the average of three independent experiments. Statistical significance was determined by two-side unpaired Student's t-test or ANOVA Turkey's test (GraphPad Prism Software, La Jolla, CA, USA). * means $p < 0.05$, ** means $p < 0.01$ and *** means $p < 0.001$. Unpaired nonparametric Mann-Whitney test (GraphPad Prism Software, La Jolla, CA, USA) was used for comparisons between groups when analyzing human prostate tissues.

RESULTS

1. Key mitotic regulators are involved in the acquisition of androgen independent PCa

1.1. Characterization of the LNCaP AI cell line as a model for androgen independent PCa and castration-resistant disease

In order to gain molecular insights into the transition to androgen independence in PCa, the LNCaP human progression model was first characterized.

LNCaP is a well-known androgen dependent PCa cell line that is widely used to explore mechanisms involved in the development and progression of the PCa. Several research groups have established an androgen independent (AI) LNCaP cell line by maintaining LNCaP cells in androgen-depleted conditions during several passages. Among them, we have used the *in vitro* model generated by Gao *et al*.[278] for our study.

Subjecting a hormone dependent PCa cell line to chronic androgen deprivation for 6 months, Gao and colleagues achieved an AI derivative of LNCaP that resembled the phenotype of an advanced recurrent PCa after progression on hormonal ablation therapy. LNCaP AI cells continued to proliferate following a long-term exposure to androgen-poor conditions, while LNCaP cells remained incapable of sustained growth in the absence of hormones[278]. In their work, they also observed that androgen independent cells lost the expression of PSA and cytokeratin 8 (CK8), two well-known prostate differentiation markers[279]. All these changes have already been described in hormone-refractory PCa, suggesting that the *in vitro*-derived cell line represents a good model for the study of a castration-resistant state.

LNCaP and its androgen independent counterpart, LNCaP AI, were then grown in both androgen and androgen-depleted conditions for 7 days, and proliferation rates were evaluated in order to assess their androgen sensitivity in our hands (Fig. 17).

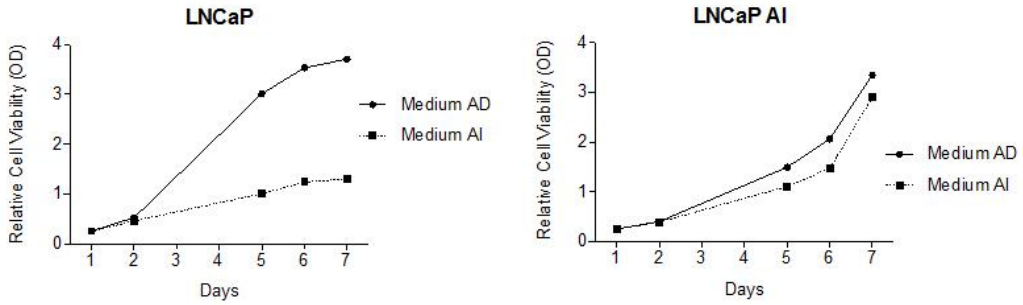

Figure 17. Cell growth of LNCaP and LNCaP AI PCa cells. A) LNCaP and **B)** LNCaP AI cell line were cultured with full media (medium AD, 10% FBS) or with androgen-depleted media (medium AI, charcoal stripped FBS). Cell growth was determined over 7 days by crystal violet assay. Results from N = 3 independent experiments are shown (mean ± SEM). AD: androgen dependent, AI: androgen independent.

As expected, androgen dependent LNCaP cells showed a significant decrease in proliferation when cultured under androgen deprivation conditions, whereas LNCaP AI cells exhibited almost identical proliferative properties when grown in either the presence or absence of androgens (Fig. 17). With these results, we were able to confirm that the LNCaP AI cell line is not dependent on androgens for growth, thus validating the model for the study of androgen independent PCa and hence castration-resistant disease. In addition, we observed that the LNCaP AI cell line presented slower growing rates compared to the androgen dependent one. This behavior was already demonstrated in previous studies[208], increasing the robustness of our work.

We also checked AR protein levels in both LNCaP and LNCaP AI cell lines (Fig. 18). Not surprisingly, we found that AR expression was significantly higher in LNCaP AI cells. Our finding supports the results obtained in other reports[278,280,281] and underscores the value of the model, since AR overexpression is one of the main characteristics of CRPC.

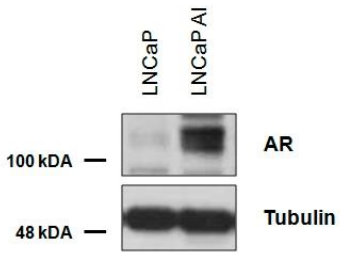

Figure 18. Protein expression levels of AR in LNCaP and LNCaP AI cells. Upregulation of AR in the androgen independent PCa cell line.

As a poof-of-concept, we further tested the levels of the master regulator kinases that are involved in the M-phase of the cell cycle and have been already associated with androgen independent PCa growth (Fig. 19). Higher protein levels of PLK1, Aurora A and CDK1 were observed in the LNCaP AI cell line. All of them are targetable candidates and its overexpression has been correlated with disease progression, highlighting the potential role of mitotic regulators as molecular drivers of hormone-refractory PCa.

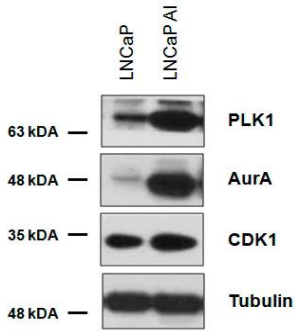

Figure 19. Protein expression levels of key regulators involved in the progression of PCa. Mitotic kinases are overexpressed in LNCaP AI cells compared to LNCaP cells.

Collectively, these results suggested that the LNCaP AI cell line is a valid model for studying androgen independence and the involvement of mitotic candidates in the progression of the disease, since it mimics the clinical scenario of castration-resistant PCa.

Once the validity of the model was confirmed, we moved towards our aim of finding

novel treatments for this letal stage of the disease. Considering that aberrant expression of mitotic proteins may have a key role in the acquisition of androgen independence in PCa, we decided to focus on the study of different cell-cycle inhibitors. We previously observed that androgen independent LNCaP cells are highly resistant to growth inhibition by well-established antimitotic agents (data not shown), and therefore novel cell-cycle targets are needed. In this regard, previous studies reported that CDK4/6 inhibitors have a significant antiproliferative activity in hormone receptor-positive cells, especially in estrogen receptor-positive (ER+) breast cancer cells[282,283]. With the same rationale and considering that deregulation of the CDK/RB-axis has been associated with tumorigenesis in many human cancers, including CRPC[153,154], the effect of palbociblib[284] and abemaciclib (LY-2835219)[285] was evaluated in both androgen dependent and independent LNCaP cells. As indicated in Figure 20, the LNCaP cell line was inhibited in a dose-dependent manner with a half-maximal inhibitory concentration (IC50) around 0.75 μM in both cases, while the LNCaP AI cell line was essentially not sensitive to low doses of CDK4/6 inhibitors.

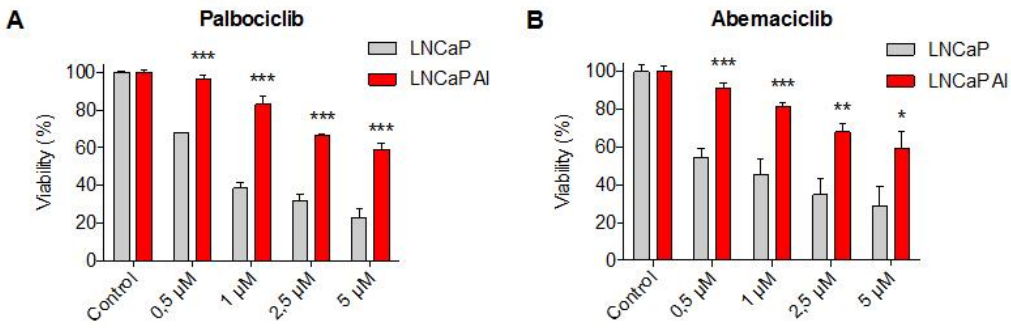

Figure 20. LNCaP and LNCaP AI differential response to CDK4/6 inhibitors. Cells were treated with increasing concentrations of **A)** palbocilib (PD-0332991) and **B)** abemaciclib (LY-2835219) for 72 h. Crystal violet data were represented as mean ± SEM. Similar results were obtained in N = 3 experiments.

These results indicate that androgen independent LNCaP cells are highly resistant to growth inhibition, confirming the work of Gao *et al*.[278] and Wang *et al*.[281], in which a partial resistance to apoptosis via overexpression of Bcl-2 was described. Given this feature, an association between LNCaP AI cells and treatment failure can be

established, making an urgent need to identify specific treatments for AI cells.

Since we were interested in the role of G_2/M regulators and mitotic kinases seem to be crucial for the progression of PCa, M-phase proteins were considered attractive treatment modalities for CRPC patients.

1.2. Quantitative proteomics unveils differentially expressed proteins between androgen dependent and independent LNCaP cells

To date, inhibitors of the M-phase cell cycle have demonstrated limited efficacy in the clinical practice in PCa and, therefore, novel strategies are needed.

In order to explore other potential mitotic regulators that might play a role in the transition to androgen independent PCa, we performed a global proteomic analysis to detect differential protein expression between androgen dependent and androgen independent LNCaP cells using SILAC in combination with shotgun mass spectrometry analysis (LC-MS/MS). Using this approach and considering that proteins are the functional molecules in the cell, we expected to identify drivers of the castration-resistant disease. To the best of our knowledge, this is the first proteomic approach studying the specific role of M-phase regulators in the transition to androgen independent PCa.

Each cell line was grown in distinct amino acid isotopic media (Fig. 21A) and both were arrested in G_2/M phase, as described in the material and methods section (Fig. 21B). Similar cell cycle arrest phenotypes were achieved using STLC, a kinesin-related motor KIF11 inhibitor, used as control. KIF11 inhibition has proven to arrest cells in prometaphase with a monoastral microtubule array, without affecting the localization and activity of other kinases[286,287]. The accumulation of cells in the second peak (G_2/M peak) detected by flow cytometry (Fig. 21C), as well as the increase of cyclin B1 and p-histone H3 protein levels (Fig. 21D), two well-known mitotic markers, demonstrated that cells were correctly arrested in mitosis. Once assured that LNCaP and LNCaP AI cells were arrested in M-phase, we collected mitotic cells from both cell lines and mixed the protein extracts 1:1 prior digestion and mass spectrometry analysis. This process was performed in three independent replicates. Next, using the MaxQuant software we were able to identify 11817 peptides and 2871 protein groups with at least

one unique peptide (FDR<5%). In addition, based on the peptide H/L ratios, protein fold-changes (FC) were calculated and statistical inference was performed to assess the differential protein abundance between LNCaP AI cells (grown in heavy media) and LNCaP cells (grown in light media). The high correlation between the three replicates was an indicator of robustness in our study (Fig. 21E). A total of 497 proteins exhibited significantly altered abundance between the two PCa cell lines (FDR < 0.05) with 198 and 299 proteins found to be up- and downregulated, respectively, in LNCaP androgen independent compared to LNCaP androgen dependent cells (see Annexes). Quality controls of the triplicates are described on the Annexes.

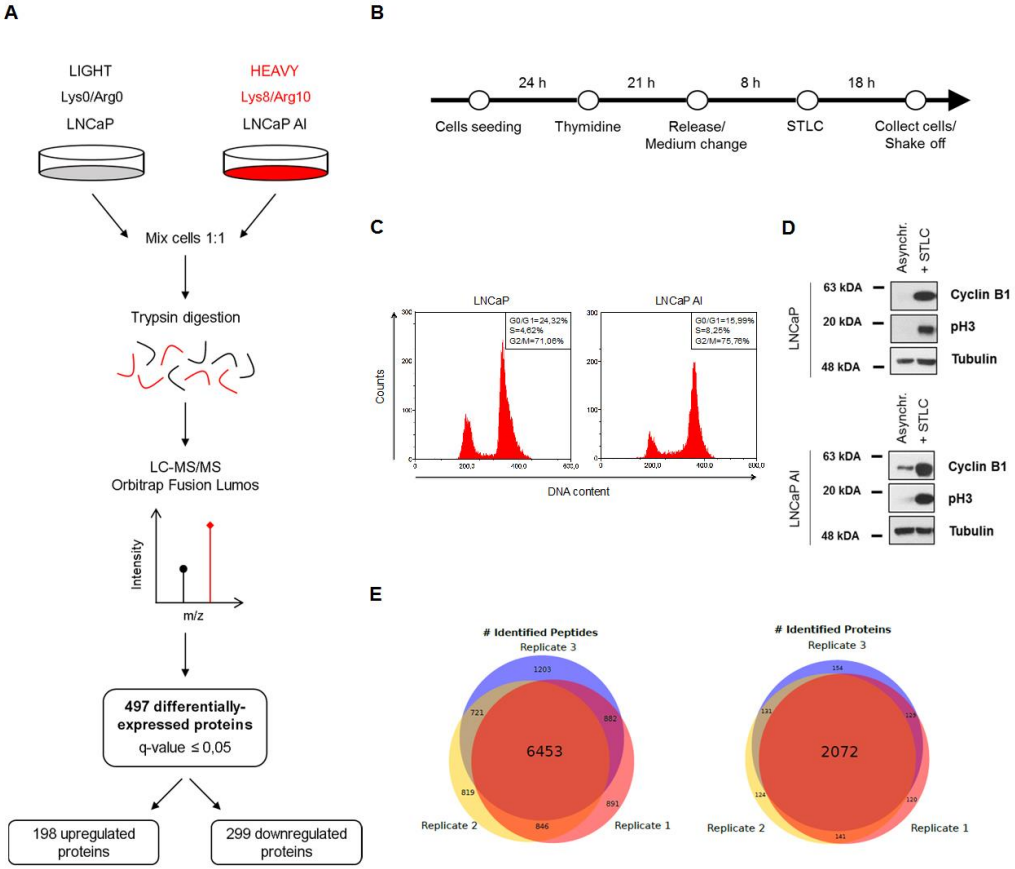

Figure 21. SILAC-based quantitative proteomic profiling of prostate cancer transition to androgen independence. A) Flow scheme summarizing the steps involved in the proteomic analysis of androgen dependent LNCaP (labeled with Lys0/arg0) and androgen indepedent (AI) LNCaP (labeled with Lys^8/Arg^{10}) cells. **B)** Timeline for the generation of highly homogenous mitotic cells. **C)** Flow cytometry analysis of PCa cell lines after mitotic arrest. **D)** Western blotting showing G_2/M phase protein levels in asynchronous and mitotic-arrested LNCaP cells. **E)** Overlap of identified proteins and peptides among the three independent replicates.

To further prioritize the list of protein candidates, different stringent criteria were applied. Since key mitotic regulators are overexpressed in CRPC patients, we decided to focus on the proteins that were found to be upregulated in androgen independent cells. We obtained a final data set of 60 proteins, consisting of the proteins that resulted highly overexpressed in the LNCaP AI cell line, with a Fold Change (FC) > 2 (Fig. 22A). Taken a look to the list, we identified proteins that were previously evaluated in the context of PCa progression, including CDK1[288], KPNA2[289], PCNA[290] and PRDX1[291], thus confirming the robustness of our proteomic approach. With the aim of finding novel potential targets, we investigated the main molecular pathways that appeared to be significantly involved in the transition to androgen independence.

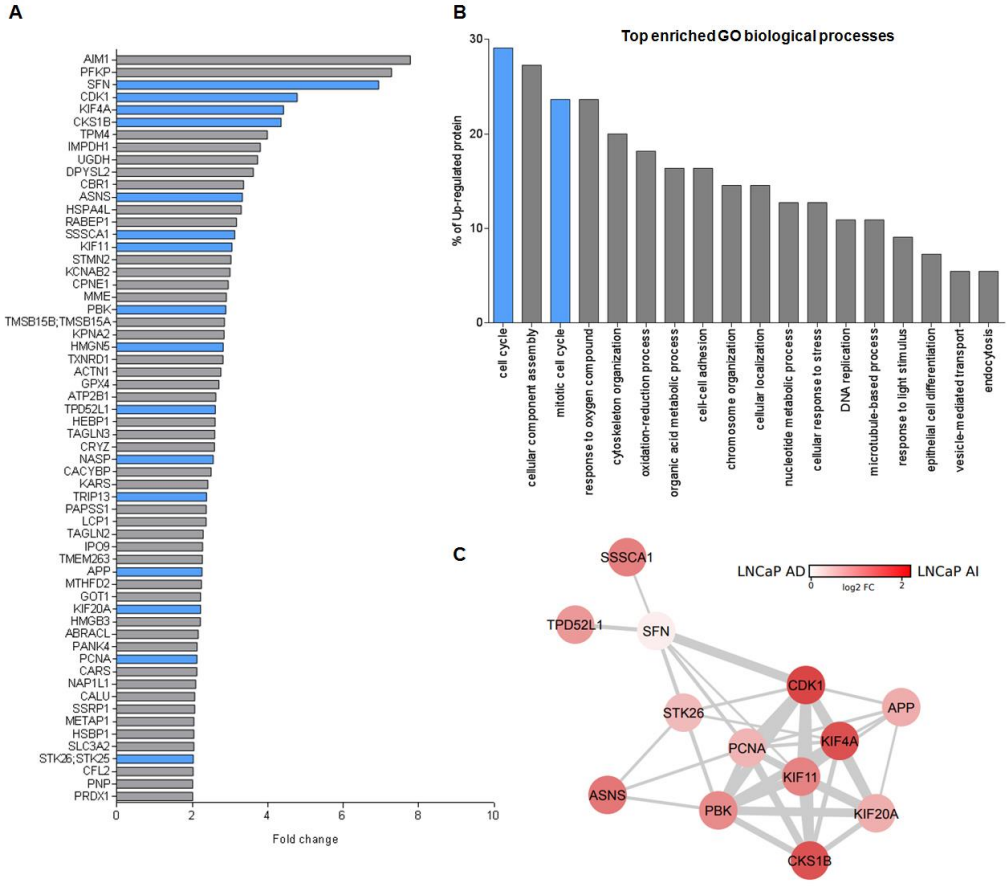

Figure 22. Cell cycle proteins are significantly deregulated in LNCaP androgen independent cells. A) 47 proteins were upregulated in LNCaP AI cells using stringent criteria (p-value < 0.05 and FC < 2). Those involved in cell cycle are represented in blue color. **B)** 'Cell cycle' and 'Mitotic cell cycle' are two of the top enriched GO biological processes in LNCaP AI

cells using DAVID functional annotation tool. **C)** Mitotic cell cycle network of the highly significantly upregulated candidates in the androgen independent LNCaP cell line.

Gene Ontology (GO) analysis of the highly differentially expressed upregulated proteins in LNCaP AI compared with LNCaP cells showed that the most enriched GO biological process was 'cell division' (Fig. 22B), confirming that higher expression of cell cycle genes, and in particular M-phase genes, functionally contributes to the progression of PCa to androgen independence, in agreement with Horning *et al.*[163].

Other enriched biological processes, such as 'response to oxygen compound', 'oxidation-reduction process' or 'organic acid metabolic process' are being investigated in the progression of many tumor types[292,293]. Indeed, aberrant or improper regulation of the redox status has been previously studied in PCa[294]. It is a possible mechanism that contribute to increased production of reactive oxygen species (ROS) and thus oxidative stress, which is hallmark of the aggressive phenotype of the disease[295,296]. Several studies seem to confirm that these processes contribute to the tumorigenesis of PCa and the development of CRPC, via activation of the AR signaling[297,298]. Moreover, metabolic alterations have been extensively studied in PCa and play an increasingly important role in the progression of PCa, as well as in its resistance to therapy, as evidenced by Giunchi *et al*.[299]. All these findings underline the utility of our approach.

Since 'mitotic cell cycle' is the focus of our work, the 13 significantly highly upregulated mitotic proteins were selected and used to generate an interplaying network to identify major interactions and sets between the obtained protein candidates (Fig. 22C). Interestingly, most identified proteins had stronger interactions with the other mitotic regulators.

Of note, some of these genes have already been identified to be involved in the acquisition of androgen independence using ChIP assays or microarray analysis (Fig. 23) and our study would therefore confirm their functional relevance. In their study, Ramos-Montoya *et al*.[191] have observed that HES6 drives castration-resistant tumor growth by enhancing a cell cycle network through a combined activity with AR and E2F1. This HES6-associated network included ASNS, CDK1, KIF4A, KIF11 KIF20A and PBK genes. CDK1 was found to be selectively upregulated by AR in androgen

indenpendet PCa[161], while Tamura *et al*.[300] classified KIF20A as one of the upregulated genes in the progression to hormone-refractory PCa.

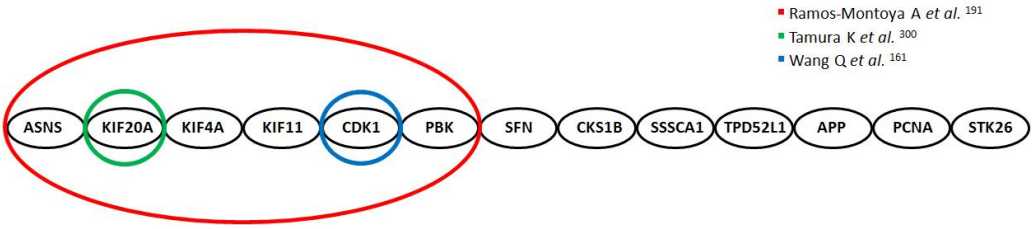

Figure 23. Mitotic candidates significantly upregulated in androgen independent LNCaP AI cells compared to androgen dependent LNCaP cells. Genes that have previously been identified to be involved in androgen independence PCa acquisition were highlighted in colors.

1.3. Identified mitotic regulators are involved in the transition to androgen independence

M-phase genes seem to play a key role in androgen independent PCa progression[161]. To narrow down which significant candidates could be of potential clinical relevance, we next subjected our protein list of mitotic candidates to an *in Silico* validation (Fig. 24) using three different PCa public data sets: Grasso *et al.* (2012)[268], Robinson *et al*. (2015)[269] and *The Cancer Genome Atlas* (TCGA). Validation of the proposed upregulated proteins revealed that 6 out of the top 13 significantly overexpressed mitotic candidates (CDK1, KIF4A, ASNS, KIF11, PBK and KIF20A) had robustly increased mRNA expression in CRPC tissue specimens not only versus benign prostate tissues but also versus localized hormone-naïve PCa tissue, were overexpressed in metastasis compared to primary tumor, and their expression increased with increasing Gleason score. The expression of all mitotic proteins is detailed in the Annexes for each of the three public databases. Interestingly, those 6 candidates were described as differentially expressed genes (DEGs) associated with HES6 overexpression in castration-resistant xenografts, as evidenced in the work Ramos-Montoya and colleagues[191].

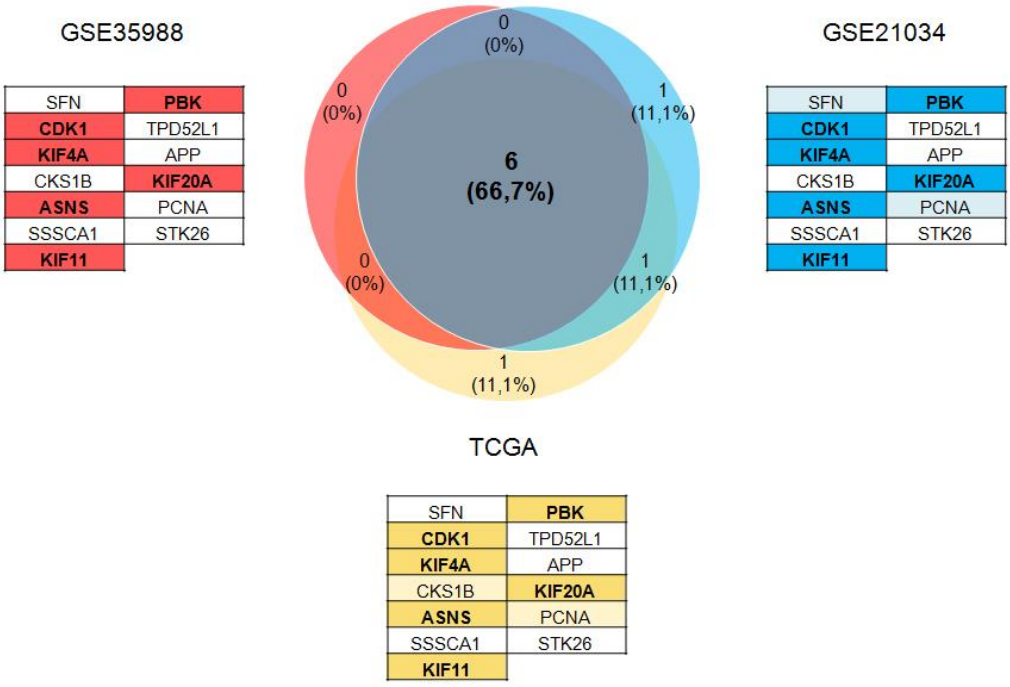

Figure 24. Analysis of gene expression levels of the cell cycle-related candidates involved in mitosis on different PCa public databases. Venn diagram representation displaying the overlap of mitotic proteins found as commonly upregulated in different clinical PCa cohorts: Grasso *et al.*[268] (GSE35988), Robinson *et al.*[269] (GSE21034) and *The Cancer Genome Atlas* (TCGA). A shading was applied to the genes that are significanty deregulated in each database. The six genes that appeared significantly overexpressed in all PCa databases are highlighted in dark color.

Three of those candidates (KIF4A, KIF11 and KIF20A) belong to the kinesin protein family, a family of motor proteins crucial for mitosis that are being studied as targets for chemotherapeutic intervention in different types of cancer[179]. CDK1 and ASNS have been already studied in the context of PCa for having an important role in the AR stability[301] and for being upregulated in cases of CRPC[302], whereas PBK has been recognized as a metastasis-promoting kinase in several tumors[303]. Surprisingly, we did not detect the twoother main kinase regulators of mitosis, namely PLK1 and AURKA, on this quantitative proteomic approach, even if both kinases have been previously extensively studied in PCa and associated to androgen independent growth. This is likely due to the relative lower abundance of kinases and the difficulty to detect them when high abundant proteins are present.

To confirm our results, the expression of the selected mitotic regulators was then studied *in vitro* by means of Western blotting in various prostate cell lines: the non-malignant normal epithelial RWPE1 cell line, the androgen dependent LNCaP cell line and three different androgen independent PCa cell lines such as LNCaP AI cells used for the proteomic screen and DU154 and PC3 (Fig. 25A and 25B). Protein expression levels of the candidates were evaluated in different STLC-arrested PCa cell lines in order to mimic the conditions of the proteomic approach (Fig. 25A), and almost all of them (except in the case of the asparagine synthetase ASNS) were correctly validated. Thus, the accuracy of the proteomic profiling and the potential of these candidates as targets for the molecular intervention of CRPC patients were highlighted.

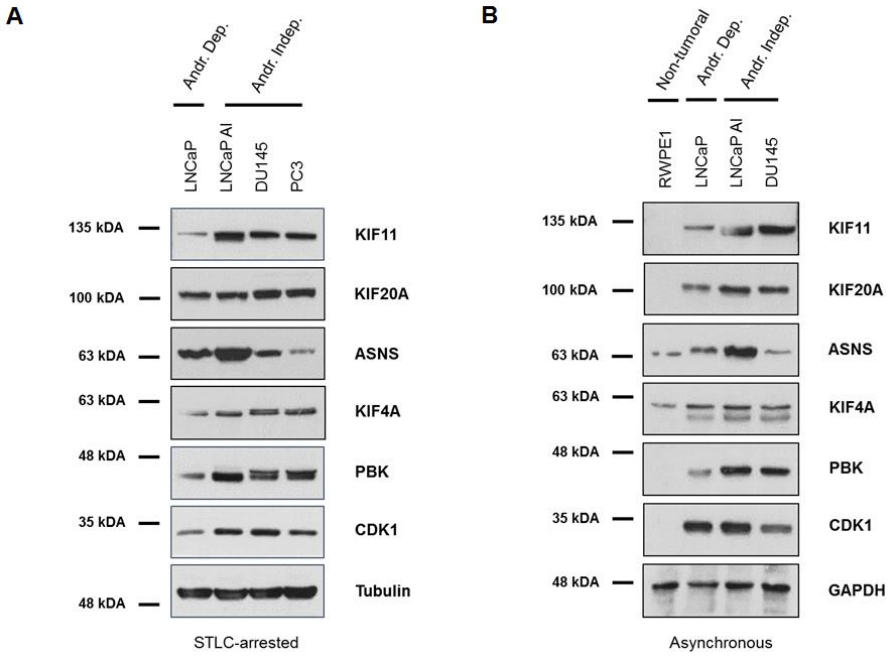

Figure 25. Protein expression validation using Western blotting of selected M-phase candidates. Cancidates were checked in different A) STLC-arrested and B) asynchronous prostate cell lines. Asynchronous cells confirmed the robustness of KIF11, KIF20A and PBK overexpression in androgen independent PCa cells. Due to the slow growing rates, the RWPE1 cell line could not be properly arrested in mitosis and protein expression levels could only be evaluated in asynchronous cells.

It should be noted that, in all cases, PCa cell lines displayed increased protein expression levels than the non-malignant RWPE1 cell line (Fig. 25B). However, KIF11, KIF20A and PBK showed consistent higher protein expression in the androgen

independent cells lines when assayed under asynchronous conditions (Fig. 25B). Our results suggested that those three specific proteins may have a key role in the transition to androgen independent PCa, and raised the possibility that elevated levels of these candidates may be a shared feature in androgen insensitive PCa cells. Based on all these observations, these three candidates have been followed up and a novel research line targeting these two kinesins has been initiated in the laboratory, in which I have also been involved. Specifically, in a collaborative project with Dr. Miquel Segura's group (Laboratory of Translational Research in Child ad Adolescent Cancer, Vall d'Hebron Research Institute (VHIR), Barcelona, Spain), we have demonstrated that KIF11 could be to a therapeutic target against high-risk neuroblastoma as well (manuscript in preparation) and another PhD thesis in our laboratory is focused in elucidating the role of a novel oral specific KIF11 inhibitor for treating mCRPC.

Apart from kinesins, PBK stood out as promising mitotic candidate to be followed up, as it is a druggable target and little is known about the effect of its inhibition in preclinical PCa mouse models. Our results concur with the results published by Warren *et al*.[304] during the course of this project (indicating a co-regulation between the AR and PBK). In particular, here we proceeded to explore the role of this kinase as a promising driver to androgen independence and to study its potential therapeutic advantages through pharmacological inhibition.

2. PBK as a therapeutic target for hormone-refractory PCa

2.1. PBK expression is increased in advanced PCa and correlates with poor prognosis

PBK is a serine/threonine kinase that act as a MAP kinase kinase by phosphorylation of P38 mitogen-activated protein kinase (MAPK)[305]. It is highly active during the M-phase of the cell cycle and, together with the cdc2/cyclin B complex, promotes cytokinesis through phosphorylation of protein regulator of cytokinesis 1 (PRC1)[306]. Cumulative reports are being focused on the critical roles of this mitotic kinase in cell division[306,307]. PBK high expression has been linked to a more aggressive phenotype in various types of cancer such as breast, colorectal, lung cancers and Ewing sarcoma[308]. Since it is upregulated in several types of cancer and its expression is hardly detectable in normal tissues (except testis and fetal tissues), PBK appears to be at first glance a promising molecular target for cancer therapy. Moreover, pharmacological inhibition of this kinase has led to decreased cell proliferation and enhanced apoptosis in several tumor types[309-312].

Increasing evidence in the last few years suggest that PBK could also have an important role in the progression PCa. Several studies have demonstrated that PBK depletion resulted in reduced cell proliferation, invasion and migration of different PCa cell lines *in vitro*. Interestingly, PBK expression has been recently associated with increased AR expression[304], and nuclear localization has been correlated with PCa grade and stage[313]. While none of the currently available inhibitors has entered clinical trials so far, PBK inhibition is regarded as a potential therapeutic approach in PCa treatment.

To further explore the role of PBK during PCa progression, we first subjected PBK to an *in Silico* validation in human samples using the above-mentioned PCa public databases (Fig. 26). As observed before[314-317], PBK expression levels were also higher with increasing Gleason score (Fig. 26A), and the kinase was found to be overexpressed in metastasis compared to primary tumor (Fig. 26B). Moreover, we found consistently elevated mRNA expression in CRPC tissues, not only versus benign prostate tissues but also versus hormone-naïve PCa tissues (Fig. 26C).

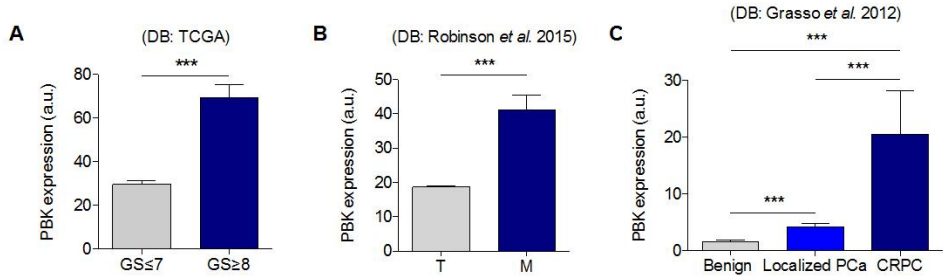

Figure 26. Analysis of PBK expression on different public data sets. A) mRNA expression levels in low-grade PCa (Gleason score ≤7) (N = 292) and intermediate- and high-grade PCa (Gleason score) (N = 205). **B)** mRNA expression levels in prostate tumors from patients with primary (N = 262) or metastatic (N = 38) PCa. **C)** mRNA expression levels in benign prostate tissue (N = 28), hormone-naïve PCa tissue (N = 59) and CRPC tissues (N=35) from a clinical PCa cohort.

Next, we assessed the protein levels of PBK in various normal (N = 8), PCa-naïve (N = 8) and CRPC (N = 8) FFPE patient samples using immunohistochemistry (Fig. 27A). Despite the apparent low number of samples, it needs to be considered their value, as patients with castration-resistant disease rarely undergo another surgery.

We devised a scoring system to determine protein expression, whereby each core was scored with a 0, 1, 2 or 3, that corresponds to no staining, low, moderate or high staining, respectively. After analysis, we found that PBK has similar staining intensities in both benign prostatic hyperplasia (BPH) and PCa-naïve tissues, but it displays significantly increased protein expression in CRPC samples (Fig. 27B). We further observed that nuclear PBK localization strongly correlates with disease progression and, as already described[308], CRPC tissues showed strong nuclear localization (Fig. 27C).

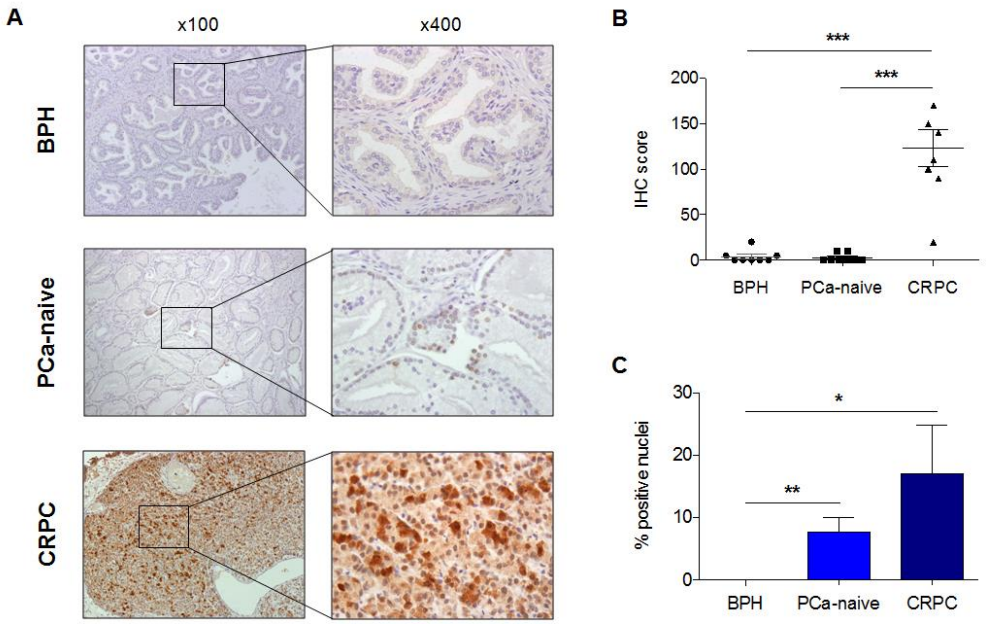

Figure 27. Elevated expression of PBK is closely correlated with pathological grade in human PCa patients. A) Representative immunohistochemistry images of PBK expression in benign, PCa-naïve and CRPC specimens under light microscopy (100x and 400x). **B)** Immunohistochemical staining score of PBK protein expression in different prostate tissues of varying disease grades. **C)** Percentage of PBK positive nuclei in different prostate tissues of varying disease grades.

To evaluate whether PBK could have a potential prognostic value in PCa, we stained different tissue microarrays (TMAs) containing radical prostatectomy primary tissues from patients treated at the Urology Department from Vall Hebron Hospital, with known clinical follow-up records (Fig. 28A). The analysis revealed that PBK expression is increased in higher Gleason grades (Fig. 28B), confirming the results observed in the public data set. In addition, PBK was able to differentiate between groups of i) patients who did not present biochemical recurrence (BCR) (N = 69), ii) patients who experienced BCR (N = 57) and iii) patients who developed metastasis (N = 21) (Fig. 28C). PBK had preferentially higher staining patterns in those patients who presented metastatic lesions. In addition, we analysed the expression of PBK in comparison with patients' outcome. We found a strong negative correlation between PBK levels and biochemical recurrence, suggesting that PBK may be a prognostic indicator of risk to relapse (Fig. 28D), with relative high sensitivity and specificity (Fig. 28E).

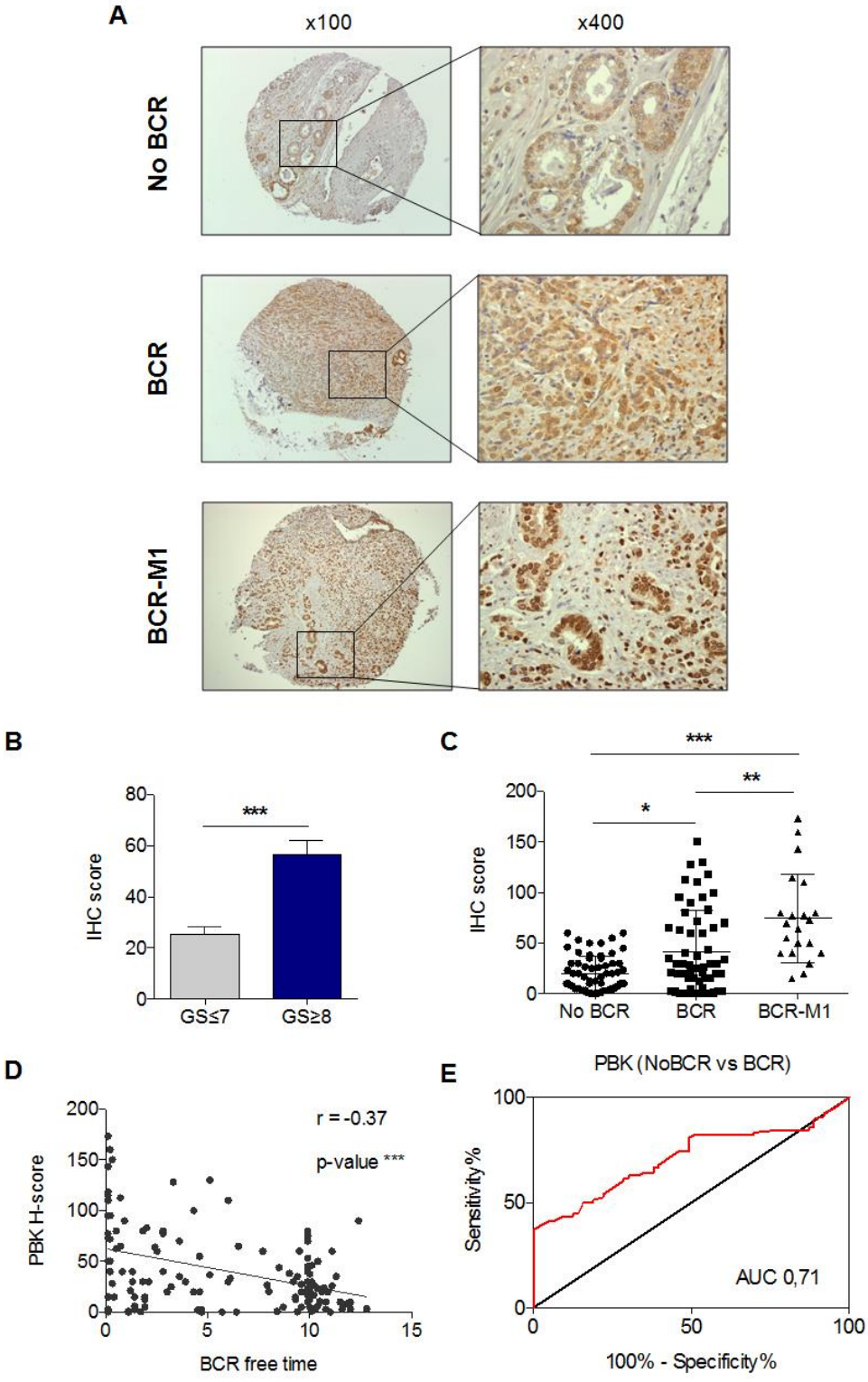
A
x100
x400
No BCR
BCR
BCR-M1
B
IHC score
***
GS≤7
GS≥8
C
IHC score
***
**
*
No BCR
BCR
BCR-M1
D
PBK H-score
r = -0.37
p-value ***
BCR free time
E
PBK (NoBCR vs BCR)
Sensitivity%
AUC 0,71
100% - Specificity%

Figure 28. Elevated expression of PBK is closely correlated with clinical outcome in human PCa patients. A) Representative IHC images of PBK expression in tissue microarrays (TMAs) containing primary tissues of no biochemical recurrent (No BCR), biochemical recurrent (BCR) and metastatic (M1) tumors of various human PCa patients. **B)** Immunohistochemical staining score of PBK protein expression in different prostate tissues of varying Gleason scores and **C)** clinical outcomes. **D)** Correlation of PBK immunohistochemistry staining score and time to biochemical recurrence. **E)** Prognostic value of PBK for distinguishing between patients with and without BCR represented as ROC curve.

Taken together, our data provide strong evidence that PBK appears to be overexpressed during the development of CRPC and therefore might play a role in the progression of PCa to an advanced-stage disease. These results also indicate that high PBK protein levels are significantly associated with biochemical recurrence and, hence, with poor prognosis. Overall, these findings were consistent with the results obtained in previous studies, thus underlining the robustness of our work.

2.2. PBK overexpression promotes androgen independent cell growth *in vitro*

Going a step further, we wanted to determine whether PBK could be a driver of androgen independence in PCa. The potential of this mitotic regulator as a target for cancer therapy has already been investigated in many tumor types, including PCa; nevertheless, its role as an oncogenic driver has not been elucidated yet. For this purpose, we evaluated the capacity of androgen dependent LNCaP cells stably overexpressing PBK to growth in androgen-depleted conditions, which is the main characteristic of CRPC.

For this purpose, we generated an LNCaP cell line stably overexpressing PBK (pINDUCER20-PBK) when induced with doxycycline. Increased PBK protein levels were confirmed by Western blotting (Fig. 29A). Once the overexpression was confirmed, cells were cultured in full or androgen-depleted media and cell proliferation was monitored. Cells received regularly doxycycline for assuring high levels of PBK during the experiment in the treatment group.

Interestingly, in the presence of androgens (AD medium), overexpression of PBK didn't seem to provide any significant growth advantage to PCa cells and no differences in shape were observed. However, results indicated that doxycycline-induced

overexpression of PBK confers androgen dependent LNCaP cells the ability to proliferate in androgen-depleted conditions (AI medium) (Fig. 29B), thus highlighting the importance of PBK in the acquisition of androgen Independence in PCa.

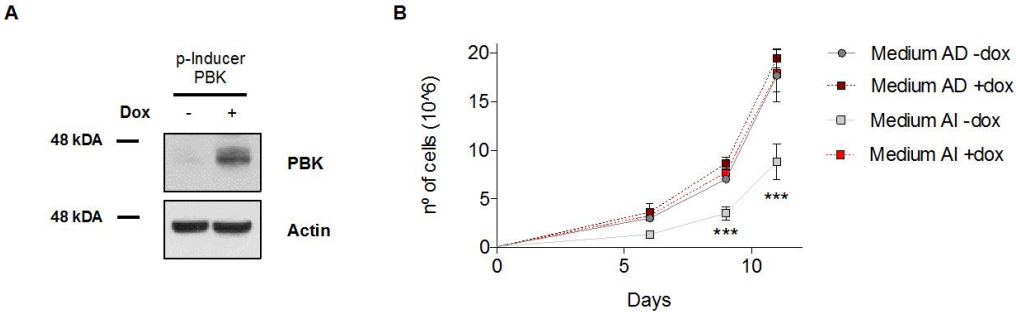

Figure 29. PBK overexpression confers androgen independence to prostate cancer cell lines. A) Western blotting showing PBK overexpression after 72h induction with 0.5 μg/mL doxycycline. **B)** LNCaP cells stably overexpressing PBK (pINDUCER20-PBK) were cultured with or without doxyxycline for 11 days. Cells were harvested, counted and reseeded at the indicated time points using culture medium with or without androgens. Three independent experiments are represented as average and standard error of the mean.

On note, this is the first report demonstrating the crucial role of this kinase in the transition to androgen independent PCa. We therefore hypothesized that the PBK overexpression observed in advanced PCa (see section 2.1) could potentially serve as a survival strategy in the progression of the disease. These findings are summarized in Fig. 30 and discussed in the Discussion section.

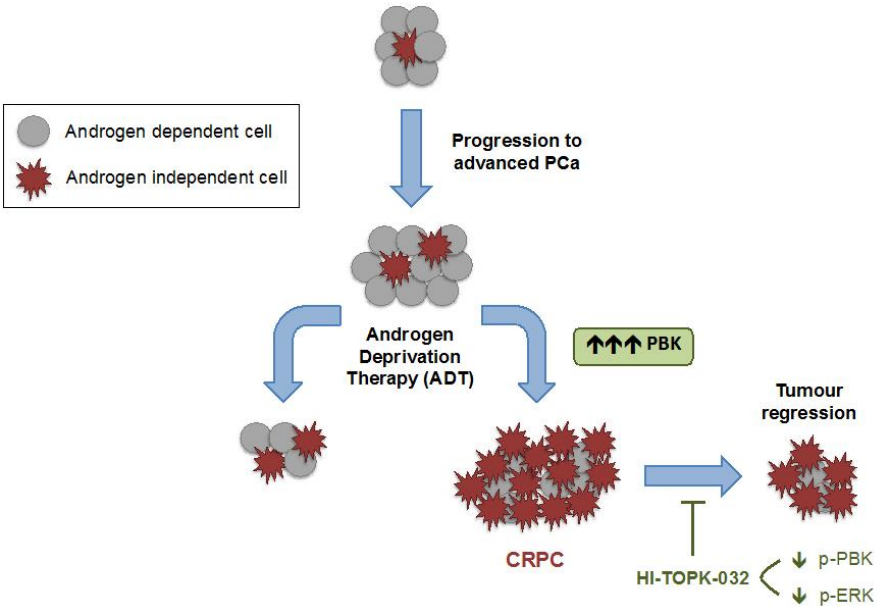

Figure 30. PBK might be as an oncogenic driver of castration-resistance in PCa. Model depicting oncogenic role of PBK in the transition of PCa to androgen independence. PBK overexpression can result in the progression of PCa to androgen independent disease after androgen deprivation therapy (ADT), leading to CRPC.

2.3. PBK Inhibitor HI-TOPK-032 Reduces PCa Cell Growth and Induces Apoptosis

Once the key role of PBK in the transition to androgen independence was confirmed, we evaluated PBK as a potential therapeutic target in PCa. In this regard, we proceeded to knock it down using lentiviral-based short hairpin RNAs in LNCaP and LNCaP AI cell lines. The knockdown efficiency of four different shRNA constructs was validated by means of Western blotting (Fig. 31A) and shPBKIII was selected for having the strongest effect on both cell lines. Results indicated that PBK suppression significantly impeded cell growth in both androgen dependent and independent PCa cells (Fig. 31B), which is consistent with the work published by Warren *et al.*[304].

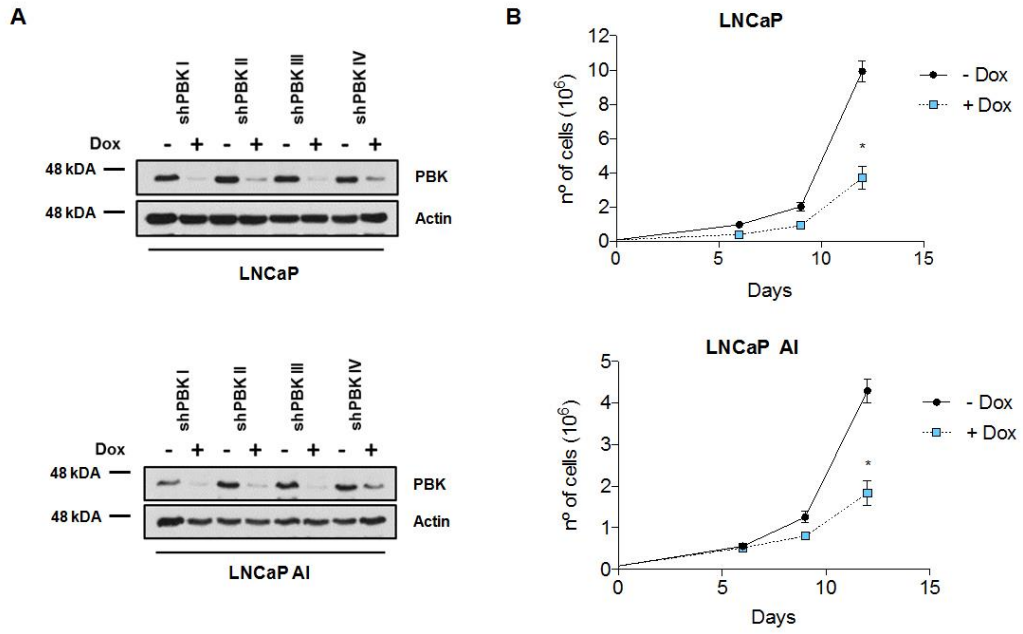

Figure 31. Inducible knockdown of PBK reduces viability in both androgen dependent and independent PCa cells. A) shRNA expression was induced by doxyxycline (1 μg/mL) for 72h and protein expression levels were validated using Western blotting in both PCa cell lines. shPBKIII was chosen for further experiments. **B)** Effect of PBK knockdown on cell proliferation was examined by cell counting for 12 days. Data represent ± SEM of three independent experiments.

Having shown that PBK knockdown resulted in a decrease in cell proliferation, we then examined whether targeting PBK kinase activity with the ATP-competitive inhibitor HI-TOPK-032 would exhibit a cytotoxic effect in PCa cells. Several PBK inhibitors are currently being used in preclinical studies; however, HI-TOPK-032 has already demonstrated a high efficacy in several tumor types[305,309,311,312]. We treated various prostate cell lines with different concentrations of HI-TOPK-032 for 72h and found a high dose-dependent decrease in cell viability in all three PCa cell lines tested, with an IC50 that ranged from 2–4 μM (Fig. 32A). Importantly, androgens dependent as well as androgen independent cells were highly sensitive to PBK inhibition, different to what had been observed with the majority of treatments tested, as reported earlier. On the contrary, it had little effect (IC50 = 10.4 μM) on the non-malignant normal RWPE1 prostate cell line, which could ultimately help to rationally utilize this inhibitor for cancer therapy. Although previous experience in the laboratory had shown that androgen

independent cell lines were commonly more resistant to other mitotic inhibitors (data not shown), HI-TOPK-32 suppressed cell proliferation in both androgen dependent and independent PCa cells, and therefore it was worth continuing to characterize its effect on PCa.

With the aim of examining the effect of the PBK inhibitor on apoptosis, LNCaP and LNCaP AI cells were treated with HI-TOPK-032 and then incubated for 72h. Results showed a dose-dependent increase in hallmarks of apoptosis such as induction of caspase-3 and PARP cleavage (Fig. 32B), thereby confirming apoptotic cell death. In addition, treatment with HI-TOPK-032 also showed increased levels of the mitotic marker p-Histone H3 (Fig. 32B), since PBK seems to play an important role in the M-phase of the cell cycle[318].

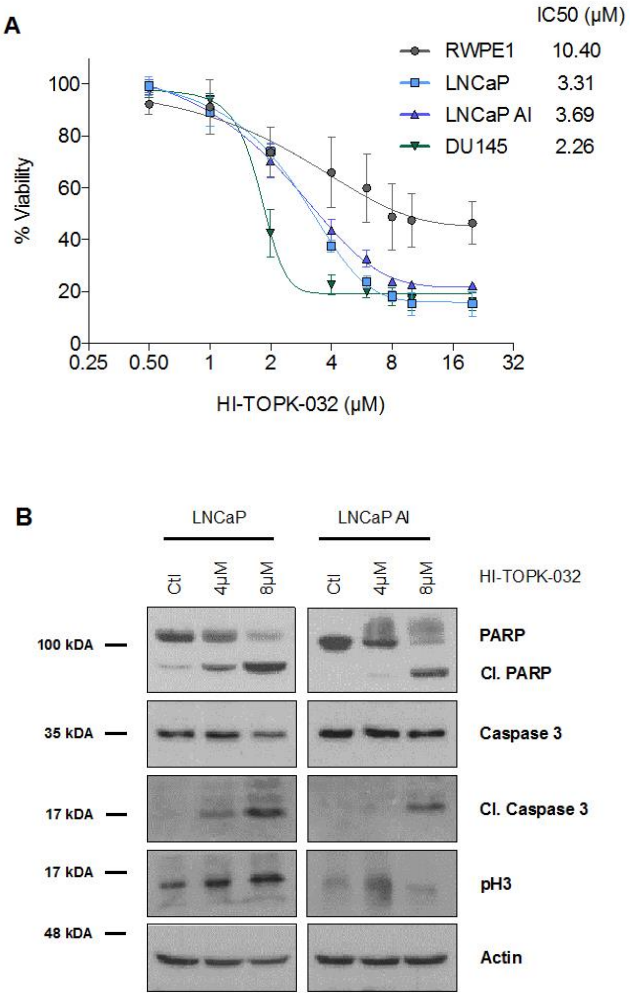

Figure 32. Pharmacological inhibition of PBK by means of HI-TOPK-032 reduces cell viability and promotes apoptosis in different PCa cell lines. A) HI-TOPK-032 inhibited PCa cell growth in a dose-dependent manner, having little effect on the normal prostate RWPE1 cell line. Cells were treated with HI-TOPK-032 and proliferation was measured after 72h by crystal violet assay. Data are shown as mean ± SEM (N = 3). **B)** HI-TOPK-032 induced apoptosis in both androgen dependent and independent LNCaP cells.

Once assured that HI-TOPK-032 was effective on PCa cell lines, we then tested the growth-inhibitory effect of PBK inhibition on a more clinically relevant model, using anchorage-independent PCa patient-derived cells (patient characteristics can be found on the material and methods section). PCa cells derived from a patient biopsy were seeded and treated with different concentrations of HI-TOPK-032 (Fig. 33A). MTS assay was performed after 72 h treatment to check the viability of the remaining spheroids and we found that increasing concentrations of the inhibitor significantly reduced cell viability (Fig. 33B). Moreover, Western blotting confirmed increased caspase-dependent apoptosis (Fig. 33C) of prostate spheroids, in agreement with previous results in the representative PCa cells growing in monolayer. Our study supports the findings of Warren *et al*.[304], who demonstrated that inhibition of PBK resulted in decreased tissue proliferation as assessed by Ki67 staining. In their work, they also observed that AR levels were reduced after treatment with HI-TOPK-032 in an *ex vivo* culture, thus confirming the role of PBK in sustaining AR levels and PCa tumor growth.

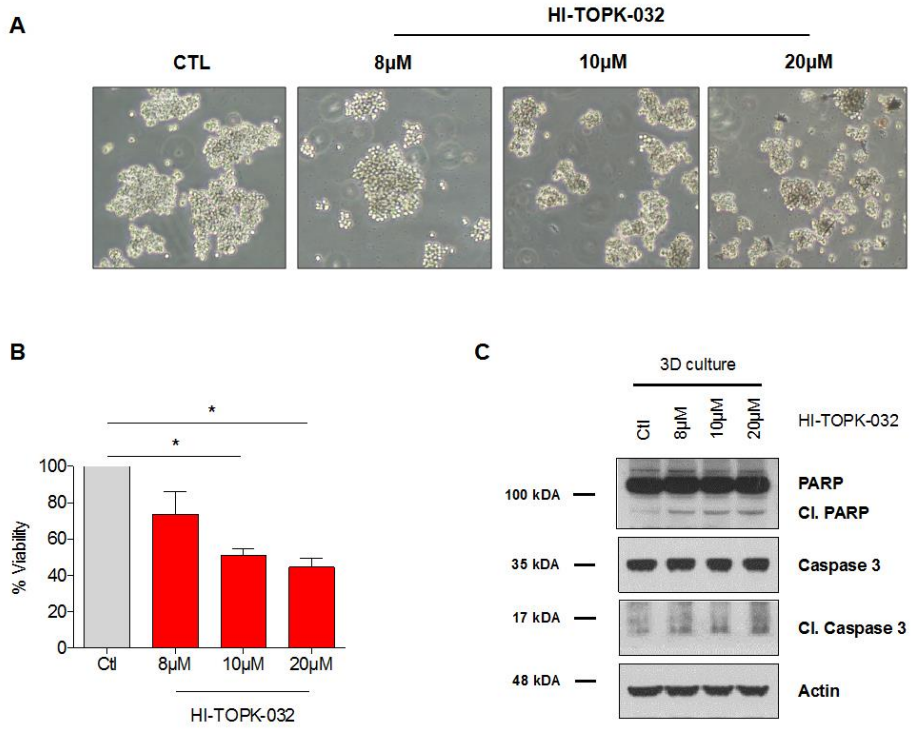

Figure 33. HI-TOPK-032 reduces cell viability and induces apoptosis in anchorage independent PCa patient-derived cells. A) Representative images of anchorage-independent tumor spheres derived from a patient biopsy after 72h treatment with the HI-TOPK-032 inhibitor. **B)** HI-TOPK-032 treated PCa patient spheres exhibited a significant decrease in cell viability. **C)** Protein levels of several apoptotic markers were assessed by means of Western blotting in PCa patient 3D cultures.

The fact that PBK inhibition promotes apoptosis in a patient-derived model obtained from a CRPC patient highlights the potential of this kinase as a valid future target for hormone-refractory PCa. Altogether, this confirm the previous results observed in PCa cell lines and empowered patient-derived cells as *ex vivo* models to evaluate novel therapies for advanced-stage PCa patients.

Finally, to further study, we explored the effect of HI-TOPK-032 on downstream targets of PBK in the patient-derived PCa culture. Since PBK expression peaks at the G_2/M-phase of the cell cycle, cells were arrested in mitosis, treated with HI-TOPK-032 for several hours and lysates were examined using Western blotting. The results pointed out that HI-TOPK-032 treatment resulted in a significant dose-dependent reduction of

both phosphorylated ERK1/2 and PBK kinase activity (assessed by p-PBK), while the total expression of PBK was not changed (Fig. 34).

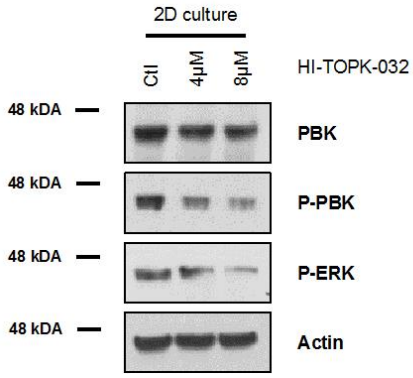

Figure 34. Effect of HI-TOPK-032 on PBK activity and MAPK signaling pathway in PCa patient cells. Cells were arrested in mitosis (as explained the section of material and methods) and treated with HI-TOPK-032 for several hours.

We could therefore confirm that HI-TOPK-032 is a selective inhibitor of PBK and showed high efficacy in PCa cells both *in vitro* and *ex vivo*. For all these reasons, we suggest that PBK plays a key role in PCa growth and survival and is therefore a potential therapeutic target for the molecular intervention of CRPC patients.

2.4. Pharmacological inhibition of PBK attenuates tumor growth *in vivo*

To validate and reinforced the obtained *in vitro* results, we analyzed the anti-tumor potential of HI-TOPK-032 was analyzed in a PCa xenograft mice model. Several studies have previously evaluated different agents targeting PBK *in vivo* in various cancer types (Table 15); however, the effect of kinase inhibition in preclinical PCa mouse models is still unknown.

Table 15. Studies assessing PBK inhibition and/or depletion in several tumor types *in vivo.*

Indication	PBK inhibitor/depletion	Mice	Year	Reference
Acute myeloid leukemia	OTS514	Tail vein injection model	2015	Alachkar H *et al.* [319]
Colorectal cancer	HI-TOPK-032	Subcutaneous xenograft	2012	Kim DJ *et al.* [309]
	HI-TOPK-032	Subcutaneous xenograft	2017	Zou J *et al.* [320]
	SKLB-C05	Subcutaneous xenograft	2019	Gao T *et al.* [321]
	OTS514 fluorescently labeled	Subcutaneous xenograft	2020	Pirovano G *et al.* [322]
Esophageal carcinoma	HI-TOPK-032	Tail vein injection model	2019	Jiang Y *et al.* [323]
Glioblastoma	OTS964 fluorescently labeled	Subcutaneous xenograft	2018	Pirovano G *et al.* [324]
	shPBK	Orthotopic model	2020	Mao P *et al.* [325]
Glioma	HI-TOPK-032	Subcutaneous xenograft	2015	Joel M *et al.* [305]
Hepatocellular carcinoma	shPBK	Subcutaneous xenograft	2017	Yang YF *et al.* [326]
	shPBK	Orthotopic model	2019	Yang Q *et al.* [327]
Lung cancer	OTS514 and OTS964	Subcutaneous xenograft	2014	Matsuo Y *et al.* [310]
Multiple myeloma	OTS964	Subcutaneous xenograft	2020	Stefka AT *et al.* [328]
Nasopharyngeal carcinoma	HI-TOPK-032	Subcutaneous xenograft	2016	Wang MY *et al.* [312]
Ovarian cancer	OTS514	Orthotopic model	2016	Ikeda Y et al. [329]
	OTS514	Subcutaneous xenograft	2019	Ma H *et al.* [330]
Prostate cancer	shPBK	Subcutaneous xenograft	2015	Sun H *et al.* [313]
T-cell leukemia/lymphoma	HI-TOPK-032	Subcutaneous xenograft	2018	Ishikawa C *et al.* [311]

With the collaboration of Dr. Alvaro Aytes' group at IDIBELL, PCa tumors derived from a NP53 (Nkx3.1CreERT2/+; Ptenflox/flox; p53flox/flox) GEM model[331], which represents a common PCa phenotype, were implanted subcutaneously into the flank of athymic nude mice as shown in Fig. 35A. Mice were previously castrated in order to mimic the clinical scenario of hormone-refractory PCa. After establishment of tumors, mice were randomized into four groups according to administration of vehicle (N = 6), enzalutamide (N = 6), HI-TOPK-032 (N = 7) or both HI-TOPK-032 and enzalutamide (N = 7). Vehicle was intraperitoneally administered each day, enzalutamide (10 mg/kg) was orally administered five times a week, and HI-TOP-032 (10 mg/kg) three times a week over a period of 28 days as seen in Figure 35B. Treatment with HI-TOPK-032 had the strongest effect on reducing PCa tumor growth (Fig. 35C) and, thus resulting in more reduced tumor volumes (Fig. 35D) and tumor weights (Fig. 35E). Those significant differences were already visible at day 17 and increased throughout the experiment (Fig. 35D). Intriguingly, although the combined treatment of HI-TOPK-032 and enzalutamide had a higher effect than the produced by enzalutamide alone, tumor growth was less affected compared to HI-TOPK-032 single treatment (Fig. 35),

suggesting that enzalutamide may negatively interfere with HI-TOPK-032 mechanism of action.

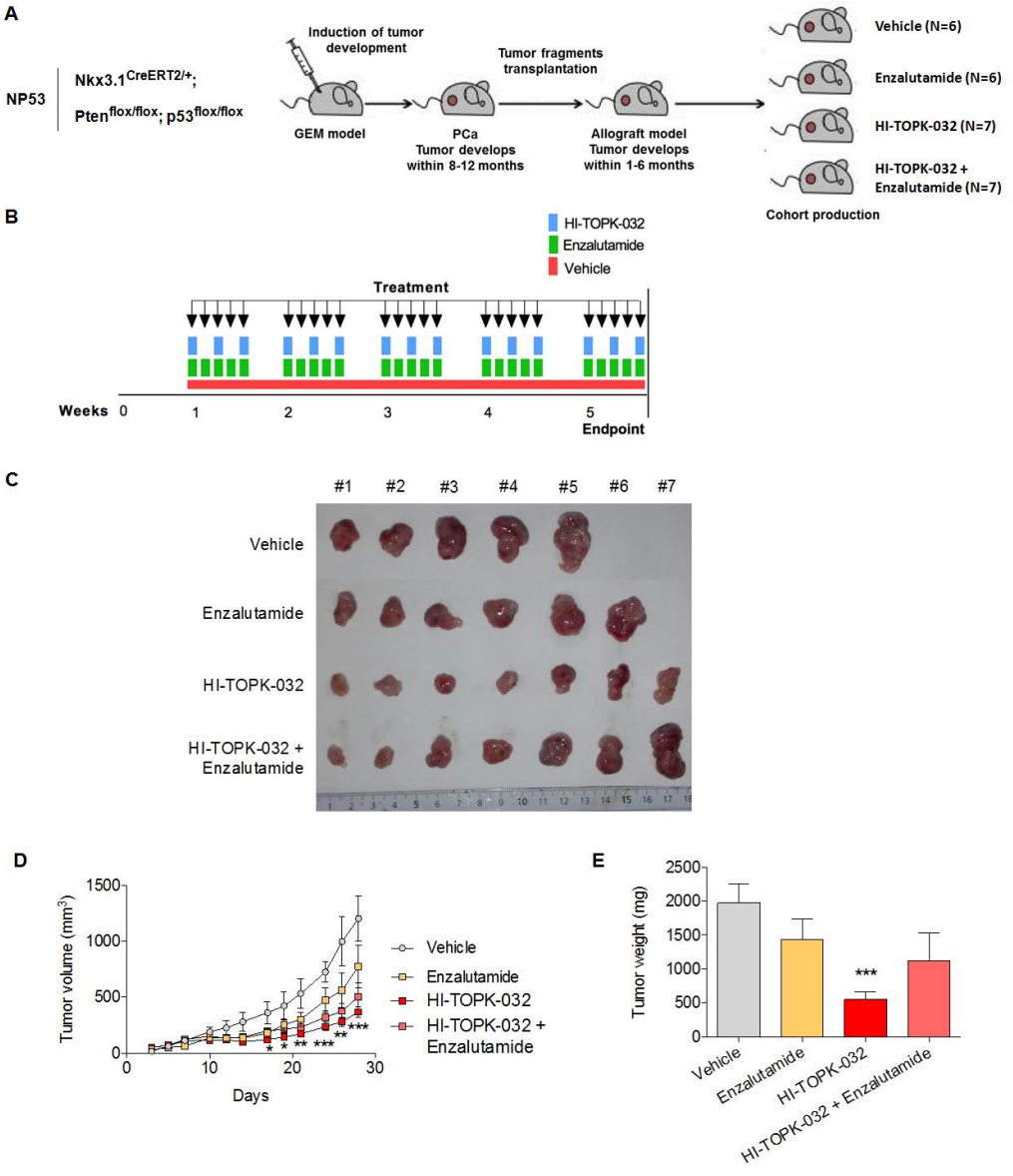

Figure 35. Tumor growth *in vivo* attenuation in PCa genetically engineered mouse (GEM) model upon inhibition of PBK. A) Experimental strategy. PCa tumors derived from a NP53 GEM model were implanted subcutaneously into the flank of immunodeficient mice. **B)** After establishment of tumors, mice were treated with vehicle, enzalutamide (10 mg/kg), HI-TOPK-032 (10 mg/kg) or HI-TOPK-032 and anzalutamide. The tumors were extracted 4 weeks after treatment and representative tumors for each group are shown. One tumor of the vehicle-treated group was excluded from the analysis due to the absence of palpable mass. **C)** Mean tumor

volumes and weights **D)** of HI-TOPK-032 treated group were significantly smaller than the control group. The results are represented as the mean ± SEM (N = 7).

Mice seemed to tolerate the intraperitoneal injection of HI-TOPK-032 without overt signs of toxicity or significant loss of body weight (Fig. 36A). In addition, tumor volume in the HI-TOPK-032 treated group positively correlated with tumor weight (Fig. 36B), confirming the accuracy of the measures.

In agreement with tumor growth data, immunohistochemical analysis revealed a significant reduction of the proliferation marker Ki67 in HI-TOPK-032 monotherapy, confirming the growth attenuation. The effect was lower when combined with enzalutamide, but higher than the produced by enzalutamide alone (Fig. 36C-D). Of note, AR nuclear staining was reduced with enzalutamide or combined treatment, while it was not significantly affected after pharmacological inhibition of PBK (Fig. 36E). Staining of p-ERK, a downstream target of PBK, and p-S6, a marker of active mTOR pathway, were strongly decreased in HI-TOPK-032 treated tumors, thus corroborating the efficacy and specificity of the PBK inhibitor. Nevertheless, this effect was less evident in the combined treatment group (Fig. 36E).

With the aim of further exploring the mechanism by which enzalutamide may reduce HI-TOPK-032 efficacy when used in combination, we treated androgen dependent and androgen independent LNCaP cells with a suboptimal death dose of enzalutamide for 48 h and then assessed PBK protein levels by Western Blotting (Fig. 36F). Because Warren and colleagues[304] reported AR binding sites at the enhancer upstream of PBK gene, we hypothesized that the reduced AR activity induced by enzalutamide treatment may decrease PBK transcription, reducing PBK protein levels and therefore diminishing the effect of HI-TOPK-032. Here, a significant reduction reduction of PBK protein expression was observed in enzalutamide-treated LNCaP cells compared to the control ones (Fig. 36F), thus reinforcing our hypothesis and underlining the utility of our study to understand the mechanistic facts of our results with the combined treatment.

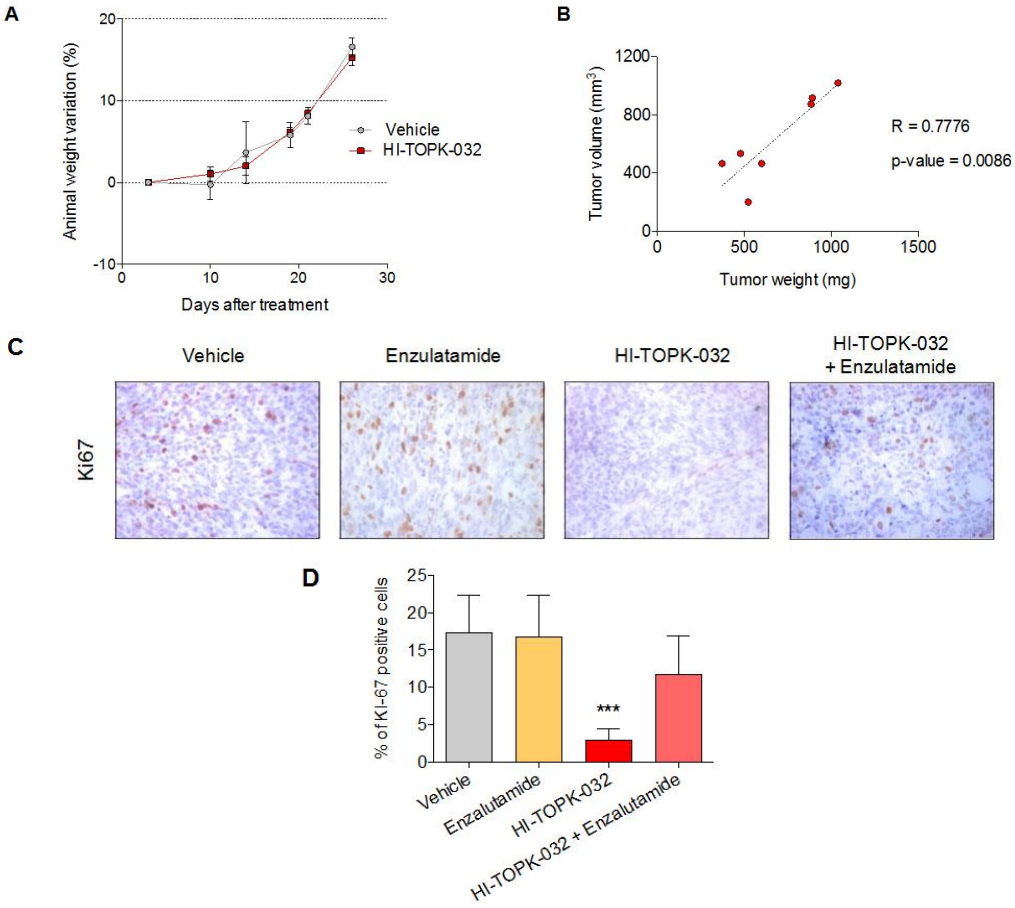
A
Animal weight variation (%)
Days after treatment
Vehicle
HI-TOPK-032
B
Tumor volume (mm3)
Tumor weight (mg)
R = 0.7776
p-value = 0.0086
C
Vehicle
Enzulatamide
HI-TOPK-032
HI-TOPK-032 + Enzulatamide
Ki67
D
% of KI-67 positive cells
***
Vehicle
Enzulatamide
HI-TOPK-032
HI-TOPK-032 + Enzulatamide
E
Vehicle
Enzulatamide
HI-TOPK-032
HI-TOPK-032 + Enzulatamide
AR
pERK
pS6

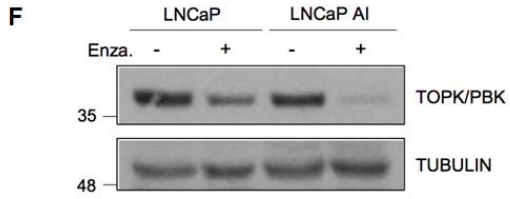

Figure 36. HI-TOPK-032 significantly reduces tumor proliferation *in vivo*. A) Body weights of vehicle- and HI-TOPK-032-treated mice throughout the experiment. **B)** Positive significant correlation between tumor volume and tumor weight of HI-TOPK-032 mice group. **C)** Representative IHC images and **D)** quantification of Ki67 positive cells in the four study groups. The results are represented as the mean ± SEM (N = 7). **E)** Representative IHC images for AR, pERK and PS6 in the four study groups. **F)** Western Blotting showing PBK protein levels after treatment with enzalutamide in both LNCaP and LNCaP AI cell lines.

Altogether, our findings suggest that HI-TOPK-32 effectively arrests PCa tumor growth through inhibition of PBK *in vivo* and offer an exciting therapeutic approach for castrated-resistant PCa. To the best of our knowledge, this is the first report assessing the efficacy of the *in vivo* pharmacological PBK inhibition in PCa mice models.

Given the promising results obtained with PBK pharmacological inhibition in a GEM xeneograft, we decided to go a step further and confirm the effects of HI-TOPK-032 on an orthotopic PCa mouse model in collaboration with Dr. MJ Vicent (Laboratory of Polymer Therapeutics, Centro de Investigación Príncipe Felipe (CIPF), Valencia, Spain). Compared to subcutaneous xenografts, othotopic models provide an appropriate tumor microenvirenment that leads to the development of tumor cells with biological and metastatic properties resembling clinical cases, thereby resulting in a more reliable translation[332].

In this case, VCaP cells, which express wild type AR and were established from a hormone-refractory PCa patient, were injected into the prostate of mice following MJ Vicent´s lab internal protocol. After establishment of tumors, mice were randomized into two groups according to administration of vehicle (N = 6) or HI-TOPK-032 (N = 6). Vehicle and HI-TOPK-032 (10 mg/kg) were intraperitoneally injected three times a week over a period of 35 days. Unexpectedly, treatment with HI-TOPK-032 did not lead to reduced tumor volume in this specific experiment (Fig. 37A-B), thus not resulting in any significant changes by luminescence (Fig. 37C-D).

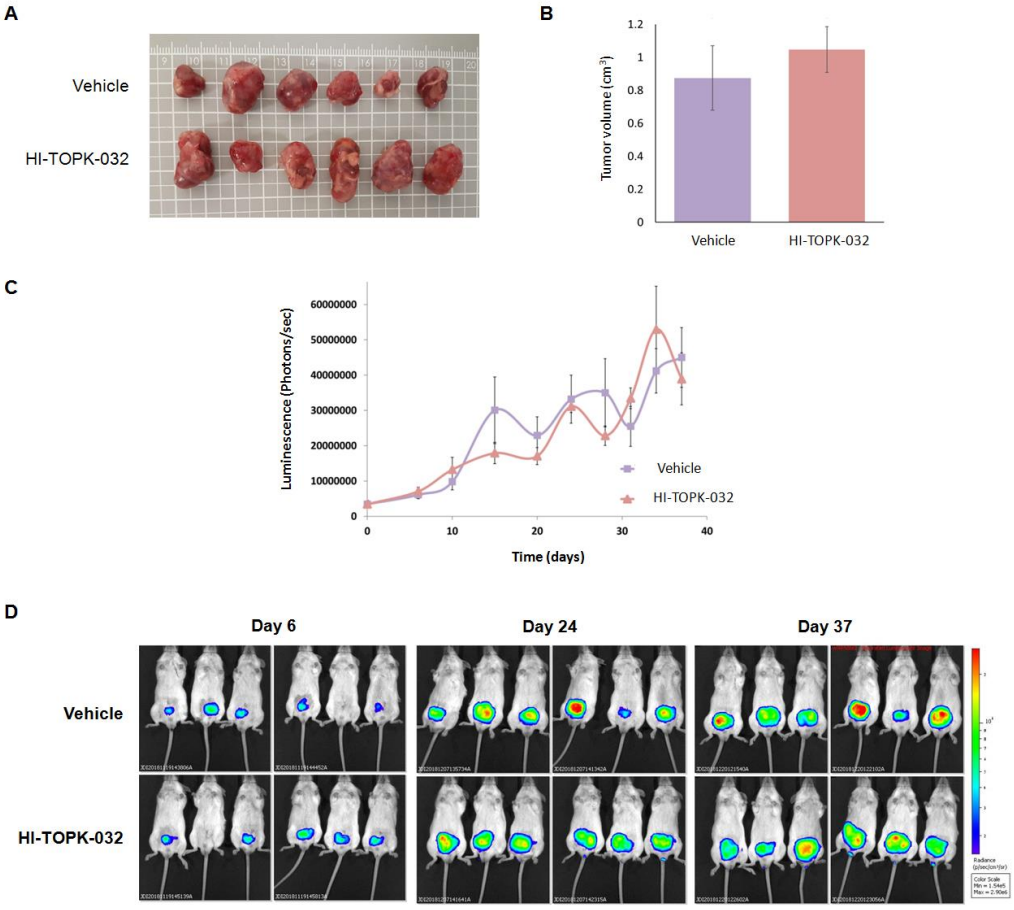

Figure 37. *In vivo* tumor growth of PCa orthotopic murine model upon inhibition of PBK. Tumors were generated following MJ Vicent´s lab internal protocol. After establishment of tumors, mice were treated with vehicle, or HI-TOPK-032 (10 mg/kg) three time as week. **A)** Tumors were extracted after 5 weeks treatment and representative tumors for each group are shown. **B)** Mean tumor volumes and **C)** luminescence of HI-TOPK-032 treated group did not show any significant change compared with the control group. The results are represented as the mean ± SEM (N = 6). **D)** Representative luminescence images from both study groups after 6, 24 and 37 days.

Based on these results, we evaluated two different scenarios that could explain the lack of HI-TOPK-032 efficacy in this setting. Once mice were sacrified, we observed that the abdominal cavity and the proximal organs of animals treated with the PBK inhibitor showed drug accumulation or precipitations (Fig. 38A), suggesting that HI-TOPK-032 was not properly dissolved and thus giving a possible explanation for the lack of HI-TOPK-032 activity detected. Although this finding may have affected the

efficacy of the inhibitor to some extent, drug solubility was not regarded as a problem in the GEM xenograft setting or during the preparation of the compound to be injected. Next, although it has been previously shown that VCaP cells express PBK levels and that non-toxic concentrations of HI-TOPK-032 inhibited cell proliferation in this cell line[308], we checked PBK protein levels of VCaP cells from Dr. MJ Vicent´s lab that were used for this particular experiment. Notably, almost undectectable PBK expression was observed in the VCaP cell line, whereas the androgen dependent LNCaP and the androgen independent DU145 and LNCaP AI cells possessed increasingly higher levels of the kinase (Fig. 38B). Accordingly, we hypothesized that the efficacy of HI-TOPK-032 is highly dependent on PBK levels, and therefore PBK inhibition represents a fresh treatment paradigm for the molecular intervention of CRPC patients whose tumors harbour high levels of this kinase. We plan to repeat in the future such experiment with PCa cell lines expressing high levels of PBK.

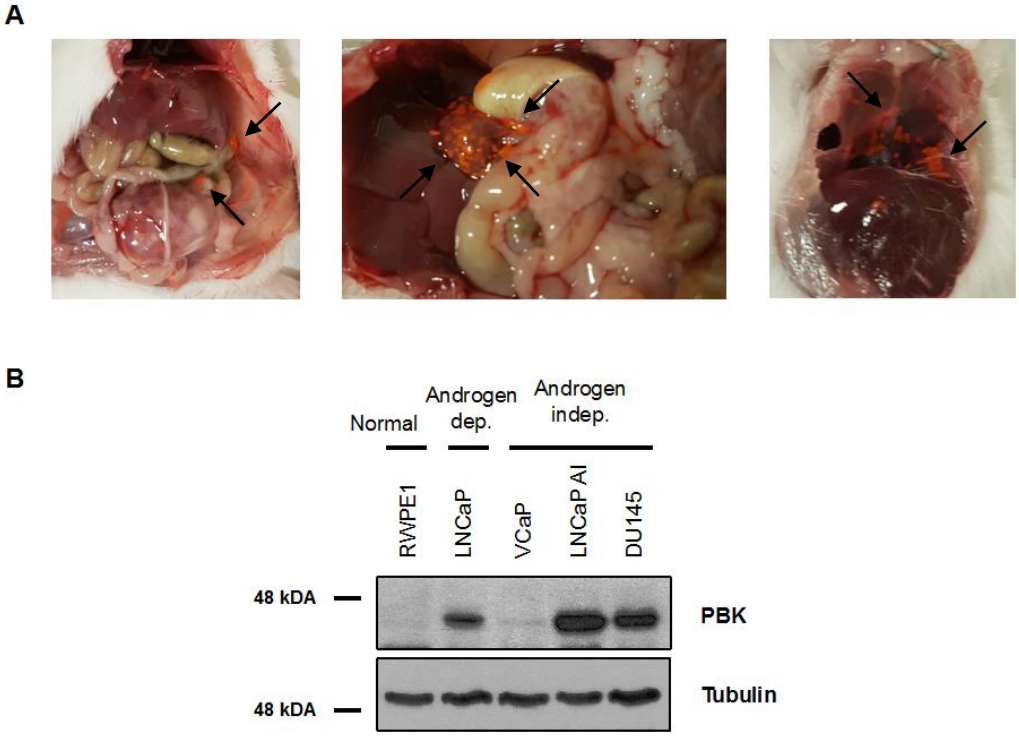

Figure 38. HI-TOPK-032 is highly dependent of PBK expression levels. A) Pictures from the abdominal cavity of HI-TOPK-032 treated mice showed accumulation of the compound, indicating poor drug solubility. **B)** PBK protein expression levels in different prostate cell lines.

2.5. FOXM1 regulates PBK high expression in advanced PCa

FOXM1 is a cell proliferation-specific transcription factor frequently overexpressed in several human solid cancers[333,334]. In PCa, high FOXM1 levels have been associated with aggressive prostate tumors and poor clinical outcomes[335]. Several evidence supports that this transcription factor promotes PCa progression by selectively regulating the transcription of typical androgen responsive genes, such as PSA and KLK2, and participates in the acquisition of chemoresistance and androgen independence[334,336]. Indeed, androgen independent PCa cells have demonstrated to have more FOXM1 binding sites than androgen independent cells. Since it has been shown that FOXM1 transcriptionally regulates PBK to enhance a malignant phenotype in adrenocortical and hepatocellular carcinomas[326], we aimed to test whether this regulation on PBK by FOXM1 also exists in PCa.

We subjected PBK to an *in Silico* analysis in order to identify potential transcription factors that could regulate PBK expression in PCa. Our findings confirmed that FOXM1 was significantly correlated with PBK in two different databases (Fig. 39). The E2F family seemed to play also an important role in the regulation of PBK in the disease. Interestingly, elevated levels of E2F1 have been previously linked to the progression of androgen independent PCa[337], which is consistent with our results. Nevertheless, we decided to continue exploring FOXM1 because it appeared as the most robust transcription factor in both PCa databases.

A

Gene	R	p-value
FOXM1	0.825	3.56e-73
E2F7	0.712	3.18e-45
MYBL2	0.697	1.39e-42
E2F8	0.688	4.04e-41
UHRF1	0.655	5.53e-36
ZNF367	0.638	1.30e-33
TCF19	0.627	2.82e-32
PTTG1	0.550	2.84e-23
E2F1	0.482	4.20e-17
VDR	0.476	1.37e-16

B

Gene	R	p-value
FOXM1	0.808	5.86e-113
UHRF1	0.763	3.78e-93
MYBL2	0.758	1.23e-91
E2F2	0.742	8.10e-86
PTTG1	0.720	2.17e-78
ZNF367	0.708	9.80e-75
E2F1	0.681	5.05e-67
E2F7	0.595	7.62e-47
E2F8	0.582	1.90e-44
TCF19	0.521	5.85e-34

Figure 39. Transcription factors regulating PBK in different stages of PCa. FOXM1 regulates PBK gene in **A)** Robinson *et al.*[269] (GSE21034) database and **B)** TCGA[270].

We further analyzed FOXM1 expression levels in three publicy available PCa databases (Fig. 40A-C). We showed that FOXM1 expression was consistently increased with increasing Gleason score. It was also upregulated in metastasis when compared to primary tumors. In addition, we revealed that this transcription factor had significantly elevated expression levels in CRPC tissues, not only compared to benign prostate tissues but also to localized hormone-naïve samples, confirming its malignant role in advanced stages of PCa.

After *in Silico* validation, we corroborated that FOXM1 protein levels were high in androgen independent PCa cells, slightly lower in androgen dependent cells and almost undetectable in non-malignant human RWPE-1 cells (Fig. 40G,H). Moreover, *in vitro* silencing of FOXM1 resulted in reduced PBK protein levels in both androgen dependent and independent LNCaP cell lines (Fig. 40I), thus validating FOXM1 as an upstream regulator of PBK in PCa.

Although we did not find upregulation of FOXM1 in our proteomic approach, CENPF was found to be overexpressed in LNCaP AI cells compared to LNCaP cells (Annexes). CENPF is a cell cycle-dependent kinetochore-associated protein that is required for kinetochore function and chromosome segregation in mitosis[338,339].

Previous studies have defined this mitotic protein as a driver of PCa progression[340], while Aytes *et al*.[331] identified FOXM1 and CENPF as synergic master co-regulators of PCa malignancy. Similar to FOXM1, we evaluated CENPF protein expression in different PCa cells and observed that it was consistently higher in androgen independent cell lines compared to both androgen dependent LNCaP and non-malignant RWPE-1 cells (Fig. 40G,H).

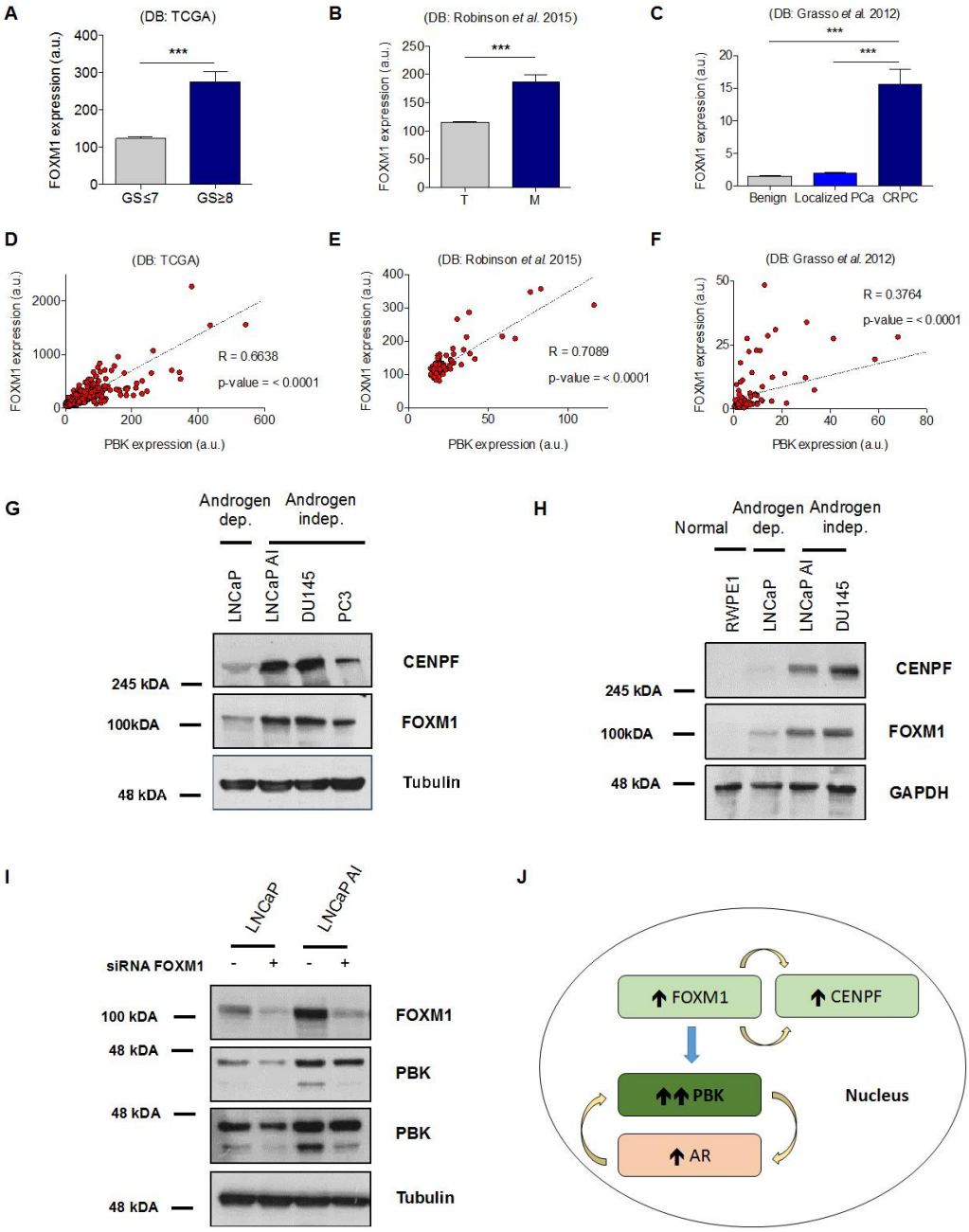

Figure 40. Regulation of PBK by FOXM1 might promote PCa progression. A) FOXM1 mRNA expression levels in low-grade PCa (Gleason score ≤7) (N = 292) and intermediate- and high-grade PCa (Gleason score) (N = 205). **B)** FOXM1 mRNA expression levels in prostate tumors from patients with primary (N = 262) or metastatic (N = 38) PCa. **C)** FOXM1 mRNA expression levels in benign prostate tissue (N = 28), hormone-naïve PCa tissue (N = 59) and CRPC tissues (N=35) from a clinical PCa cohort. **D)-F)** FOXM1 and PBK mRNA levels are

correlated in three different cohorts. **G),H)** Western blotting showing FOXM1 and CENPF expression in different PCa cell lines and in non-malignant human RWPE-1 cells. **I)** FOXM1 depletion results in reduced PBK expression, as shown by Western blotting. **J**) Model depicting a potential oncogenic pathway in the transition of PCa to androgen independence.

All these findings suggest that enhanced expression of PBK in advanced PCa disease might be a result of increased CENPF expression, which may lead to enhanced FOXM1 activity (Fig. 40J). Furthermore, the three candidates render indicative factors of PCa aggressiveness and, hence, promising targets for the molecular intervention of hormone-refractory patients.

.

DISCUSSION

1. Clinical challenges in the management of PCa

Despite its slow growth, PCa is still a lethal disease. It is the second most commonly diagnosed invasive malignancy and the fifth leading cause of cancer-related deaths among men worldwide[29]. The introduction of the PSA blood test has led to a dramatic increase in the early detection of the disease, when potentially curative treatment options are more effective. Upon early detection and when the tumor is confined to the prostate, PCa has demonstrated excellent cancer-specific survival rates[29]. However, once the cancer disseminates outside the prostate, current treatments such as ADT and chemotherapy commonly fail in the long run[90]. In fact, the 5-year survival of patients with metastatic PCa drops below 30%. Androgens play a crucial role in the initiation and progression of the disease and thus, ADT has been the mainstay of treatment for locally advanced, metastatic and recurring PCa for over 40 years. Almost all patients initially respond to different types of androgen-ablation therapies, however, remissions are temporary and most of them develop resistance and progress to a castration resistant state. Upon progression to CRPC, the disease remains essentially untreatable, and the median survival for those patients is less than 2 years[88]. Moreover, further insights into the molecular mechanisms governing the transition to androgen independence are needed, and therefore the clinical management of PCa remains a challenge.

Cancer genomics have delivered major advances in the management of solid malignancies, including PCa. Metastatic CRPC patients with homologous recombination repair (HRR) gene alterations are currently treated with PARP inhibitors, resulting in decreased PSA levels and improving progression-free survival (PFS)[341,342]. Recently, data from a whole-genome sequencing (WGS) study revealed distinct genotypes with potential clinical impact in metastatic CRPC, including MSI, homologous recombinant deficiency (HRD) enriched with BRCA2 alterations and CDK12 aberrations, among others[343]. However, only a small subset of patients is eligible for this treatment and potential therapeutic tools that can work in a broader number of PCa patients are clinically necessary.

Since the therapeutic benefits of current standard regimens are still very limited[92,132], there remains a keen interest in matching these patients with effective targeted treatments. Increasing evidence in recent years suggests that the AR selectively

upregulates M-phase cell cycle genes in androgen insensitive PCa cells[161], being therefore one of possible the underlying causes of CRPC development, along with the already well-established AR signaling pathway, and the focus of the present work.

Genomic and transcriptomic studies have already enabled a better understanding of the disease progression. In this context, some studies have reported that in early PCa already exists a side-population whose growth depends more on mitotic networks and less on androgen signaling[163,191], together suggesting an important role of M-phase genes in the transition to castration resistance. Notably, enrichment of mitotic proteins has been found in CRPC chemotherapy-resistant tumors[162], while Horning *et al.*[163] identified a subpopulation of PCa cells with enhanced cell cycle-related genes that had the potential to develop androgen independence. Mitotic aberrations, which contribute to tumor resistance and seem to confer PCa cells a growing advantage under androgen-depleted conditions, represent potentially actionable vulnerabilities that can enhance the effectiveness of existing therapies. Thus, identifying those novel potential targets for the treatment of CRPC represents an opportunity that cannot be missed.

In this work, we have carried out a proteomic approach in order to identify new mitotic regulators involved in the acquisition of prostate tumors androgen independence. Notably, this is the first study that examines the role of key mitotic regulators at the proteomic (instead of genomic) level in PCa. Several studies have already used state-of-art technologies for evaluating molecular mechanisms involved in CRPC development, providing great insights in the progression of the disease[237,238,245]. However, none of them focused on the involvement of M-phase candidates in the transition to androgen independence.

One of the major obstacles in PCa research has been the lack of cell lines that closely mimic the transition to androgen independence. Although DU145 and PC3 represent two “classical” well-known and broadly used in the literature androgen independent PCa cell lines, the behavior of these cells does not fully mirror clinical disease progression, since they are reported to be AR-negative[344,345]. Some other PCa cell lines, such as the 22Rv1, which express AR and were derived from a xenograft that was serially propagated in mice after castration-induced relapse of the parental, may also be considered good models for the study of CRPC, but lack thus far an accurate counterpart to study the whole progression process. At the time of initiation of this

project, LNCaP androgen independent sublines, including LNCaP AI, had been generated by several groups to provide more clinically relevant tools for *in vitro* and *in vivo* studies. LNCaP AI cells were established by culturing the androgen sensitive LNCaP cell line under hormone deprivation conditions for several passages, maintaining its AR nucleotide sequence and loosing the expression of well-known differentiation markers, thus better representing the transition to a castration resistant state[278]. Several studies have previously used this model to investigate the role of crucial mitotic kinases in androgen independent PCa[161,208,346]. In their work, Deeraksa *et al*.[208] demonstrated that PLK1 is reprogrammed for high-level expression in androgen independent LNCaP cells, highlighting the need to explore its properties for therapies in CRPC. Interestingly, LNCaP AI cells presented slower proliferation rates compared to their androgen dependent counterpart in our hands, Despite being already described in previous studies[208], this finding was not consistent with the aggressive and highly proliferative phenotype that characterizes the advanced PCa disease. We hypothesized that this phenomenon may be due to an in vitro artifact produced during the cell line establishment, without having any additional effect on the behavior of the cell culture and its clinical relevance.

Of note, AR was also overexpressed in androgen independent LNCaP AI cells, validating the *in vitro* model for the study of castration resistance in PCa. Although both androgen dependent and independent cell lines expressed AR, we observed that AR is strongly upregulated in LNCaP AI cells compared to LNCaP cells. Collectively, our findings suggested that the LNCaP AI cell line is a good starting point for studying androgen independence, since it mimics the clinical scenario of CRPC.

Considering that our attention was focused on G_2/M candidates, we checked the expression of the different key mitotic regulators that have been widely studied in the progression of the disease. Although expression levels of other mitotic kinases including BUB1[347], Aurora B[348] and NEK2[349] have been positively correlated with Gleason score and clinicopathological stage of PCa, efforts have been primarily focused on the study of motor proteins and PLK1 and Aurora A kinases. Liu *et al*.[350] reported that CDK1, the central driver of mitosis, is overexpressed in PCa and contributes to tumorigenesis by promoting cell proliferation. Upregulation of CDK1 in androgen independent PCa was also described by Chen and colleagues[301]. They demonstrated that this kinase is responsible for increasing AR expression and stability

in response to low androgen levels. Other studies revealed that Aurora A levels were significantly elevated in prostate tumors[351], and especially in AR-positive CRPC tumors[194], when compared with non-neoplastic samples. Moreover, PLK1, a critical regulator of the cell cycle, is also found to be overexpressed in PCa and linked to tumor grades[204,205]. Its expression is correlated not only with tumorigenesis, but also with AR expression and activity[207]. Kinesins, which play an important role during disease progression, have also been extensively studied in PCa. The expression of KIF11, for example, might be an independent parameter for PCa aggressiveness and could be used as a prognostic biomarker[352]. In our study, higher protein levels of CDK1, Aurora A, PLK1 and KIF11 were observed in the LNCaP AI cell line, corroborating the results from previous studies and highlighting a potential role of mitotic regulators as molecular drivers of hormone-refractory PCa.

Overall, we believed that expression of mitotic proteins may be part of the reprogramming process to allow PCa cells to grow under androgen-depleted conditions and, consequently, are attractive targets for the treatment of CRPC patients.

2. High-throughput quantitative proteomics unveils actionable mitotic candidates for the treatment of CRPC

Progression to CRPC is still a major clinical problem and mechanisms involved in this lethal disease remain to be elucidated.

Mitotic regulators have been described to be involved in the acquisition of resistance in several cancer types[353-355]. In PCa, resistance to taxol or androgen ablation therapies has been linked to PLK1 overexpression[204-207]. High levels of Aurora A are associated to resistance to androgen depletion regimens and progression to NEPC[103,194], while upregulation of KIF11 has been observed in docetaxel-resistant PCa cells[188]. Based on this evidence, efforts have been focused on the development of inhibitors targeting these mitotic proteins during the last decades. Several small molecule inhibitors have entered clinical trials for PCa (Table 4-6), especially in the setting of castration-resistance, but have failed to demonstrate benefit in the long-term. Therefore, identifying new mitotic markers for effective patient stratification, discovering novel potential targets and improving combination therapies becomes of utmost importance.

In this study, we performed a high-throughput quantitative proteomics analysis to gain molecular insights into the involvement of mitotic regulators in the acquisition of prostate tumors castration resistance. Advances in the field of proteomics have provided the opportunity to study the proteomic signature of virtually any biological specimen and it has been applied to various areas of science, such as the discovery of biomarkers or disease-specific targets for drug development[356,357]. Here, we arrested both androgen dependent and independent LNCaP cells in mitosis and performed a proteomic analysis to compare the differential global protein expression between the two PCa cell lines. We identified over 2800 proteins and specified over 450 proteins as significantly differentially expressed between both cell lines.

Several studies previously used proteomics aiming at unveiling the mechanisms of PCa progression. Saraon *et al*.[245] benefited from the SILAC technique to associate enzymes of the ketogenic pathway with androgen independent PCa, while Iglesias-Gato *et al*.[246] employed a SILAC-based approach to compare the protein expression of prostate bone metastasis and primary tumors and identified increased levels of proteins involved in cell cycle progression. Furthermore, distict kinase phosphorylation signatures in mCRPC compare to hormone-naïve primary prostate tissues have been

described using phosphoproteomics[261], confirming that kinases have a key role in driving resistance to hormonal therapies in PCa. However, to our knowledge this is the first quantitative proteomic study focused on the involvement of M-phase regulators in the critical transition to androgen independence.

Since key mitotic proteins seem to be overexpressed in CRPC, only candidates that were found to be upregulated in the LNCaP AI cell line were further investigated in the current work. As expected due to the G_2/M arrest of the cells, we noticed that the most enriched biological process was cell division, suggesting that higher expression of cell cycle genes may contribute to the clinical progression of PCa. Moreover, 6 proteins among our top mitotic upregulated candidates (CDK1, KIF4A, ASNS, KIF11, PBK and KIF20A) have been previously described to be altered in PCa progression. Our results were consistent with the work of Ramos-Montoya and colleagues[191], who associated these six candidates with a cell cycle network involved in CRPC tumor growth. Besides, CDK1 and ASNS have been shown to be involved in both AR stability and development of CRPC[301,302]. KIF20A was found by Tamura *et al*[300] as one of the upregulated genes observed in the progression to hormone-refractory PCa, while high expression of KIF4A[358] and KIF11[352] have been previously associated with poor clinical outcomes and PCa tumor progression. Here, a new research line targeting the actionable kinesin KIF11 has been initiated in the lab based on these proteomics results. All these findings highlight the robustness of our study and support that high activities of mitotic regulators are linked to advanced PCa disease.

Surprisingly, neither PLK1 nor AURKA were detected on our quantitative proteomic approach, even If these mitotic kinases have demonstrated to have higher protein levels in androgen independent PCa cell lines and have been already linked to androgen independent PCa growth[191,192,208]. In both cases, it might be explained by the relative lower abundance of kinases and the difficulty to detect them when high abundant proteins are present.

After validating our M-phase protein candidates and confirming their important role in different public databases, we decided to futher explore the serine/threonine mitotic kinase PBK for the following reasons: (i) it is a kinase, which are mostly expressed in actively dividing cells and are therefore main targets of anticancer therapies, (ii) it has been shown to be involved in the development and progression of different tumor

types, including PCa, and (iii) it is a druggable target with some pharmacological inhibitor already available. Nevertheless, it is important to emphasize that our study contains many potential candidates that are being further evaluated in our laboratory. Overall, these data underline the potential value of using proteomics to identify clinical actionable targets and therefore expand the therapeutic options for a group of patients who currently lack effective treatments. A proteomic-based approach using human CRPC samples would allow us to continue investigating the molecular mechanisms involved in the transition to the lethal disease of PCa and confirm the validity as well as the robustness of our findings.

3. PBK expression as a biomarker of poor prognosis

TOPK/PBK may be involved in the development and growth of various cancer types, such as breast, lung, colorectal cancers and hematological malignancies, where it is associated with poor clinical outcomes[319,320,329].

Performing clinical validation on samples representing different stages of the disease, including benign, hormone-naïve and hormone-refractory (CRPC) specimens, we found that higher expression of PBK was strongly correlated with tumor aggressive features. Interestingly, PBK nuclear localization was predominantly detected in advanced disease, particularly in CRPC tissue samples, suggesting that both PBK expression and localization could have relevant clinical implications in castration-resistant state. Our findings are in good agreement with earlier studies, where PBK expression was significantly associated with PCa progression[304] and nuclear localization correlated well with cancer grade and stage[308].

More importantly, our immunohistochemical analysis in tissue microarrays demonstrated that PBK could be considered as a promising indicator of relapse. Assessing PBK expression, we were able to discriminate between patients who did not present biochemical recurrence and those who experienced it, highlighting the potential role of the kinase as a molecular marker to asses response to therapy. In this regard, we will compare in the future TOPK/PBK expression on biopsies for which we know the clinical outcome in regard to the anti-hormonal therapy that patients have been submitted to. Here, we corroborated previous reports demonstrated that higher expression of PBK was an independent prognostic factor of recurrence in the early stage of PCa.

Despite the retrospective nature of our study, our data provide strong evidence that PBK is overexpressed during the development of CRPC and, hence, might be involved in the progression of the disease to advanced stages, where no effective therapeutic options are available to date. Since the kinase appears to be highly activated in cancer and its expression is hardly detectable in normal tissues[316], it was suggested as a promising molecular target, and our attention was focused on the impact of PBK inactivation in PCa, primarily hormone-refractory.

4. PBK overexpression – consequence or driver in PCa?

Despite the already well-defined correlation between tumor progression and PBK expression, no data supporting the specific role of this kinase in the acquisition of androgen independence in PCa has been described yet. Going a step further, we wanted to investigate the capacity of androgen dependent LNCaP cells overexpressing PBK to grow under hormone-depleted conditions, which is the main characteristic of castration resistance.

In their work, Brown-Clay *et al*.[308] generated stable LNCaP and VCaP cell lines overexpressing PBK in order to evaluate whether PCa cells with low endogenous PBK levels exhibits increased invasiveness upon ectopic expression of the kinase. They showed that PBK overexpression resulted in increased invasiness and cell proliferation of the transfected clones, suggesting that PBK high levels are associated with the proliferative potential of PCa cells and thus provide a more aggressive cell type. Nevertheless, its role as a driver of androgen independent PCa was still unknown.

Here, we identified PBK for the first time as a novel master regulator of androgen independence that is able to maintain cell growth of androgen dependent PCa in the absence of androgens. The potential of this mitotic kinase as a target for cancer therapy has already been investigated in many types of cancer; however, this is the first study confirming its role as a driver in the transition to androgen independent PCa. PBK overexpression has shown to increase invasiveness and thus metastatic capacity *in vitro* and *in vivo* in PCa[308], but so far no study has shown the potential of this protein as a driver of androgen independence. Moreover, this statement can be expanded to other mitotic kinases and tumor types that are dependent on hormones to grow, such as breast cancer, highlighting the unique feature of our finding.

The castration resistant state develops under selective pressure of androgen deprivation; hence, PBK overexpression appear to serve as a key survival strategy allowing PCa cells to become increasingly aggressive and gain androgen independent properties. This observation not only fits with other reports providing evidence of the importance of M-phase cell cycle genes in the development of resistance mechanisms[222], but also offers a fresh treatment paradigm for the molecular intervention of CRPC patients. In this case, overexpression of just one mitotic protein was sufficient for androgen dependent LNCaP cells to acquire androgen independent

properties, reinforcing the crucial role of PBK in the whole process.

Altogether, our findings support that PBK overexpression is not a consequence but a driver of androgen independent PCa, and thus PBK could be considered a promising therapeutic target for the androgen independent disease. Inhibition of this kinase offers therefore an exciting treatment approach for CRPC patients who have limited therapeutic options. A further exploration of the signaling pathways involved in this transition will allow us to better understand the mechanism by which PBK promotes castration-resistant growth and identifiy other potential drug targets.

5. Is PBK a potential therapeutic target for the treatment of CRPC patients?

Several studies previously investigated the effect of PBK inhibition in different types of cancer. As examples, PBK promotes cell migration and invasion in lung cancer by modulating a PI3K/PTEN/AKT-dependent signaling pathway[303], knockdown of this kinase inhibits proliferation and clonogenicity in breast cancer[306], and the pharmacological inhibition of PBK effectively suppresses colon cancer growth[305]. In PCa, PBK enhances the aggressive phenotype by increasing the invasive ability via β-catenin-TCF/LEF-mediated matrix metalloproteinases production, and by acting within a reciprocal feedback loop with the AR[308]. In addition, this serine/threonine kinase has been identified as a downstream target of different oncogenic transcription factors, including c-Myc and E2F, which have significant roles in PCa biology[315,359]. Knockdown of PBK results in reduced cell proliferation and migration in PCa cells *in vitro*[308,313], but its effect in preclinical PCa mice models remains to be elucidated. Although no PBK inhibitor is approved for any tumor yet, PBK is regarded as a potential therapeutic approach in PCa treatment.

In PCa, Sun *et al*.[313] reported that knocking down PBK resulted in a decreased migration of circulating tumor cells (CTCs) in PCa. Moreover, PBK has been associated with AR signaling, having key roles in both tumor invasion and metastasis regulation[304]. Although none of the currently available inhibitors has entered clinical trials to date, we believe that PBK inhibition could be a promising therapeutic target for the treatment of CRPC patients.

HI-TOPK-032, which has already demonstrated high efficacy in preclinical studies in several tumors (Table 15), resulted in decreased cell viability in androgen dependent and independent cell lines. Consistently with other studies[305,312], we observed that PBK pharmacological inhibition in PCa cells caused increased expression of the mitotic marker pH3, followed by an increase of apoptosis, as shown by elevated levels in both caspase-3 and cleavage PARP well-known apoptotic markers. Importantly, HI-TOPK-032 had little effect on the non-malignant RWPE1 prostate cell line, and thus we confirmed that PBK inhibition might be a promising target for the molecular intervention of androgen independent PCa. Depletion of PBK by means of shRNAs confirmed the specificity of the pharmacological inhibitor in our hands as a proof-of-concept.

In this context, we proved that the selective PBK inhibitor HI-TOPK-032 also reduced viability of anchorage-independent PCa patient-derived cells grown *ex vivo*.

Notably, this is the first report that tested the effect of therapeutically targeting PBK on CRPC patient-derived tumor spheres. Data from Warren *et al*.[304] revealed a decresed in PCa tissue proliferation after treatment with HI-TOPK-032, as assessed by Ki67 staining, but on hormone-naïve primary patient tumors. Ikeda and colleagues[329] had already described the tumor suppressive effects of PBK inhibition in patient-derived ovarian cancer cells. Again, we detected a caspase-dependent apoptosis of the prostate spheroids, in agreement with the results observed in LNCaP cells growing in monolayer. Taken together, these findings empowered the use of patient-derived cells as *ex vivo* models to evaluate novel therapies for advanced-stage PCa patients and highlighted the potential of PBK as a valid future target for the hormone-refractory disease.

Analysis of PBK kinase activity and its downstream target ERK1/2 showed a dose-dependent marked reduction of phosphorylated forms of these proteins in the HI-TOPK-032 treated patient-derived PCa culture. These results are in agreement with other reports that demonstrated that HI-TOPK-32 inhibited cancer cell growth by reducing ERK-RSK phosphorylation as well as increasing cell apoptosis through regulation of the abundance of cleaved PARP[309], underlining the robustness of our study. Although little is still known about the ‘in-depth’ mechanism of this kinase in carcinogenesis, our work further emphasizes the role of PBK in tumor cell growth by regulating ERK signaling pathway.

Several pharmacological agents targeting PBK, such as HI-TOPK-032 and OTS514, have been previously investigated *in vivo* for various cancer types, presenting an interesting avenue of cancer-targeted therapy. However, the effects of PBK inhibitors in PCa xenograft models are, to date, unknown. In the present study, we validated and reinforced the obtained *in vitro* and *ex vivo* results using a NP53 (Nkx3.1CreERT2/+; Ptenflox/flox; p53flox/flox) GEM model, which represents a common PCa phenotype and was already employed to investigate disease malignancy[331]. Of note, mice were previously castrated in order to mimic the clinical scenario of hormone-refractory PCa. Concordantly with previous studies in other cancers (Table 15), our findings revealed that the intravenous administration of 10 mg/kg HI-TOPK-021 in pre-established

subcutaneous PCa xenografts led to a marked tumor growth attenuation without significant loss of animal body weight. Surprisingly, when this PBK inhibitor was combined with enzalutamide, the effect on tumor growth reduction was lower than the observed with HI-TOPK-032 alone, but higher than the produced by enzalutamide as single agent. Here, based on previous evidence and the results obtained by Warren *et al*.[304] in which they uncover a novel interplay between AR and PBK, we hypothesized that enzalutamide treatment decreased PBK transcription levels, thereby diminishing protein levels and leading to reduced HI-TOPK-032 efficacy. We observed that treatment of both androgen dependent and androgen independent LNCaP cells with enzalutamide at suboptimal doses resulted in a marked decrease of PBK protein levels, thus confirming our hypothesis. In this context, our study demonstrated that HI-TOPK-032 activity is highly dependent on PBK protein expression levels. This finding was further reinforced by the lack of HI-TOPK-032 efficacy observed in the orthotopic PCa mouse model, which was established using a PCa cell line that harbors very low levels of this kinase.

In agreement with tumor growth data, immunohistochemical analysis indicated a strongly reduction in the % of Ki67 positive cells in the treated group, confirming the *in vivo* antitumor potential of the PBK inhibitor in PCa. Moreover, staining of downstream targets of PBK and markers of mTOR pathway were strongly decreased in HI-TOPK-032 treated tumors, thus corroborating the efficacy and specificity of the PBK inhibitor. Nevertheless, Western Blotting analysis of the extracted tumors at the end of the experiment did not resulted in a decrease in p-PBK levels (data not shown), contrary to the results observed at our *in vitro* studies. This is likely due to the late collection of the samples, since mice were sacrified a couple of days after the last HI-TOPK-032 dosis and we hypothesized that a reduction of PBK phosphorylated form could only be seen shortly after PBK pharmacological treatment.

Going a step further, we wanted to determine how PBK might be regulated. FOXM1 and CENPF have been described as synergistic drivers of PCa progression[331], while the former has been already associated with increased metastatic potential and with the acquisition of chemoresistance and androgen independence[334,336,360]. Indeed, a transcriptional regulation of PBK and FOXM1 has been demonstrated in other tumor types[326,361]. Our study supports that a correlation between PBK and FOXM1 also exists in advanced human PCa. We therefore hypothesized that higher PBK expression in

CRPC is prompted by enhanced FOXM1 activity, which in turns may lead to increased CENPF expression. However, further analyses are required to confirm this mechanism.

All these findings confirmed PBK as an important molecular target for the treatment of PCa and demonstrated the therapeutic potential of HI-TOPK-32 not only i*n vitro* in PCa cell lines and patient-derived cultures, but also *in vivo* in preclinical mouse models, without significant signs of toxicity. Our results strengthen and broaden the crucial role of PBK in cellular survival and pave the way to further explore this kinase as a potential treatment option for CRPC patients.

Targeting different pathways simultaneously could potentially be an effective strategy for the treatment of cancer, and particularly of hormone-refractory PCa. Although the combination of HI-TOPK-032 with enzalutamide decreased its therapeutic potential, the combined treatment may still provide modest clinical benefits compared to enzalutamide monotherapy. Moreover, the combination of PBK inhibition and chemotherapy agents remains to be elucidated.

The novelty of our study relies on the efficacy demonstrated by HI-TOPK-032 in a patient-derived PCa culture and *in vivo* in a preclinical mice model. Thus, we conclude that PBK inhibition represents a promising therapeutic option when aiming at specifically targeting hormone-refractory PCa, especially for patients whose tumors present with high levels of PBK. Clinical trials will be essential to evaluate and fully validate the utility of this small molecule inhibitor in CRPC patients.

At present, we are planning to decipher the mechanisms that are involved in the acquisition of resistance to PBK inhibition. For this purpose, we would take advantage of preclinical models and perform high-throughput quantitative proteomics to compare sensitive and resistant tumors with the aim of identifying proteins that are associated with resistance. Next steps will also include another orthotopic model to confirm the results obtained from the PCa subcutaneous xenograft. Phosphoproteomics will be key in order to examine PBK signaling pathway, thus providing a better overview of the relevance of PBK in CRPC and maximizing clinical response.

Overall, we demonstrated that (i) several mitotic regulators become upregulated during the progression of PCa, (ii) a significant correlation between PBK expression and clinical outcome in PCa patients, (iii) strong tumor-suppressive effects of HI-TOPK-032 both *in vitro* and *in vivo*, and (iv) a key role of PBK coordinating and driving the

transition to an androgen independent state in PCa. The unique properties presented in this study prompted us to continue investigating and underscored the importance of our approach for unveiling novel candidates that will be follow up by our group (Fig. 41). The mechanistic role of PBK and its potential downstream targets in the acquisition of androgen independence still requires better exploration; however, our data provided sufficient evidence that PBK is a critical regulator of androgen independence, thereby highlighting PBK inhibition as an attractive treatment approach for CRPC patients.

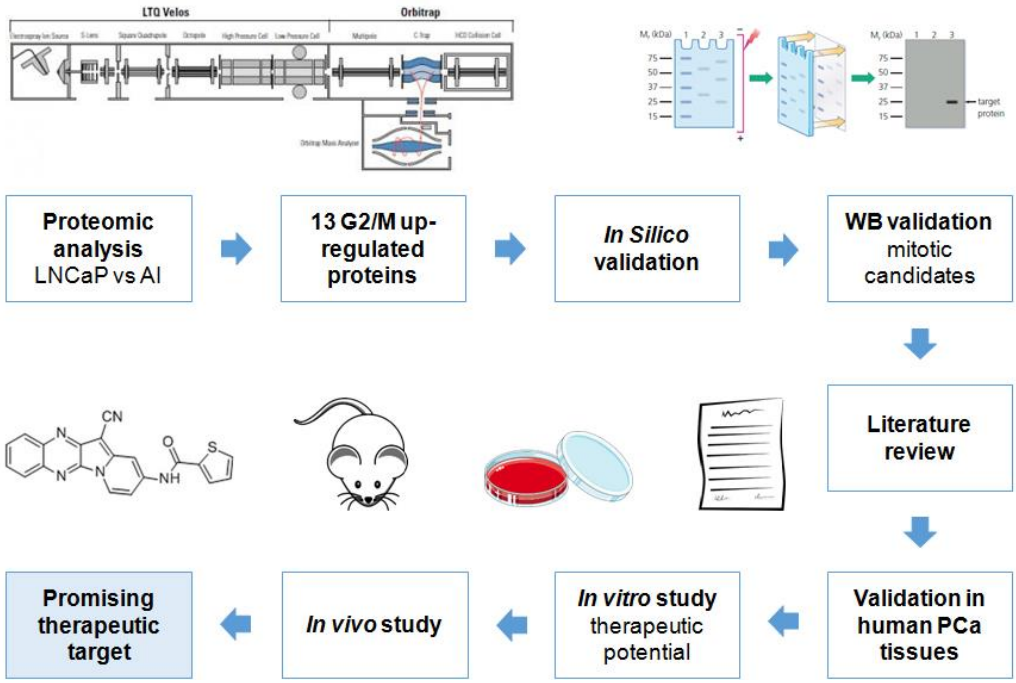

Figure 41. Workflow followed in the study in order to identify potential therapeutic targets for the molecular intervention of CRPC patients.

CONCLUSSIONS

First: A high-thoughput quantitative proteomic approach enables the identification of actionable mitotic proteins as potential therapeutic targets for the treatment of CRPC.

Second: Higher expression of cell cycle genes, and in particular M-phase genes, functionally contributes to the progression of PCa to androgen independence.

Third: The serine/threonine mitotic kinase PBK is overexpressed in CRPC tissues, not only compared to benign prostate tissue but also to localized hormone-naïve samples, indicating that PBK might play a role in the progression of PCa. Higher protein levels of PBK are associated with biochemical recurrence and, hence, with poor prognosis.

Fourth: PBK overexpression promotes cell proliferation of androgen dependent PCa in androgen-depleted conditions, highlighting the role of this kinase as a driver in the transition to androgen independent disease.

Fifth: Pharmacological inhibition of PBK strongly suppresses PCa growth *in vitro*, *ex vivo* and *in vivo*; and therefore offers a novel treatment paradigm for the molecular intervention of CRPC patients.

Sixth: Enzalutamide decreases PBK transcription levels, thereby diminishing PBK protein levels and reducing HI-TOPK-032 efficacy. The activity of HI-TOPK-032 is highly dependent on PBK expression levels and thus, PBK inhibition represents an encouraging therapeutic option for CRPC patient whose tumors present with high PBK levels.

Seventh: Higher expression of PBK in advanced PCa disease might be a result of enhanced FOXM1 activity, which also leads to increased CENP-F expression. All three candidates render indicative factors of PCa aggressiveness and, hence, promising targets for the treatment of hormone-refractory PCa.

ANNEXES

Annex 1. Quality controls from the quantitative proteomics approach using three independent replicates

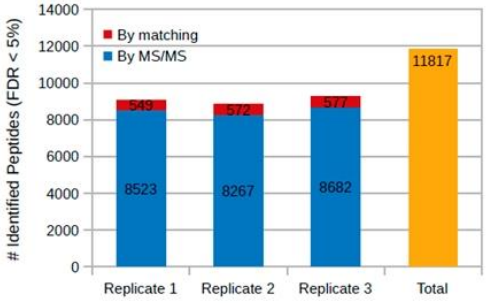

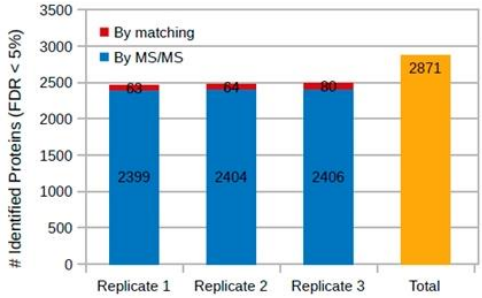

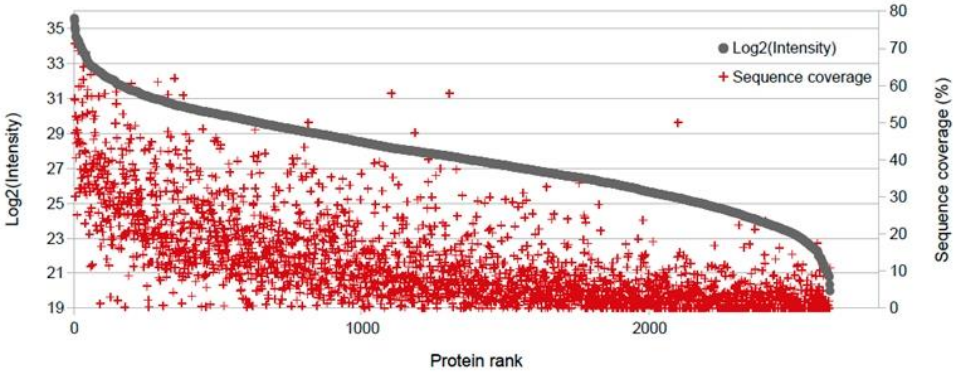

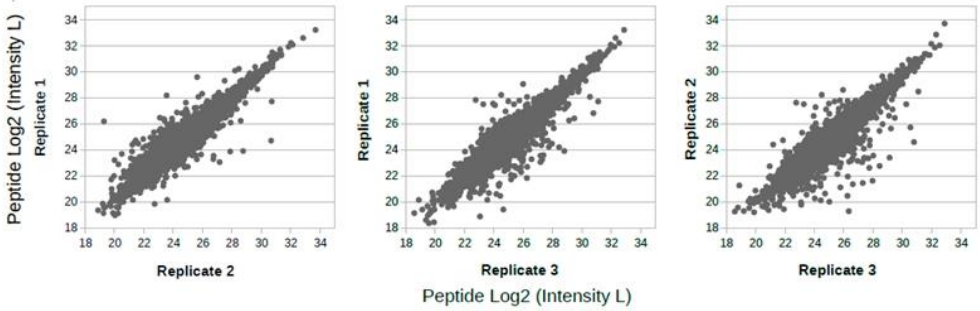

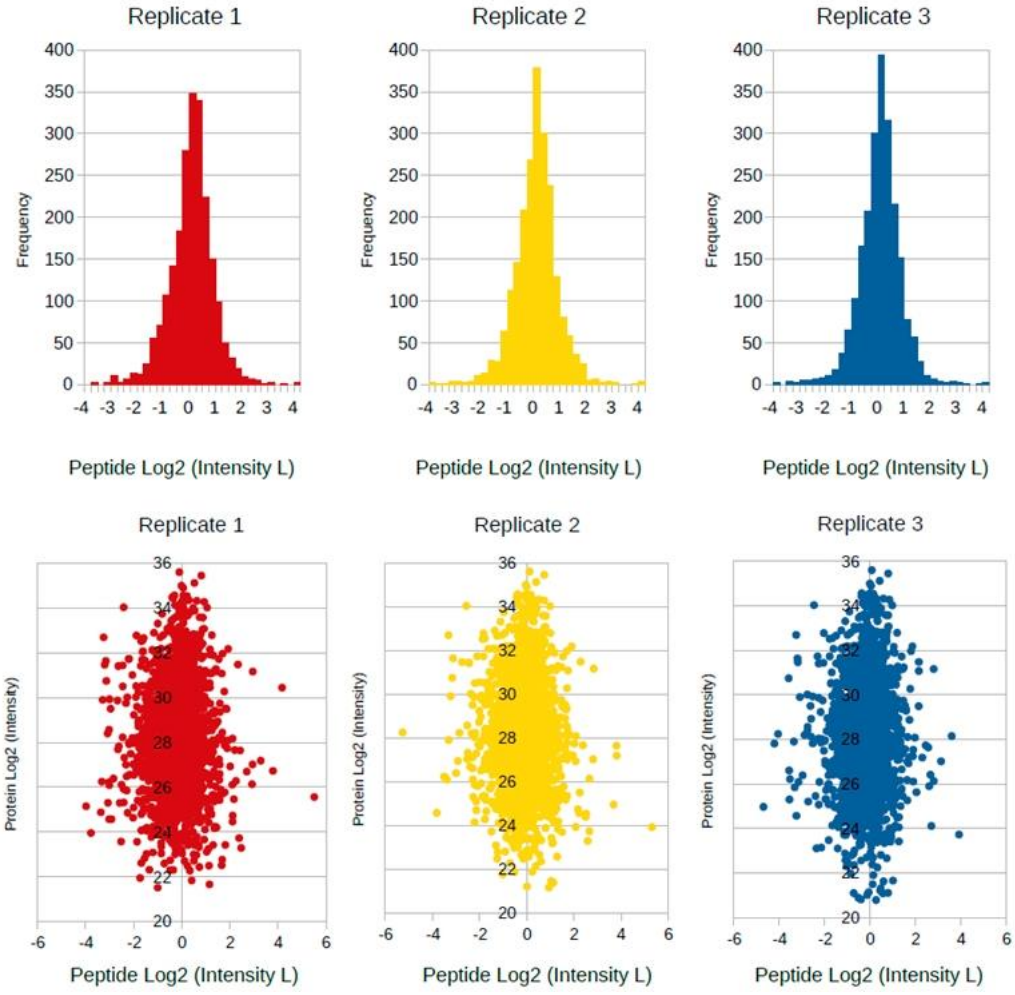
Replicate 1
Replicate 2
Replicate 3
Frequency
Peptide Log2 (Intensity L)
Protein Log2 (Intensity)

Annex 2. List of significantly upregulated proteins (q-value ≤ 0.05) in LNCaP androgen independent cells

Protein IDs	Genes	log2 Ratio L/H Rep. 1	log2 Ratio L/H Rep. 2	log2 Ratio L/H Rep. 3	T-test p-value	T-test q-value	T-test Difference	Fold Change
Q9Y4K1	AIM1	-2,942439318	-2,810319662	-3,12816143	0,000968354	0,029740126	-2,960306803	7,782894513
Q01813	PFKP	-2,951886177	-2,838911533	-2,80310297	0,000244862	0,029228323	-2,86463356	7,283508446
P31947	SFN	-2,919511795	-2,661931992	-2,805663824	0,00070981	0,029228323	-2,795702537	6,943689984
P06493	CDK1	-2,336426258	-2,284040213	-2,149877071	0,000605336	0,029228323	-2,256781181	4,779239878
O95239	KIF4A	-2,116531134	-2,171174765	NaN	0,008112808	0,049329832	-2,143852949	4,419407455
P61024	CKS1B	-1,893828154	-2,020022154	-2,451303482	0,00626792 1	0,045164187	-2,12171793	4,352118774
P67936	TPM4	-1,921969533	-2,089057446	-1,976363659	0,000607234	0,029228323	-1,995796879	3,988363434
P20839	IMPDH1	-2,01303339	-2,074847937	-1,695459366	0,003695883	0,038153714	-1,927780231	3,804693483
O60701	UGDH	-1,929260731	-1,904927135	-1,866235495	9,32533E-05	0,023795133	-1,90014112	3,73249705
Q16555	DPYSL2	-1,666074872	-1,750820875	-2,149324417	0,006385709	0,045261668	-1,855406721	3,618537497
P16152	CBR1	-1,767824292	-1,707127213	-1,770194769	0,000139317	0,024566889	-1,748382092	3,359815687
P08243	ASNS	-1,698885202	-1,701327324	-1,803929567	0,000397935	0,029228323	-1,734714031	3,328135176
O95757	HSPA4L	-1,554294109	-1,720847487	-1,887759209	0,00311417	0,03757262	-1,720966935	3,296572785
Q15276	RABEP1	-1,824319839	-1,629426599	-1,54210937	0,002499762	0,035903561	-1,665285269	3,171763649
O60232	SSSCA1	-1,580531359	-1,711803317	-1,639278412	0,000532932	0,029228323	-1,643871029	3,125032144
P52732	KIF11	-1,46152854	-1,629379988	-1,73534894	0,002446288	0,035903561	-1,608752489	3,04988002
Q93045	STMN2	-1,68329227	-1,723602176	-1,384105086	0,004465833	0,03977371	-1,596999844	3,025135667
Q13303	KCNAB2	-1,787474275	-1,565451026	-1,398733377	0,005015733	0,041372413	-1,583886226	2,997762784
Q99829	CPNE1	-1,59158361	-1,685850382	-1,407407165	0,002730241	0,035910878	-1,561613719	2,951838351
P08473	MME	-1,35236299	-1,670477748	-1,587988973	0,003823744	0,038172726	-1,536943237	2,901790242
Q96KB5	PBK	-1,287235856	-1,650672674	-1,655214429	0,006280523	0,045164187	-1,531040986	2,889942897
P0CG35; P0CG34	TMSB15B; TMSB15A	-1,576715589	-1,716683626	-1,244460821	0,008462065	0,049828543	-1,512620012	2,853277394
P52292	KPNA2	-1,582459688	-1,469312906	-1,465556622	0,000648254	0,029228323	-1,505776405	2,839774563
P82970	HMGN5	-1,274947405	-1,625130296	-1,587172985	0,005456601	0,043030222	-1,495750229	2,820107638

(continued)

Protein IDs	Genes	log2 Ratio L/H Rep. 1	log2 Ratio L/H Rep. 2	log2 Ratio L/H Rep. 3	T-test p-value	T-test q-value	T-test Difference	Fold Change
Q16881	TXNRD1	-1,541564345	-1,535405993	-1,394404292	0,001038122	0,029918461	-1,49045821	2,809782017
P12814	ACTN1	-1,428249598	-1,471447587	-1,485942006	0,000140467	0,024566889	-1,46187973	2,754670441
P36969	GPX4	-1,680324316	-1,358171225	-1,267176151	0,007539866	0,048266875	-1,435223897	2,704241315
P20020	ATP2B1	-1,496513486	-1,424760938	-1,25586319	0,002614224	0,035910878	-1,392379204	2,625112415
Q16890	TPD52L1	-1,536599994	-1,236890554	-1,37801218	0,003890475	0,038172726	-1,383834243	2,609610049
Q9NRV9	HEBP1	-1,306845546	-1,394349456	-1,444666982	0,000847863	0,029228323	-1,381953994	2,606211189
Q9UI15	TAGLN3	-1,305153489	-1,528671384	-1,288535833	0,003159681	0,03757262	-1,374120235	2,59209795
Q08257	CRYZ	-1,37428844	-1,510151863	-1,226261973	0,003560169	0,037765449	-1,370234092	2,58512509
P49321	NASP	-1,449006677	-1,170501947	-1,435841918	0,004473771	0,03977371	-1,351783514	2,552274523
Q9HB71	CACYBP	-1,417487979	-1,319444418	-1,223731399	0,00179016	0,034136686	-1,320221265	2,497044038
Q15046	KARS	-1,34192884	-1,060670018	-1,411588907	0,007042804	0,046880576	-1,271395922	2,413950214
Q15645	TRIP13	-1,064262033	-1,241718173	-1,438878417	0,007428548	0,047914758	-1,248286208	2,375590564
O43252	PAPSS1	-1,243912816	-1,260567665	-1,231493831	4,57394E-05	0,019037885	-1,245324771	2,370719163
P13796	LCP1	-1,238542318	-1,226631761	-1,260146141	6,23878E-05	0,019838945	-1,241773407	2,364890536
P37802	TAGLN2	-1,307078719	-1,183835864	-1,091801405	0,002715769	0,035910878	-1,194238663	2,288240455
Q96P70	IPO9	-1,372394919	-1,165879846	-1,013140678	0,007643497	0,048290015	-1,183805148	2,271751683
Q8WUH6	TMEM263	-1,080862284	-1,273814201	-1,188021064	0,002226437	0,035880789	-1,180899183	2,267180387
P05067	APP	-1,103195429	-1,251204014	-1,164657593	0,001336747	0,03337557	-1,173019012	2,254830538
P13995	MTHFD2	-1,014783859	-1,274172187	-1,203201175	0,004391518	0,03977371	-1,164052407	2,240859828
P17174	GOT1	-1,251204014	-1,000432849	-1,193834782	0,00433436	0,039769023	-1,148490548	2,216818335
O95235	KIF20A	-1,179956913	-1,00396204	-1,261410475	0,004347474	0,039769023	-1,148443143	2,216745493
O15347	HMGB3	-1,186880708	-1,028639913	-1,215989113	0,002579616	0,035903561	-1,143836578	2,209678653
Q9P1F3	ABRACL	-1,13520658	-1,131523728	-1,058870673	0,000502315	0,029228323	-1,108533661	2,156263756
Q9NVE7	PANK4	-1,082975149	-1,095046639	NaN	0,003528372	0,037765449	-1,089010894	2,12728141
P12004	PCNA	-1,172295451	-1,04236424	-1,044813871	0,001555997	0,033986413	-1,086491187	2,123569296

(continued)

Protein IDs	Genes	log2 Ratio L/H Rep. 1	log2 Ratio L/H Rep. 2	log2 Ratio L/H Rep. 3	T-test p-value	T-test q-value	T-test Difference	Fold Change
P49589	CARS	-1,172423482	-0,933421612	-1,145090461	0,004822341	0,040790074	-1,083645185	2,119384263
P55209	NAP1L1	-1,168385386	-1,013641	-1,00489676	0,002489121	0,035903561	-1,062307715	2,088269219
O43852	CALU	-1,122672677	-0,877115965	-1,136257052	0,006426561	0,045341313	-1,045348565	2,063864942
Q08945	SSRP1	-1,17287159	-0,977902651	-0,985136092	0,003706679	0,038153714	-1,045303444	2,063800395
P53582	METAP1	-1,104202509	-0,911653221	-1,075395703	0,003369134	0,037650691	-1,030417144	2,042614773
O75506	HSBP1	-1,049700499	-1,086240292	-0,953377068	0,001477562	0,03337557	-1,029772619	2,041702437
P08195	SLC3A2	-0,953377068	-1,138421297	-0,996894896	0,00293071	0,036778013	-1,02956442	2,041407815
Q9P289; O00506	STK26; STK25	-1,024603367	-0,97555685	-1,049979091	0,000461243	0,029228323	-1,016713103	2,023304004
Q9Y281	CFL2	-0,945607722	-1,002090335	-1,093222141	0,001794907	0,034136686	-1,013640066	2,018998818
P00491	PNP	-1,161758661	-0,91096288	-0,943958819	0,006066307	0,044865282	-1,00556012	2,007722835
Q06830	PRDX1	-1,052346349	-0,984698653	-0,977682948	0,000560675	0,029228323	-1,004909317	2,006817351
Q99729	HNRNPAB	-1,032735705	-0,995086432	-0,934554219	0,000837698	0,029228323	-0,987458785	1,982689533
Q9Y237	PIN4	-1,12816143	-0,906582832	-0,892896116	0,006048585	0,044865282	-0,975880126	1,966840716
O95456	PSMG1	-1,058593631	-0,83673209	-1,006549358	0,004761536	0,040653212	-0,967291693	1,9551668
Q96C90	PPP1R14B	-0,952184439	-1,010421753	-0,905350924	0,001009077	0,029918461	-0,955985705	1,939904599
Q14914	PTGR1	-1,010135412	-0,816313028	-1,006046653	0,004554413	0,03977371	-0,944165031	1,924074993
Q15293	RCN1	-0,873655677	-0,988775611	-0,966651976	0,001395821	0,03337557	-0,943027755	1,922558843
Q9UKK9	NUDT5	-0,867026627	-1,088141561	-0,812210679	0,008255729	0,049329832	-0,922459622	1,895343875
Q8IUI8	CRLF3	-1,002594471	-0,896233082	-0,837781787	0,002785246	0,036291158	-0,912203113	1,881917147
P52434	POLR2H	-0,844385684	-0,956354082	-0,919683337	0,001318304	0,03337557	-0,906807701	1,874892269
Q9H3K6	BOLA2	-0,89017427	-0,833011448	-0,978708208	0,002207217	0,035880789	-0,900631309	1,866882733
Q8NBF2	NHLRC2	-0,812539279	-0,879392087	-0,994217634	0,003492254	0,037765449	-0,895383	1,860103632
P08133	ANXA6	-0,881664574	-0,808755755	-0,994724512	0,00363354	0,037972349	-0,895048281	1,859672119
O00515	LAD1	-1,019773126	-0,863066196	-0,760348678	0,007249521	0,047216325	-0,881062667	1,841731392

(continued)

Protein IDs	Genes	log2 Ratio L/H Rep. 1	log2 Ratio L/H Rep. 2	log2 Ratio L/H Rep. 3	T-test p-value	T-test q-value	T-test Difference	Fold Change
Q9UHV9	PFDN2	-0,8972404	-0,996244073	-0,747859955	0,006656107	0,04538544	-0,880448143	1,840947064
Q15311	RALBP1	-0,887759149	-0,871685982	NaN	0,00581559	0,044186939	-0,879722565	1,840021426
Q9Y5K5	UCHL5	-0,951587796	-0,901340008	-0,768417239	0,003887937	0,038172726	-0,873781681	1,832459967
Q9Y696	CLIC4	-0,990228832	-0,794852495	-0,819014072	0,004981482	0,041372413	-0,8680318	1,825171207
Q9Y266	NUDC	-0,981268167	-0,717034817	-0,888772488	0,007962243	0,049154011	-0,862358491	1,818007928
Q58FF6	HSP90AB4P	-0,991172612	-0,862431526	-0,730052948	0,007574302	0,048266875	-0,861219029	1,816572605
P62942	FKBP1A	-0,925695658	-0,878843009	-0,755229414	0,003532121	0,037765449	-0,853256027	1,806573594
P23921	RRM1	-0,924480021	-0,834144831	-0,796846926	0,001972712	0,034770826	-0,851823926	1,804781177
O14896	IRF6	-0,810895503	-0,885886729	-0,857980967	0,000659658	0,029228323	-0,851587733	1,804485728
P17812	CTPS1	-0,87428546	-0,778545022	-0,891030312	0,001703164	0,033986413	-0,847953598	1,799945966
Q9Y617	PSAT1	-0,926075339	-0,795102	-0,81811434	0,002267324	0,035903561	-0,84643056	1,798046785
P08238	HSP90AB1	-0,930093944	-0,739329636	-0,850799441	0,004309846	0,03974924	-0,840074341	1,790142384
P63104	YWHAZ	-0,877979815	-0,807272494	-0,797760069	0,000933368	0,029740126	-0,827670793	1,774817634
P06753	TPM3	-0,913645804	-0,80661273	-0,746054709	0,003533074	0,037765449	-0,822104414	1,767983014
P60983	GMFB	-0,802151859	-0,761115074	-0,83963716	0,000800472	0,029228323	-0,800968031	1,742269777
P07195	LDHB	-0,863383532	-0,74588275	-0,785090148	0,001867572	0,03463919	-0,79811881	1,738832312
P06454	PTMA	-0,870660663	-0,771378517	-0,735262215	0,002599204	0,035910878	-0,792433798	1,731993839
P60174	TPI1	-0,813853025	-0,74097079	-0,80041337	0,000812568	0,029228323	-0,785079062	1,72318675
Q9Y6E2	BZW2	-0,866789341	-0,647268474	-0,815493405	0,007211009	0,047216325	-0,776517073	1,712990408
P41250	GARS	-0,825867057	-0,783582389	-0,703720927	0,002150265	0,035637944	-0,771056791	1,706519371
P21266	GSTM3	-0,892896116	-0,717473507	-0,69928515	0,006367479	0,045261668	-0,769884924	1,705133769
Q01082	SPTBN1	-0,847355604	-0,695281208	-0,743644178	0,003446904	0,037765449	-0,762093663	1,695950031
Q04917	YWHAH	-0,740884423	-0,809496701	-0,735782087	0,000971265	0,029740126	-0,762054404	1,69590388
P27348	YWHAQ	-0,783079445	-0,68894124	-0,751292348	0,001388942	0,03337557	-0,741104345	1,671454803
Q8IYF1	TCEB3B	-0,803309739	-0,700972319	-0,704340816	0,002072168	0,035414197	-0,736207624	1,665791255

(continued)

Protein IDs	Genes	log2 Ratio L/H Rep. 1	log2 Ratio L/H Rep. 2	log2 Ratio L/H Rep. 3	T-test p-value	T-test q-value	T-test Difference	Fold Change
P55327	TPD52	-0,716595948	-0,715893388	-0,756254792	0,000334066	0,029228323	-0,729581376	1,658157877
P10599	TXN	-0,748632967	-0,676899254	-0,721328914	0,000852154	0,029228323	-0,715620379	1,64218923
P00441	SOD1	-0,74355799	-0,69937396	-0,693141162	0,000496356	0,029228323	-0,712024371	1,638101067
P42166; P42167	TMPO	-0,713607788	-0,716595948	-0,700617313	4,76794E-05	0,019037885	-0,710273683	1,636114463
O60493	SNX3	-0,823667824	-0,69090873	-0,602931917	0,008160806	0,049329832	-0,705836157	1,631089738
P14324	FDPS	-0,792188942	-0,660837352	-0,655901372	0,004006295	0,038820489	-0,702975889	1,627859164
Q9UK76	HN1	-0,768671274	-0,71650815	-0,576183558	0,006924404	0,046395022	-0,687120994	1,6100673
Q9H2G2	SLK	-0,668391526	-0,734395266	-0,656725228	0,001238413	0,032546011	-0,686504006	1,609378881
Q92973	TNPO1	-0,742351174	-0,631150842	-0,67464143	0,002238237	0,035882098	-0,682714482	1,605157076
P21333	FLNA	-0,734048426	-0,69233793	-0,587172985	0,004212046	0,039641878	-0,671186447	1,592381976
P29966	MARCKS	-0,612210929	-0,703632295	-0,683831215	0,001730987	0,033986413	-0,666558146	1,587281651
P99999	CYCS	-0,629846156	-0,682213664	-0,651223958	0,00053916	0,029228323	-0,654427926	1,573991692
P61086	UBE2K	-0,704694927	-0,677981734	-0,541316569	0,006167028	0,04509081	-0,641331077	1,559767587
P60033	CD81	-0,594357431	-0,682033896	-0,622180641	0,001666439	0,033986413	-0,632857323	1,550633053
Q9NVQ4	FAIM	-0,736041903	-0,567837477	-0,581977785	0,007262864	0,047216325	-0,628619055	1,546084376
P26639	TARS	-0,673104048	-0,59234935	-0,617674589	0,001440005	0,03337557	-0,627709329	1,545109763
P17844	DDX5	-0,626953006	-0,69438988	-0,561692655	0,00370415	0,038153714	-0,627678514	1,54507676
O43707	ACTN4	-0,649477541	-0,662114322	-0,568810403	0,002166704	0,035637944	-0,626800756	1,544136997
O75347	TBCA	-0,736734688	-0,593592763	-0,547745943	0,008164526	0,049329832	-0,626024465	1,543306346
Q15185	PTGES3	-0,681674123	-0,605020165	-0,58630836	0,002176452	0,035637944	-0,624334216	1,541499281
P55060	CSE1L	-0,692962766	-0,561888158	-0,580820858	0,004438752	0,03977371	-0,611890594	1,528260622
P08134	RHOC	-0,650580764	-0,495285839	-0,667846799	0,00813657	0,049329832	-0,604571134	1,520526683
P82979	SARNP	-0,664937854	-0,569102168	-0,573374569	0,002680935	0,035910878	-0,60247153	1,518315418
P25685	DNAJB1	-0,680414379	-0,603026927	-0,511973977	0,006550764	0,04538544	-0,598471761	1,514111826

(continued)

Protein IDs	Genes	log2 Ratio L/H Rep. 1	log2 Ratio L/H Rep. 2	log2 Ratio L/H Rep. 3	T-test p-value	T-test q-value	T-test Difference	Fold Change
O75534	CSDE1	-0,606537044	-0,620492578	-0,56510973	0,000774101	0,029228323	-0,597379784	1,512966227
Q9NZD2	GLTP	-0,616169453	-0,537842691	-0,621993244	0,002093832	0,03542163	-0,592001796	1,507336786
Q9NRX5	SERINC1	-0,653335273	-0,536948025	-0,55522722	0,003835191	0,038172726	-0,58183684	1,496753703
O43175	PHGDH	-0,623211384	-0,523060083	-0,586500585	0,002555147	0,035903561	-0,577590684	1,492354918
P46940	IQGAP1	-0,566376805	-0,629193425	-0,501005948	0,004254853	0,039641878	-0,565525393	1,479926363
P20645	M6PR	-0,595121682	-0,497842222	-0,574828148	0,002828469	0,036517311	-0,555930684	1,470116701
Q6DD88	ATL3	-0,491596609	-0,57075429	-0,593783975	0,003127795	0,03757262	-0,552044958	1,466162446
Q96T37	RBM15	-0,531768262	-0,519441307	-0,590051055	0,001580397	0,033986413	-0,547086875	1,461132361
Q7Z4H3	HDDC2	-0,521854758	-0,559149146	-0,53873682	0,000398559	0,029228323	-0,539913575	1,453885419
P04792	HSPB1	-0,611833394	-0,471447617	-0,527470827	0,005724899	0,0438241	-0,536917279	1,450869016
P26583	HMGB2	-0,562181413	-0,51752764	-0,509645164	0,000951937	0,029740126	-0,529784739	1,443713766
O43765	SGTA	-0,522859275	-0,49855721	-0,559442937	0,0011257	0,031915683	-0,526953141	1,440882948
P33176	KIF5B	-0,509442449	-0,59387958	-0,457856894	0,005754141	0,043938107	-0,520392974	1,434345895
Q9BZZ5	API5	-0,543594837	-0,429642737	-0,584000349	0,007833603	0,048753036	-0,519079308	1,433040425
Q9BRT8; Q8IUF1; Q5RIA9; Q5JTY5; Q4V339	CBWD1; CBWD2; CBWD5; CBWD3; CBWD6	-0,605683982	-0,49415952	-0,448266685	0,008104384	0,049329832	-0,516036729	1,430021392
Q5TFE4	NT5DC1	-0,511569321	-0,455544204	-0,562865198	0,003672345	0,038153714	-0,509992907	1,424043195
Q9BV86	NTMT1	-0,539630353	-0,422233045	-0,560225785	0,007099294	0,047023519	-0,507363061	1,421449713
O14974	PPP1R12A	-0,572404623	-0,466340005	-0,481505543	0,004243918	0,039641878	-0,506750057	1,420845864
Q9Y265	RUVBL1	-0,495592803	-0,559834421	-0,461214244	0,003252216	0,037650691	-0,505547156	1,419661674
P08237	PFKM	-0,540324926	-0,483261138	-0,45585984	0,002535477	0,035903561	-0,493148635	1,407513378

(continued)

Protein IDs	Genes	log2 Ratio L/H Rep. 1	log2 Ratio L/H Rep. 2	log2 Ratio L/H Rep. 3	T-test p-value	T-test q-value	T-test Difference	Fold Change
P07900	HSP90AA1	-0,533862352	-0,42212534	-0,487897933	0,004507868	0,03977371	-0,481295208	1,395996387
O60264	SMARCA5	-0,535953403	-0,503450572	-0,393525958	0,008041441	0,049329832	-0,477643311	1,392467167
P50395	GDI2	-0,534061551	-0,460585266	-0,435095161	0,003852766	0,038172726	-0,47658066	1,39144189
P43487	RANBP1	-0,528371215	-0,444879025	-0,42728433	0,004431017	0,03977371	-0,466844857	1,382083573
P00390	GSR	-0,462261736	-0,494466811	-0,432745636	0,001477543	0,03337557	-0,463158061	1,378556179
P48163	ME1	-0,511670411	-0,405774593	-0,442545414	0,004656003	0,040159667	-0,453330139	1,369197098
P11142	HSPA8	-0,526870012	-0,397145808	-0,424707204	0,007615364	0,048277939	-0,449574341	1,365637274
Q15819; Q13404	UBE2V2; UBE2V1	-0,520447373	-0,420078188	-0,395830631	0,007253315	0,047216325	-0,445452064	1,361740747
P54577	YARS	-0,495899796	-0,393965274	-0,444136947	0,004350954	0,039769023	-0,444667339	1,361000257
P22234	PAICS	-0,480678797	-0,435628563	-0,415650487	0,001870979	0,03463919	-0,443985949	1,360357603
P49736	MCM2	-0,412944108	-0,445302993	-0,463936269	0,001140526	0,032039366	-0,44072779	1,35728886
Q9P258	RCC2	-0,451857299	-0,428785563	-0,421048194	0,000454533	0,029228323	-0,433897018	1,350877654
Q7Z3B4	NUP54	-0,435841918	-0,431355536	-0,425351918	4,97397E-05	0,019037885	-0,430849791	1,348027372
P51114	FXR1	-0,431783348	-0,462471187	-0,396049827	0,001985328	0,034770826	-0,430101454	1,347328321
P24666	ACP1	-0,487074673	-0,417596042	-0,367371023	0,006632314	0,04538544	-0,424013913	1,341655163
P47755	CAPZA2	-0,350497216	-0,436055243	-0,466235578	0,006819285	0,045790902	-0,417596012	1,335699999
O75369	FLNB	-0,470198482	-0,408168405	-0,364572465	0,005426799	0,043030222	-0,414313118	1,332664031
P78406	RAE1	-0,397036225	-0,438292861	-0,381283373	0,001752084	0,033986413	-0,405537486	1,324582301
Q9Y547	HSPB11	-0,406318933	-0,361319214	-0,410232514	0,001593727	0,033986413	-0,392623554	1,312778534
P15924	DSP	-0,341758102	-0,456490785	-0,373174876	0,007597856	0,048266875	-0,390474588	1,310824541
Q9UI26	IPO11	-0,331934482	-0,390117377	-0,439889073	0,006424691	0,045341313	-0,387313644	1,307955669
Q9NRR5	UBQLN4	-0,433600456	-0,374065727	-0,335483313	0,005562389	0,043119077	-0,381049832	1,302289171
O00764	PDXK	-0,431462526	-0,313826323	-0,382722557	0,008136173	0,049329832	-0,376003802	1,297742187
Q9BUB7	TMEM70	-0,319155425	-0,407624751	-0,38183704	0,005015106	0,041372413	-0,369539072	1,291940002

(continued)

Protein IDs	Genes	log2 Ratio L/H Rep. 1	log2 Ratio L/H Rep. 2	log2 Ratio L/H Rep. 3	T-test p-value	T-test q-value	T-test Difference	Fold Change
P35637	FUS	-0,349931389	-0,389126211	-0,307894796	0,004486444	0,03977371	-0,348984132	1,273663467
P08758	ANXA5	-0,324580252	-0,344942093	-0,370052665	0,001437092	0,03337557	-0,346525004	1,271494308
P11216	PYGB	-0,306145579	-0,346758395	-0,374733448	0,003361778	0,037650691	-0,342545807	1,267992144
P60981	DSTN	-0,360420465	-0,360083252	-0,303693116	0,00303573	0,03748147	-0,341398944	1,266984561
Q8NF37	LPCAT1	-0,343464702	-0,364124089	-0,312781334	0,001917507	0,034770826	-0,340123375	1,265864843
O75874	IDH1	-0,382058531	-0,334453881	-0,302523732	0,004596009	0,03977371	-0,339678715	1,265474744
O75934	BCAS2	-0,312200516	-0,362105161	-0,295958072	0,003765347	0,038172726	-0,32342125	1,25129439
P30153	PPP2R1A	-0,345169276	-0,333080113	-0,272859275	0,004938499	0,041372413	-0,317036221	1,245768692
P52565	ARHGDIA	-0,307778239	-0,358058631	-0,275245428	0,005844979	0,04419537	-0,3136941	1,242886107
O00743	PPP6C	-0,298071802	-0,338795274	-0,298423707	0,001874293	0,03463919	-0,311763595	1,241224083
Q15149	PLEC	-0,320195824	-0,269272536	-0,314638555	0,002851767	0,036523545	-0,301368972	1,232313199
P28838	LAP3	-0,257614136	-0,311619312	-0,322735786	0,004544549	0,03977371	-0,297323078	1,228862142
Q7Z739	YTHDF3	-0,289362371	NaN	-0,288772047	0,000650043	0,029228323	-0,289067209	1,221850021
P33316	DUT	-0,240375444	-0,30812791	-0,312084287	0,006516928	0,04538544	-0,286862547	1,219984271
P52788	SMS	-0,258096725	-0,273456156	-0,274530023	0,000390001	0,029228323	-0,268694301	1,204717016
P67775; P62714	PPP2CA; PPP2CB	-0,256889939	-0,277270645	-0,256044507	0,000693227	0,029228323	-0,263401697	1,200305543
P40925	MDH1	-0,249748722	-0,288181335	-0,2507191	0,002308363	0,035903561	-0,262883052	1,199874114
O00429	DNM1L	-0,267475814	-0,223916709	-0,230079964	0,003187087	0,03757262	-0,240490829	1,181394523
P48147	PREP	-0,25507772	-0,209515691	-0,253868252	0,003894806	0,038172726	-0,239487221	1,180572974
P04406	GAPDH	-0,204140648	-0,251567632	-0,255319506	0,004794269	0,040777917	-0,237009262	1,178546974
P33993	MCM7	-0,231678233	-0,179001376	-0,231432438	0,006632222	0,04538544	-0,214037349	1,159929683
Q32MZ4	LRRFIP1	-0,194339216	-0,216982484	-0,219338864	0,001434121	0,03337557	-0,210220188	1,156864734
P31943	HNRNPH1	-0,214870766	-0,216485962	-0,161049291	0,008402197	0,049762719	-0,197468673	1,146684637
P49588	AARS	-0,180657059	-0,186500579	-0,221691549	0,004235999	0,039641878	-0,196283062	1,145742675

(continued)

Protein IDs	Genes	log2 Ratio L/H Rep. 1	log2 Ratio L/H Rep. 2	log2 Ratio L/H Rep. 3	T-test p-value	T-test q-value	T-test Difference	Fold Change
Q93074	MED12	-0,207767874	-0,179001376	-0,176833302	0,002804422	0,036386182	-0,187867517	1,139078771
O60869	EDF1	-0,211136878	-0,154323995	-0,176578134	0,0082646	0,049329832	-0,180679669	1,133417725
Q96AY2	EME1	-0,177088574	-0,165686935	-0,161049291	0,000804191	0,029228323	-0,1679416	1,123454425
P47756	CAPZB	-0,173255324	-0,137241185	-0,174789935	0,00570296	0,043765573	-0,161762148	1,118652658
P63267; P68133; P68032; P62736	ACTG2; ACTA1; ACTC1; ACTA2	-0,156655431	-0,153546005	-0,135928735	0,001877892	0,03463919	-0,148710057	1,108577827
Q9H1E5	TMX4	-0,085696608	-0,115832359	-0,096801519	0,007738663	0,048457643	-0,099443495	1,071360117
P18206	VCL	-0,075327188	-0,092207417	-0,096801519	0,005445079	0,043030222	-0,088112041	1,062978223
P05423	POLR3D	-0,079156123	-0,08488071	-0,073683143	0,001660228	0,033986413	-0,079239992	1,056461353

Annex 3. Validation of the top upregulated mitotic candidates obtained in the proteomic profiling using Grasso *et al.*[268], Robinson *et al.*[269] and TCGA270 publicly available databases

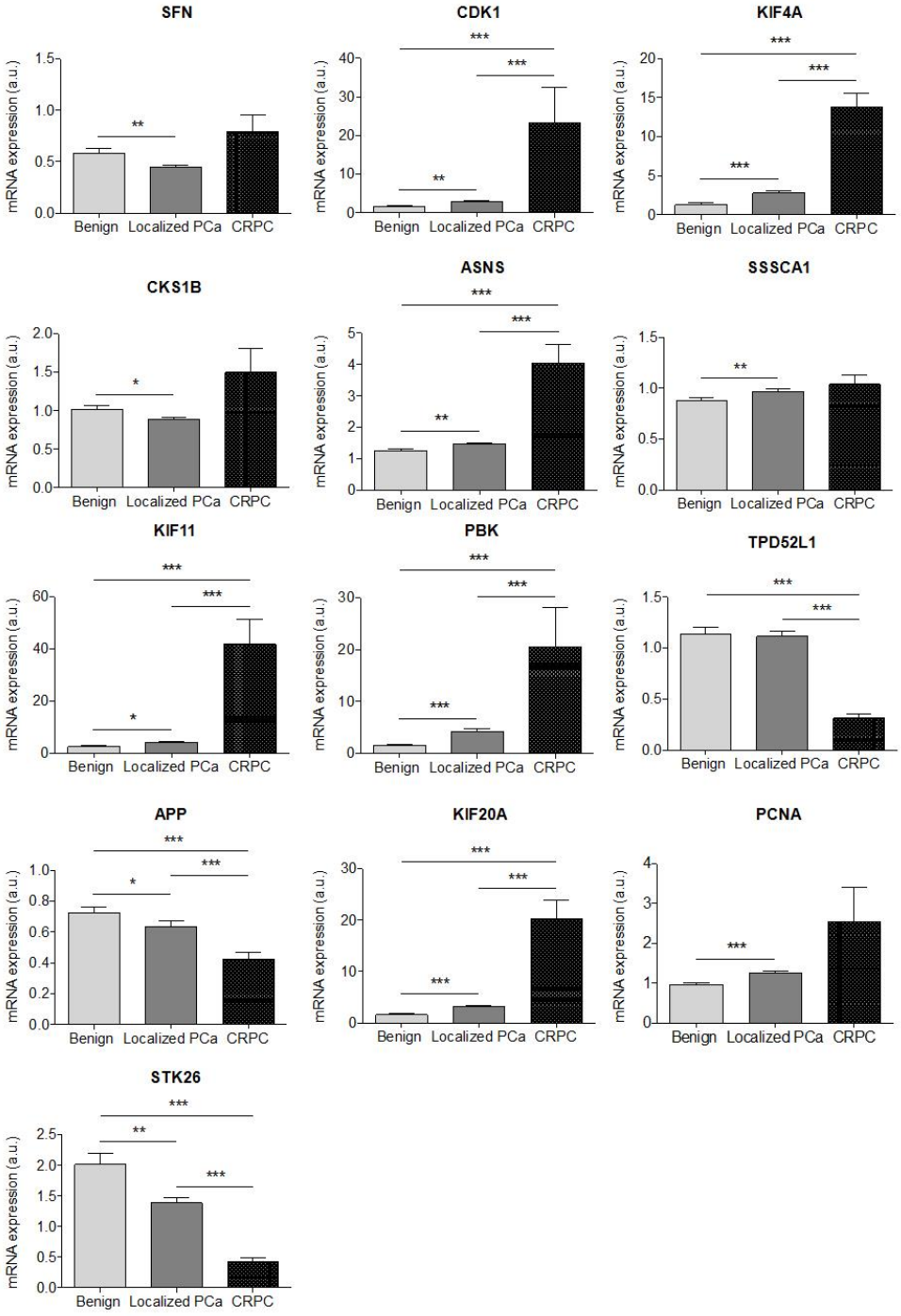

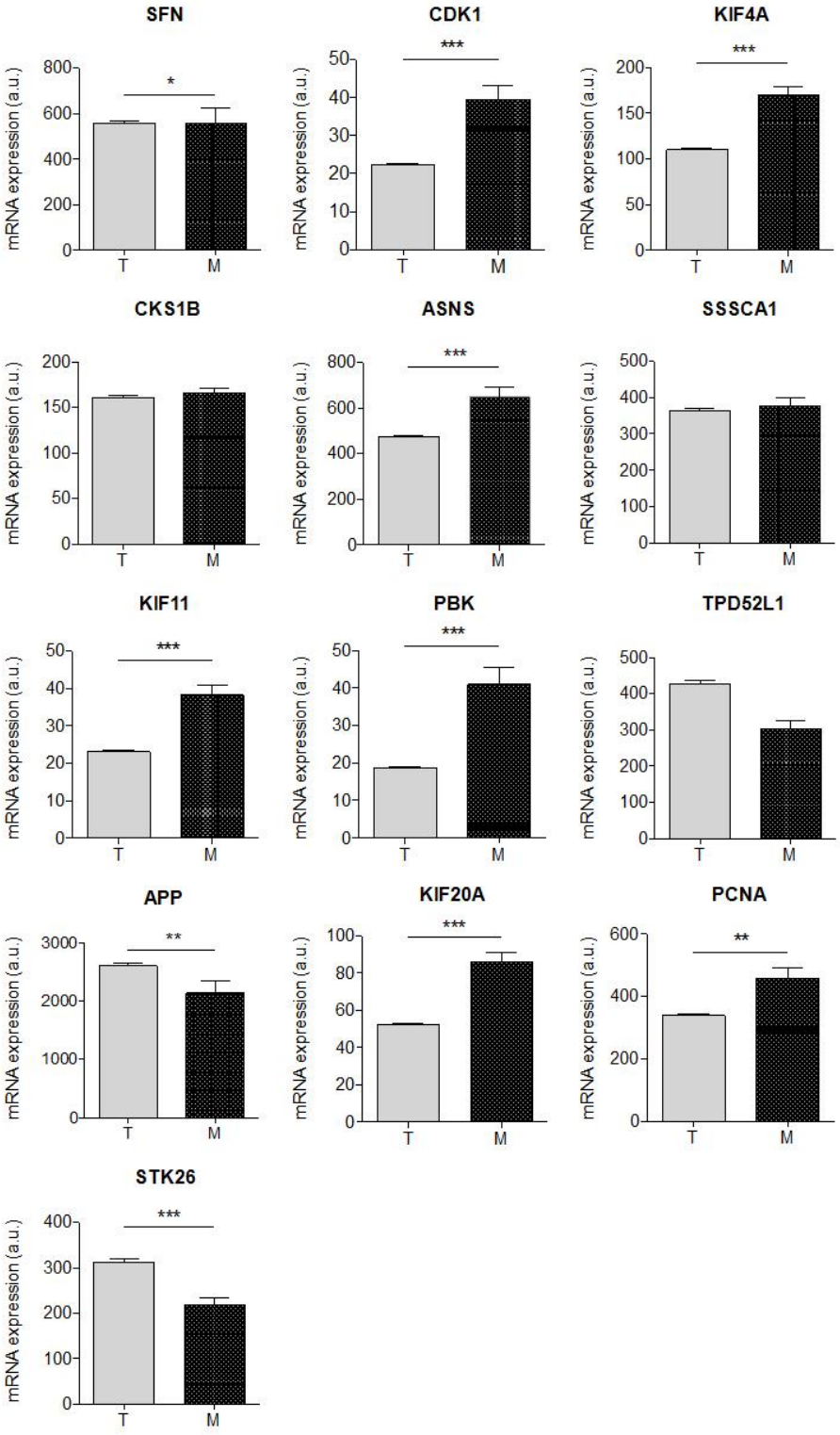
SFN
CDK1
KIF4A
CKS1B
ASNS
SSSCA1
KIF11
PBK
TPD52L1
APP
KIF20A
PCNA
STK26
mRNA expression (a.u.)
T
M
*
**
***

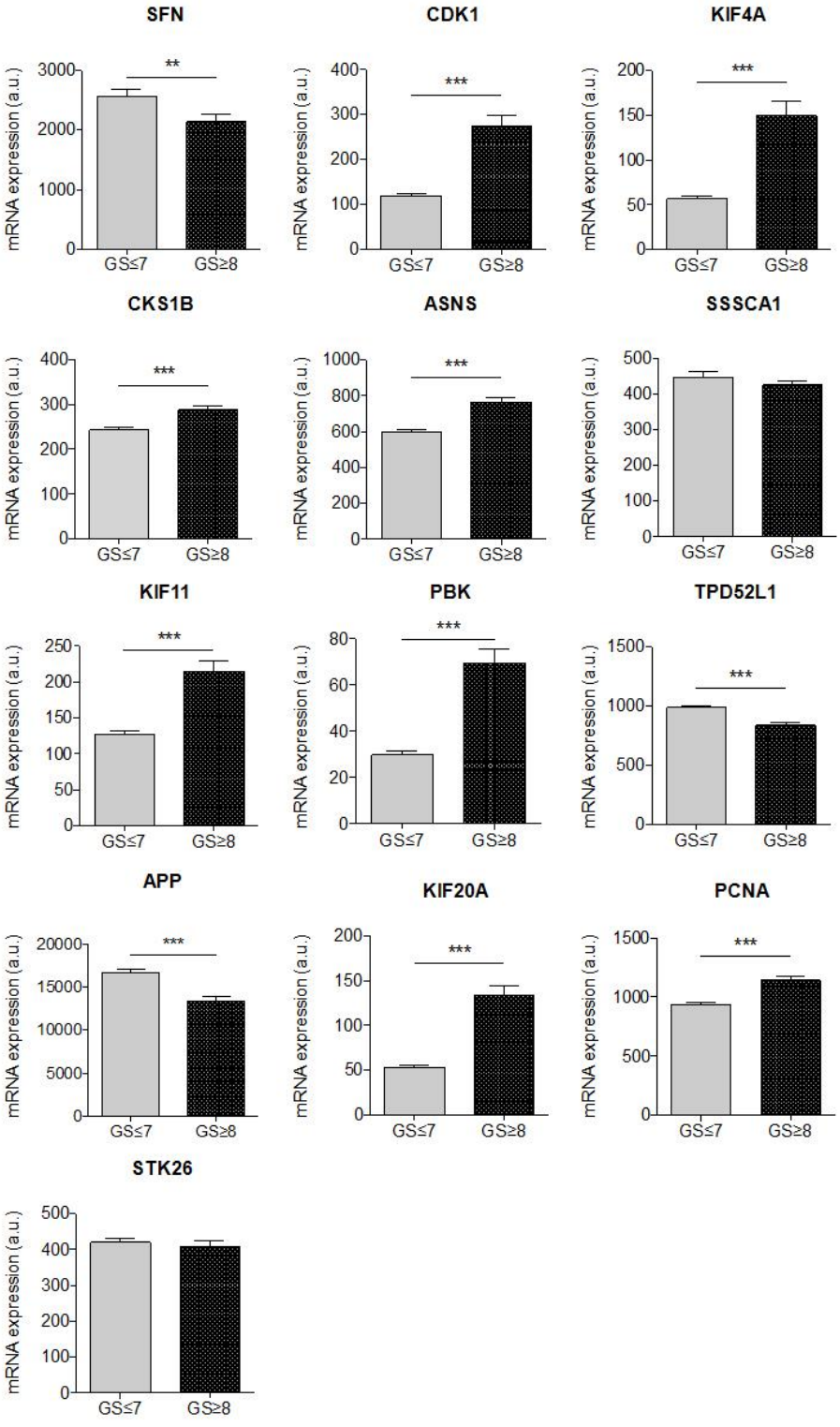
SFN
CDK1
KIF4A
CKS1B
ASNS
SSSCA1
KIF11
PBK
TPD52L1
APP
KIF20A
PCNA
STK26
mRNA expression (a.u.)
GS≤7
GS≥8
**
***

BIBLIOGRAPHY

1. Stabile A *et al*. Multiparametric MRI for prostate cancer diagnosis: current status and future directions. *Nat Rev Urol*. 2020. 17:41-61.
2. Kumar VL, Majumder PK. Prostate gland: Structure, functions and regulation. *Int Urol Nephrol*. 1995. 27:231-43.
3. Audet-Walsh É, Yee T, Tam IS, Giguère V. Inverse regulation of DHT synthesis enzymes 5α-reductase types 1 and 2 by the androgen receptor in prostate cancer. *Endocrinology*. 2017. 158:1015-1021.
4. Lee CH, Akin-Olugbade O, Kirschenbaum A. Overview of prostate anatomy, histology, and pathology. *Endocrinol. Metab. Clin. North Am*. 2011. 40:565-575.
5. Salem O, Hansen CG. The hippo pathway in prostate cancer. *Cells*. 2019. 8:E370.
6. Uzgare AR, Xu Y, Isaacs JT. In vitro culturing and characteristics of transit amplifying epithelial cells from human prostate tissue. *J Cell Biochem*. 2004. 91:196-205.
7. Hudson DL *et al*. Epithelial cell differentiation pathways in the human prostate: identification of intermediate phenotypes by keratin expression. *J Histochem Cytochem*. 2001. 49:271-8.
8. Maitland NJ, Frame FM, Polson ES, Lewis JL, Collins AT. Prostate cancer stem cells: do they have a basal or luminal phenotype? *Horm Cancer*. 2011. 2:47-61.
9. Collins AT, Maitland NJ. Prostate cancer stem cells. *Eur J Cancer*. 2006. 42:1213-8.
10. Yuan TC, Veeramani S, Lin MF. Neuroendocrine-like prostate cancer cells: neuroendocrine transdifferentiation of prostate adenocarcinoma cells. *Endocr Relat Cancer*. 2007. 14:531-47.
11. Huang YH, Zhang YQ, Huang JT. Neuroendocrine cells of prostate cancer: biologic functions and molecular mechanisms. *Asian J Andro*l. 2019. 21:291-295.
12. Vashchenko N, Abrahamsson PA. Neuroendocrine differentiation in prostate cancer: implications for new treatment modalities. *Eur Urol*. 2005. 47:147-155.

13. Kuehnel W. Color atlas of cytology, histology and microscopic anatomy. 4th edition. *Thieme*. 2003.
14. McNeal JE. The zonal anatomy of the prostate. Prostate. 1981. 2:35–49.
15. Selman SH. The McNeal prostate: a review. Urology. 2011. 78:1224–8.
16. Hammerich KH, Ayala GE, Wheeler TM. Anatomy of the prostate gland and surgical pathology of prostate cancer. *Cambridge Univ Press*. 2009. 1–10.
17. Lee JJ *et al*. Biologic differences between peripheral and transition zone prostate cancer. *Prostate*. 2015. 75:183-190.
18. Cohen RJ *et al*. Central Zone Carcinoma of the Prostate Gland: A Distinct Tumor Type With Poor Prognostic Features. J Urol. 2008. 179:1762–7.
19. Murphy AB, Macejko A, Taylor A, Nadler RB. Chronic prostatitis: management strategies. Drugs. 2009. 69:71-84.
20. Duclos AJ, Lee CT, Shoskes DA. Current treatment options in the management of chronic prostatitis. Ther Clin Risk Manag. 2007. 3:507-12.
21. Sfanos KS, De Marzo AM. Prostate cancer and inflammation: the evidence. *Histopathology*. 2012. 60:199-215.
22. Sarma AV, Wei JT. Clinical practice. Benign prostatic hyperplasia and lower urinary tract symptoms. *N Engl J Med*. 2012. 367:248-57.
23. Pinheiro LC, Martins Pisco J. Treatment of benign prostatic hyperplasia. *Tech Vasc Interv Radiol*. 2012. 15:256-60.
24. Gandaglia G *et al*. The role of chronic prostatic inflammation in the pathogenesis and progression of benign prostatic hyperplasia (BPH). *BJU Int*. 2013. 112:432-41.
25. Alcaraz, A, Hammerer P, Tubaro A, Shröder FH, Castro R. Is there evidence of a relationship between benign prostatic hyperplasia and prostate cancer? Findings of a literature review. *Eur Urol*. 2009. 55:864-73.
26. Zeng L, Kyprianou N. Apoptotic regulators in prostatic intraepithelial neoplasia (PIN): value in prostate cancer detection and prevention. *Prostate Cancer Prostatic Dis*. 2005. 8:7-13.

27. Bostwick DG, Qian J. High-grade prostatic intraepithelial neoplasia. *Mod Pathol*. 2004. 17:360-79.
28. Montironi R, Mazzucchelli R, Lopez-Beltran A, Cheng L, Scarpelli M. Mechanisms of disease: high-grade prostatic intraepithelial neoplasia and other proposed preneoplastic lesions in the prostate. *Nat Clin Pract Urol*. 2007. 4:321-32.
29. Bray F *et al*. Global cancer statistics 2018: GLOBOCAN estimates of incidence and mortality worldwide for 36 cancers in 185 countries. *CA Cancer J Clin*. 2018. 68:394-424.
30. Stattin P *et al*. Prostate cancer mortality in areas with high and low prostate cancer incidence. *J Natl Cancer Inst*. 2014. 106:dju007.
31. Neppl-Huber C *et al*. Changes in incidence, survival and mortality of prostate cancer in Europe and the United States in the PSA era: additional diagnoses and avoided deaths. *Ann Oncol*. 2012. 23:1325-34.
32. Siegel RL, Miller KD, Jemal A. Cancer statistics, 2019. *CA Cancer J Clin*. 2019. 69:7-34.
33. Howlander N et al. SEER Cancer Statistics Review, 1975-2016. National Cancer Institute, Bethesda. 2018.
34. Labbé DP et al. Role of diet in prostate cancer: the epigenetic link. *Oncogene*. 2015. 34:4683-91.
35. Damaschke NA, Yang B, Bhusari S, Svaren JP, Jarrard DF. Epigenetic susceptibility factors for prostate cancer with aging. *Prostate*. 2013. 73:1721-30.
36. Chornokur G, Dalton K, Borysova ME, Kumar NB. Disparities at presentation, diagnosis, treatment, and survival in African American men, affected by prostate cancer. *Prostate*. 2011. 71:985-97.
37. Moses KA, Paciorek AT, Penson DF, Carroll PR, Master VA. Impact of ethnicity on primary treatment choice and mortality in men with prostate cancer: data from CaPSURE. *J Clin Oncol*. 2010. 28:1069-74.
38. Eeles R *et al*. The genetic epidemiology of prostate cancer and its clinical implications. *Nat Rev Urol*. 2014. 11:18-31.
39. Bratt O, Drevin L, Akre O, Garmo H, Stattin P. Family history and probability of prostate cancer, differentiated by risk category: a nationwide population-based

study. *J Natl Cancer Inst*. 2016. 108:djw110.

40. Jansson KF *et al*. Concordance of tumor differentiation among brothers with prostate cancer. *Eur Urol*. 2012. 62:656-61.
41. Frankel S, Smith GD, Donovan J, Neal D. Screening for prostate cancer. *Lancet*. 2003. 361:1122-8.
42. Pienta KJ. Critical appraisal of prostate-specific antigen in prostate cancer screening: 20 years later. *Urology*. 2009. 73:S11-20.
43. Strope SA, Andriole GL. Prostate cancer screening: current status and future perspectives. *Nat Rev Urol*. 2010. 7:487-93.
44. Wolf *et al*. American Cancer Society guideline for the early detection of prostate cancer: update 2010. *CA Cancer J Clin*. 2010. 60:70-98.
45. Hoffman RM. Clinical practice. Screening for prostate cancer. *N Engl J Med*. 2011. 365:2013-9.
46. Pashayan N *et al*. Stage shift in PSA-detected prostate cancers – effect modification by Gleason score. J Med Screen. 2009. 16:98-101.
47. Catalona WJ *et al*. Selection of optimal prostate specific antigen cutoffs for early detection of prostate cancer: receiver operating characteristic curves. *J Urol*. 1994. 152:2037-42.
48. Gjertson CK, Albertsen PC. Use and assessment of PSA in prostate cancer. *Med Clin North Am*. 2011. 95:191-200.
49. Prensner JR, Rubin MA, Wei JT, Chinnaiyan AM. Beyond PSA: next generation of prostate cancer biomarkers. *Sci Transl Med*. 2012. 4:127rv3.
50. Hayes JH, Barry MJ. Screening for prostate cancer with the prostate-specific antigen test: a review of current evidence. *JAMA*. 2014. 311:1143-9.
51. Kang BJ *et al*. Diagnosis of prostate cancer via nanotechnological approach. I*nt J Nanomedicine*. 2015. 10:6555-69.
52. Lilja H, Ulmert D, Vickers AJ. Prostate-specific antigen and prostate cancer: prediction, detection and monitoring. *Nat Rev Cancer*. 2008. 8:268-78.
53. Steuber T, O'Brien MF, Lilja H. Serum markers for prostate cancer: a rational approach for the literature. *Eur Urol*. 2008. 54:31-40.
54. Catalona *et al*. Comparison of digital rectal examination and serum prostate specific antigen in the early detection of prostate cancer: results of a multicenter clinical trial of 6,630 men. *J Urol*. 1994. 151:1283-90.

55. Grosselaar C, Kranse R, Roobol MJ, Roemeling S, Schröder FH. The interobserver variability of digital rectal examination in a large randomized trial for the screening of prostate cancer. *Prostate*. 2008. 68:985-93.
56. Mottet N, *et al*. EAU-ESTRO-SIOG guidelines on prostate cancer. Part 1: Screening, diagnosis and local treatment with curative intent. *Eur Urol*. 2017. 71:618-629.
57. Ismail MT, Gomella LG. Transrectal prostate biopsy. *Urol Clin North Am*. 2013. 40:457-72.
58. Scattoni *et al*. Extended and saturation prostatic biopsy in the diagnosis and characterization of prostate cancer: a critical analysis of the literature. *Eur Urol*. 2007. 52:1309-22.
59. Welch HG, Fisher ES, Gottlieb DJ, Barry MJ. Detection of prostate cancer via biopsy in the Medicare-SEER population during the PSA era. *J Natl Cancer Inst*. 2007. 99:1395-400.
60. Simmons LAM *et al*. The PICTURE study: diagnostic accuracy of multiparametric MRI in men requiring a repeat prostate biopsy. *Br J Cancer*. 2017. 116:1159-1165.
61. Ahmed HU *et al*. Diagnostic accuracy of multi-parametric MRI and TRUS biopsy in prostate cancer (PROMIS): a paired validating confirmatory study. *Lancet*. 2017. 389:815-822.
62. Salami SS *et al*. Combining urinary detection of TMPRSS2:ERG and PCA3 with serum PSA to predict diagnosis of prostate cancer. *Urol Oncol*. 2013. 31:566-71.
63. Humphrey PA. Gleason grading and prognostic factors in carcinoma of the prostate. *Mod Pathol*. 2004. 17:292-306.
64. Epstein JI *et al*. The 2014 International Society of Urological Pathology (ISUP) consensus conference on Gleason grading of prostatic carcinoma: definition of grading patterns and proposal for a new grading system. *Am J Surg Pathol*. 2016. 40:244-52.
65. Arora R *et al*. Heterogeneity of Gleason grade in multifocal adenocarcinoma of the prostate. *Cancer*. 2004. 100:2362-6.
66. Lotan TL, Epstein JI. Clinical implications of changing definitions within the Gleason grading system. *Nat Rev Urol*. 2010. 7:136-42.

67. Leapman MS *et al*. Application of a prognostic Gleason grade grouping system to assess distant prostate cancer outcomes. *Eur Urol*. 2017. 71:750-759.
68. Brierley A *et al*. TNM classification of malignant tumors. UICC International Union Against Cancer. 8th edn. 2016.
69. Buyyounouski MK *et al*. Prostate cancer – major changes in the American Joint Committee on Cancer eighth edition cancer staging manual. *CA Cancer J Clin*. 2017. 67:245-253.
70. Cheng L, Montironi R, Bostwick DG, Lopez-Beltran A, Berney DM. Staging of prostate cancer. *Histopathology*. 2012. 60:87-117.
71. Partin AW *et al*. Combination of prostate-specific antigen, clinical stage, and Gleason score to predict pathological stage of localized prostate cancer. A multi-institutional update. *JAMA*. 1997. 277:1445-51.
72. EAU Guidelines. Edn. Presented at the EAU Annual Congress Barcelona 2019. ISBN 978-94-92671-04-2.
73. Shen MM, Abate-Shen C. Molecular genetics of prostate cancer: new prospects for old changes. *Genes Dev*. 2010. 24:1967-2000.
74. Beltran H *et al*. Targeted next-generation sequencing of advanced prostate cancer identifies potential therapeutic targets and disease heterogeneity. *Eur Urol*. 2013. 63:920-6.
75. Hodgson MC, Bowden WA, Agoulnik IU. Androgen receptor footprint on the way to prostate cancer progression. *World J Urol*. 2012. 30:279-85.
76. Taylor BS *et al*. Integrative genomic profiling of human prostate cancer. *Cancer Cell*. 2010. 18:11-22.
77. Sharma A *et al*. The retinoblastoma tumor suppressor controls androgen signaling and human prostate cancer progression. *J Clin Invest*. 2010. 120:4478-92.
78. Aparicio A, Den RB, Knudsen KE. Time to stratify? The retinoblastoma protein in castrate-resistant prostate cancer. *Nat Rev Urol*. 2011. 8:562-8.
79. Wang S *et al*. Prostate-specific deletion of the murine Pten tumor suppressor gene leads to metastatic prostate cancer. *Cancer Cell*. 2003. 4:209-21.
80. Knudsen BS, Vasioukhin V. Mechanisms of prostate cancer initiation and progression. *Adv Cancer Res*. 2010. 109:1-50.
81. Bowen C, Gelmann EP. NKX3.1 activates cellular response to DNA damage.

Cancer Res. 2010. 70:3089-97.

82. Gurel B *et al*. NKX3.1 as a marker of prostatic origin in metastatic tumors. *Am J Surg Pathol*. 2010. 34:1097-105.
83. Wang J, Cai Y, Ren C, Ittmann M. Expression of variant TMPRSS2/ERG fusion messenger RNAs is associated with aggressive prostate cancer. *Cancer Res*. 2006. 66:8347-51.
84. Mosquera JM *et al*. Morphological features of TMPRSS2-ERG gene fusion prostate cancer. *J Pathol*. 2007. 212:91-101.
85. Saric T *et al*. Genetic pattern of prostate cancer progression. *Int J Cancer*. 1999. 81:219-24.
86. Heinlein CA, Chang C. Androgen receptor in prostate cancer. *Endocr Rev*. 2004. 25:276-308.
87. Feldman BJ, Feldman D. The development of androgen-independent prostate cancer. *Nat Rev Cancer*. 2001. 1:34-45.
88. Yap TA *et al*. Drug discovery in advanced prostate cancer: translating biology into therapy. *Nat Rev Drug Discov*. 2016. 15:699-718.
89. Zong Y, Goldstein AS. Adaptation or selection—mechanisms of castration-resistant prostate cancer. *Nat Rev Urol*. 2013. 10:90-8.
90. Saraon P, Drabovich AP, Jarvi KA, Diamandis EP. Mechanisms of androgen-independent prostate cancer. *EJIFCC*. 2014. 25:42-54.
91. Yuan X *et al*. Androgen receptor functions in castration-resistant prostate cancer and mechanisms of resistance to new agents targeting the androgen axis. *Oncogene*. 2014. 33:2815-25.
92. Kahn B, Collazo J, Kyprianou N. Androgen receptor as a driver of therapeutic resistance in advanced prostate cancer. *Int J Biol Sci*. 2014. 10:588-95.
93. Devlin HL, Mudryj M. Progression of prostate cancer: multiple pathways to androgen independence. *Cancer Lett*. 2009. 274:177-86.
94. Pienta KJ, Bradley D. Mechanisms underlying the development of androgen-independent prostate cancer. *Clin Cancer Res*. 2006. 12:1665-71.
95. Schröder FH. Progress in understanding androgen-independent prostate cancer (AIPC): a review of potential endocrine-mediated mechanisms. *Eur Urol*. 2008. 53:1129-37.
96. Blatt EB, Raj GV. Molecular mechanisms of enzalutamide resistance in

prostate cancer. *Cancer Drug Resist*. 2019. 2:189-197.

97. Bluemn EG *et al*. Androgen receptor pathway-independent prostate cancer is sustained through FGF signaling. *Cancer Cell*. 2017. 32:474-489.
98. Vlachostergios PJ, Puca L, Beltran H. Emerging variants of castration-resistant prostate cancer. *Curr Oncol Rep*. 2017. 19:32.
99. Huang Y, Jiang X, Liang X, Jiang G. Molecular and cellular mechanisms of castration resistant prostate cancer. *Oncol Lett*. 2018. 15:6063-6076.
100. Aggarwal R, Zhang T, Small EJ, Armstrong AJ. Neuroendocrine prostate cancer: subtypes, biology, and clinical outcomes. *J Natl Compr Netw*. 2014. 12:719-26.
101. Nadal R, Schweizer M, Kryvenko ON, Epstein JI, Eisenberger MA. Small cell carcinoma of the prostate. *Nat Rev Urol*. 2014. 11:213-9.
102. Shevrin DH. Genomic predictors for treatment of late stage prostate cancer. *Asian J Androl*. 2016. 18:586-91.
103. Beltran H *et al*. Molecular characterization of neuroendocrine prostate cancer and identification of new drug targets. *Cancer Discov*. 2011. 1:487-95.
104. Aparicio A *et al*. Molecular characterization of clinically defined aggressive variant prostate cancer in prospectively collected tissues and corresponding patient derived xenografts. *J Clin Oncol*. 2015. 33:5055-5055.
105. Lee JK *et al*. N-Myc drives neuroendocrine prostate cancer initiated from human prostate epithelial cells. *Cancer Cell*. 2016. 29:536-547.
106. Tzelepi V *et al*. Modeling a lethal prostate cancer variant with small-cell carcinoma features. *Clin Cancer Res*. 2012. 18:666-77.
107. Beltran H *et al*. Divergent clonal evolution of castration-resistant neuroendocrine prostate cancer. *Nat Med*. 2016. 22:298-305.
108. Miller KD *et al*. Cancer treatment and survivorship statistics, 2019. *CA Cancer J Clin*. 2019. 10.3322/caac.21565.
109. Hayes JH *et al*. Active surveillance compared with initial treatment for men with low-risk prostate cancer: a decision analysis. *JAMA*. 2010. 304:2373-80.
110. Bill-Axelson A *et al*. Radical prostatectomy versus watchful waiting in early prostate cancer. *N Engl J Med*. 2011. 364:1708-17.
111. Freedland SJ *et al*. Risk of prostate cancer-specific mortality following biochemical recurrence after radical prostatectomy. *JAMA*. 2005. 294:433-9.

112. Wildmark A *et al*. Endocrine treatment, with or without radiotherapy, in locally advanced prostate cancer (SPCG-7/SFUO-3): an open randomized phase III trial. *Lancet*. 2009. 373:301-8.
113. Lin CC, Gray PJ, Jemal A, Efstathiou JA. Androgen deprivation with or without radiation therapy for clinically node-positive prostate cancer. *J Natl Cancer Inst*. 2015. 107.pii:djv119.
114. Zaorsky NG *et al*. Evolution of advanced technologies in prostate cancer radiotherapy. *Nat Rev Urol*. 2013. 10:565-79.
115. Miller DC *et al*. Long-term outcomes among localized prostate cancer survivors: health-related quality-of-life changes after radical prostatectomy, external radiation, and brachytherapy. *J Clin Oncol*. 2005. 23:2772-80.
116. Carreira *et al*. Tumor clone dynamics in lethal prostate cancer. *Sci Transl Med*. 2014. 6:254ra125.
117. Huggins C, Hodges CV. Studies on prostatic cancer. I. The effect of castration, of estrogen and of androgen injection on serum phosphatases in metastatic carcinoma of the prostate. *Cancer Res*. 1941. 1:293-97.
118. Pagliarulo V *et al*. Contemporary role of androgen deprivation therapy for prostate cancer. *Eur Urol*. 2012. 61:11-25.
119. Fakhrejahani F, Madan RA, Dahut WL. Management options for biochemically recurrent prostate cancer. *Curr Treat Options Oncol*. 2017. 18:26.
120. Tolkach Y, Joniau S, Van Poppel H. Luteinizing hormone-releasing hormone (LHRH) receptor agonists vs antagonists: a matter of the receptors?. *BJU Int*. 2013. 111:1021-30.
121. Chen Y, Clegg NJ, Sher HI. Anti-androgens and androgen-depleting therapies in prostate cancer: new agents for an established target. *Lancet Oncol*. 2009. 10:981-91.
122. Sharifi N, Gulley JL, Dahut WL. Androgen deprivation therapy for prostate cancer. *JAMA*. 2005. 294:238-44.
123. Fizazi K *et al*. Abiraterone acetate for treatment of metastatic castration-resistant prostate cancer: final overall survival analysis of the COU-AA-301 randomised, double-blind, placebo-controlled phase 3 study. *Lancet Oncol*. 2012. 13:983-92.
124. Sher HI *et al*. Antitumour activity of MDV3100 in castration-resistant prostate

cancer: a phase 1-2 study. *Lancet*. 2010. 375:1437-46.

125. Attard G *et al*. Selective inhibition of CYP17 with abiraterone acetate is highly active in the treatment of castration-resistant prostate cancer. *J Clin Oncol*. 2009. 27:3742-8.
126. De Bono *et al*. Abiraterone and increased survival in metastatic prostate cancer. *N Engl J Med*. 2011. 364:1995-2005.
127. Sher HI *et al*. Increased survival with enzalutamide in prostate cancer after chemotherapy. *N Engl J Med*. 2012. 367:1187-97.
128. Beer TM *et al*. Enzalutamide in metastatic prostate cancer before chemotherapy. *N Engl J Med*. 2014. 371:424-33.
129. Nevedomskaya E, Baumgart SJ, Haendler B. Recent advances in prostate cancer treatment and drug discovery. *Int J Mol Sci*. 2018. 19.pii:E1359.
130. Fizazi K *et al*. Darolutamide in nonmetastatic castration-resistant prostate cancer. *N Engl J Med*. 2019. 380:1235-1246.
131. Bastos DA, Antonarakis ES. Darolutamide for castration-resistant prostate cancer. *Onco Targets Ther*. 2019. 12:8769-8777.
132. Dagher R *et al*. Approval summary: Docetaxel in combination with prednisone for the treatment of androgen-independent hormone-refractory prostate cancer. *Clin Cancer Re*s. 2004. 10:8147-51.
133. Tannock IF *et al*. Docetaxel plus prednisone or mitoxantrone plus prednisone for advanced prostate cancer. *N Engl J Med*. 2004. 351:1502-12.
134. Paller CJ, Antonarakis ES. Cabazitaxel: a novel second-line treatment for metastatic castration-resistant prostate cancer. *Drug Des Devel Ther*. 2011. 5:117-24.
135. De Leeuw R *et al*. Novel actions of next-generation taxanes benefit advanced stages of prostate cancer. *Clin Cancer Res*. 2015. 21:795-807.
136. Seruga B, Tannock IF. Chemotherapy-based treatment for castration-resistant prostate cancer. *J Clin Oncol*. 2011. 29:3686-94.
137. Sridhar SS *et al*. Castration-resistant prostate cancer: from new pathophysiology to new treatment. *Eur Urol*. 2014. 65:289-99.
138. Tse BW *et al*. From bench to bedside: immunotherapy for prostate cancer. *Biomed Res Int*. 2014. 2014:981434.
139. Sheikh NA *et al*. Sipuleucel-T immune parameters correlate with survival: an

analysis of the randomized phase 3 clinical trials in men with castration-resistant prostate cancer. *Cancer Immunol Immunother*. 2013. 62:137-47.

140. Kantoff PW *et al*. Sipuleucel-T immunotherapy for castration-resistant prostate cancer. *N Engl J Med*. 2010. 363:411-22.
141. Borghaei H *et al*. Nivolumab versus docetaxel in advanced nonsquamous non-small-cell lung cancer. *N Engl J Med*. 2015. 373:1627-39.
142. Slovin SF *et al*. Ipilimumab alone or in combination with radiotherapy in metastatic castration-resistant prostate cancer: results from an open-label, multicenter phase I/II study. *Ann Oncol*. 2013. 24:1813-21.
143. Kwon ED *et al*. Ipilimumab versus placebo after radiotherapy in patients with metastatic castration-resistant prostate cancer that had progressed after docetaxel chemotherapy (CA184-043): a multicentre, randomized, double-blind, phase 3 trial. *Lancet Oncol*. 2014. 15:700-12.
144. Kantoff PW *et al*. Overall survival analysis of a phase II randomized controlled trial of a Poxviral-based PSA-targeted immunotherapy in metastatic castration-resistant prostate cancer. *J Clin Oncol*. 2010. 28:1099-105.
145. Morgan TM, Koreckij TD, Corey E. Targeted therapy for advanced prostate cancer: inhibition of the PI3K/Akt/mTOR pathway. *Curr Cancer Drug Targets*. 2009. 9:237-49.
146. Kinkade CW *et al*. Targeting AKT/mTOR and ERK MAPK signaling inhibits hormone-refractory prostate cancer in a preclinical mouse model. *J Clin Invest*. 2008. 118:3051-64.
147. Sonnenburg DW, Morgans AK. Emerging therapies in metastatic prostate cancer. *Curr Oncol Rep*. 2018. 20:46.
148. Mateo J *et al*. DNA-repair defects and olaparib in metastatic prostate cancer. *N Engl J Med*. 2015. 373:1697-708.
149. Bono JSD *et al*. PROfound: a randomized phase III trial evaluating olaparib in patients with metastatic castration-resistant prostate cancer and a deleterious homologous recombination DNA repair aberration. J Clin Oncol. 2017. 35:TPS5091-TPS5091.
150. Ryan CJ *et al*. TRITON3: An international, randomized, open-label, phase III study of the PARP inhibitor rucaparib vs. physician's choice of therapy for patients with metastatic castration-resistant prostate cancer (mCRPC)

associated with homologous recombination deficiency (HRD). J Clin Oncol. 2018. 36:TPS389-TPS389.

151. Collins I, Garrett MD. Targeting the cell division cycle in cancer: CDK and cell cycle checkpoint kinase inhibitors. *Curr Opin Pharmacol*. 2005. 5:366-73.
152. Wesierska-Gadek J, Maurer M, Zulehner N, Komina O. Whether to target single or multiple CDKs for therapy? That is the question. *J Cell Physiol*. 2011. 226:341-9.
153. Comstock CE *et al*. Targeting cell cycle and hormone receptor pathways in cancer. *Oncogene*. 2013. 32:5481-91.
154. Stice JP *et al*. CDK4/4 therapeutic intervention and viable alternative to taxanes in CRPC. *Mol Cancer Res*. 2017. 15:660-669.
155. Finn RS *et al*. The cyclin-dependent kinase 4/6 inhibitor palbociclib in combination with letrozole versus letrozole alone as first-line treatment of oestrogen receptor-positive, HER2-negative, advanced breast cancer (PALOMA-1/TRIO-18): a randomised phase 2 study. *Lancet Oncol*. 2015. 16:25-35.
156. Palmbos PL *et al*. Cotargeting AR signaling and cell cycle: A randomized phase II study of androgen deprivation therapy with or without palbociclib in RB-positive metastatic hormone sensitive prostate cancer (mHSPC). *J Clin Oncol*. 2018. 36:251-251.
157. Batra A, Winquist E. Emerging cell cycle inhibitors for treating metastatic castration-resistant prostate cancer. *Expert Opin Emerg Drugs*. 2018. 23:271-282.
158. Kelly WK *et al*. c15-153: Randomized phase IB/II study of enzalutamide with and without ribociclib in patients with metastatic castrate resistant, chemotherapy naïve prostate cancer that retains RB expression. *J Clin Oncol*. 2018. 36:TPS384-TPD384.
159. Lewis C *et al*. c15-149: A phase 1b study of the oral CDK4/6 inhibitor ribociclib in combination with docetaxel plus prednisone in metastatic castration resistant prostate cancer (mCRPC)-A prostate cancer clinical trials consortium study. *J Clin Oncol*. 2018. 36:e17028-e17028.
160. Perez de Castro I, de Carcer G, Malumbres M. A census of mitotic cancer genes: new insights into tumor cell biology and cancer therapy.

Carcinogenesis. 2007. 28:899-912.

161. Wang Q *et al*. Androgen receptor regulates a distinct transcription program in androgen-independent prostate cancer. *Cell*. 2009. 138:245-56.
162. Sircar K *et al*. Mitosis phase enrichment with identification of mitotic centromere-associated kinesin as a therapeutic target in castration-resistant prostate cancer. *PLoS One*. 2012. 7:e31259.
163. Horning AM *et al*. Single-cell RNA-seq reveals a subpopulation of prostate cancer cells with enhanced cell-cycle-related transcription and attenuated androgen response. *Cancer Res*. 2018. 78:853-864.
164. Nigg EA. Mitotic kinases as regulators of cell division and its checkpoints. *Nat Rev Mol Cell Biol*. 2001. 2:21-32.
165. Malumbres M, Barbacid M. Mammalian cyclin-dependent kinases. *Trends Biochem Sci*. 2005. 30:630-41.
166. García-Reyes B *et al*. The emerging role of cyclin-dependent kinases (CDKs) in pancreatic ductal adenocarcinoma. *Int J Mol Sci*. 2018. 19.pii:E3219.
167. Dominguez-Brauer C *et al*. Targeting mitosis in cancer: emerging strategies. *Mol Cell*. 2015. 60:524-36.
168. Kim HS, Fernandes G, Lee CW. Protein phosphatases involved in regulating mitosis: facts and hypothesis. *Mol Cells*. 2016. 39:654-62.
169. McGranahan N, Burrell RA, Endesfelder D, Novelli MR, Swanton C. Cancer chromosomal instability: therapeutic and diagnostic challenges. EMBO Rep. 2012. 13:528-38.
170. Vargas-Rondón N, Villegas VE, Rondón-Lagos M. The role of chromosomal instability in cancer and therapeutic responses. *Cancers (Basel)*. 2017. 10.pii:E4.
171. Janssen A, Medema RH. Mitosis as an anti-cancer target. *Oncogene*. 2011. 30:2799-809.
172. Sudakin V, Yen TJ. Targeting mitosis for anti-cancer therapy. *BioDrugs*. 2007. 21:225-33.
173. Wissing MD, van Diest PJ, van der Wall E, Gelderblom H. Antimitotic agents for the treatment of patients with metastatic castrate-resistant prostate cancer. *Expert Opin Investig Drugs*. 2013. 22:635-61.
174. Penna LS, Henriques JAP, Bonatto D. Anti-mitotic agents: Are they emerging

molecules for cancer treatment?. *Pharmacol Ther*. 2017. 173:67-82.

175. Dumontet C, Jordan MA. Microtubule-binding agents: a dynamic field of cancer therapeutics. *Nat Rev Drug Discov*. 2010. 9:790-803.
176. Jordan MA, Wilson L. Microtubules as a target for anticancer drugs. *Nat Rev Cancer*. 2004. 4:253-65.
177. Marzo I, Naval J. Antimitotic drugs in cancer chemotherapy: promises and pitfalls. *Biochem Pharmacol*. 2013. 86:703-10.
178. Salmela AL, Kallio MJ. Mitosis as an anti-cancer drug target. *Chromosoma*. 2013. 122:431-49.
179. Rath O, Kozielski F. Kinesins and cancer. *Nat Rev Cancer*. 2012. 12:527-39.
180. Voultsiadou A, Sarli V. Recent advances of kinesin motor inhibitors and their clinical progress. *Rev Recent Clin Trials*. 2011. 6:271-7.
181. Blagden SP *et al*. A phase I trial of ispinesib, a kinesin spindle protein inhibitor, with docetaxel in patients with advanced solid tumors. *Br J Cancer*. 2008. 98:894-9.
182. Beer TM *et al*. Southwest oncology group phase II study of ispinesib in androgen-independent prostate cancer previously treated with taxanes. *Clin Genitourin Cancer*. 2008. 6:103-9.
183. Holen K *et al*. A phase I trial of MK-0731, a kinesin spindle protein (KSP) inhibitor, in patients with solid tumors. *Invest New Drugs*. 2012. 30:1088-95.
184. Infante JR *et al*. A phase I study to assess the safety, tolerability, and pharmacokinetics of AZD4877, an intravenous Eg5 inhibitor in patients with advanced solid tumors. *Cancer Chemother Pharmacol*. 2012. 69:165-72.
185. Tanenbaum ME *et al*. Kif15 cooperates with Eg5 to promote bipolar spindle assembly. *Curr Biol*. 2009. 19:1703-11.
186. Liu M *et al*. Kinesin-12, a mitotic microtubule-associated motor protein, impacts axonal growth, navigation, and branching. *J Neurosci*. 2010. 30:14896-906.
187. Xing ND *et al*. A potent chemotherapeutic strategy in prostate cancer: S-(methoxytrityl)-L-cysteine, a novel Eg5 inhibitor. *Asian J Androl*. 2011. 13:236-41.
188. Wiltshire C *et al*. Docetaxel-resistant prostate cancer cells remain sensitive to S-trityl-L-cysteine-mediated Eg5 inhibition. *Mol Cancer Ther*. 2010. 9:1730-9.
189. Strebhardt K, Ulrich A. Targeting polo-like kinase 1 for cancer therapy. *Nat*

Rev Cancer. 2006. 6:321-30.

190. Keen N, Taylor S. Aurora-kinase inhibitors as anticancer agents. *Nat Rev Cancer*. 2004. 4:927-36.
191. Ramos-Montoya A *et al*. HES6 drives a critical AR transcriptional programme to induce castration-resistant prostate cancer through activation of an E2F1-mediated cell cycle network. *EMBO Mol Med*. 2014. 6:651-61.
192. Oppermann FS *et al*. Combination of chemical genetics and phosphoproteomics for kinase signaling analysis enables confident identification of cellular downstream targets. Mol Cell Proteomics. 2012. 11:O111.012351.
193. Malumbres M. Physiological relevance of cell cycle kinases. *Physiol Rev*. 2011. 91:973-1007.
194. Kivinummi K *et al*. The expression of AURKA is androgen regulated in castration-resistant prostate cancer. *Sci Rep*. 2017. 7:17978-89.
195. Kollareddy M *et al*. Aurora kinase inhibitors: progress towards the clinic. *Invest New Drugs*. 2012. 30:2411-32.
196. Otto T, Sicinski P. Cell cycle proteins as promising targets in cancer therapy. *Nat Rev Cancer*. 2017. 17:93-115.
197. Dees EC *et al*. Phase I study of aurora A kinase inhibitor MLN8237 in advanced solid tumors: safety, pharmacokinetics, pharmacodynamic, and bioavailability of two oral formulations. *Clin Cancer Res*. 2012. 18:4775-84.
198. Beltran H *et al*. A phase 2 study of the aurora kinase A inhibitor alisertib for patients with neuroendocrine prostate cancer (NEPC). *Ann Oncol*. 2016. 27:1-36.
199. Lin J *et al*. A phase I/II study of the investigational drug alisertib in combination with abiraterone and prednisone for patients with metastatic castration-resistant prostate cancer progressing on abiraterone. *Oncologist*. 2016. 21:1296-97e.
200. Barr FA, Sillje HH, Nigg EA. Polo-like kinases and the orchestration of cell division. *Nat Rev Mol Cell Biol*. 2004. 5:429-40.
201. Petronczki M, Lenart P, Peters JM. Polo on the rise-from mitotic entry to cytokinesis with Plk1. *Dev Cell*. 2008. 14:646-59.
202. Luo J, Liu X. Polo-like kinase 1, on the rise from cell cycle regulation to

prostate cancer development. *Protein Cell*. 2012. 3:182-97.

203. Takai N, Hamanaka R, Yoshimatsu J, Miyakawa I. Polo-like kinases (Plks) and cancer. *Oncogene*. 2005. 24:287-91.
204. Hou X *et al*. Plk1-dependent microtubule dynamics promotes androgen receptor signaling in prostate cancer. *Prostate*. 2013. 73:1352-63.
205. Zhang Z *et al*. Plk1 inhibition enhances the efficacy of androgen signaling blockade in castration-resistant prostate cancer. *Cancer Res*. 2014. 74:6635-47.
206. Thoma C. Prostate cancer: PLK-1 inhibition improves abiraterone efficacy. *Nat Rev Urol*. 2014.11:603.
207. Zhang Z, Chen L, Wang H, Ahmad N, Liu X. Inhibition of Plk1 represses androgen signaling pathway in castration-resistant prostate cancer. *Cell Cycle*. 2015. 14:2142-8.
208. Deeraksa A *et al*. Plk1 is upregulated in androgen-insensitive prostate cancer cells and its inhibition leads to necroptosis. *Oncogene*. 2013. 32:2973-83.
209. Gutteridge RE, Ndiaye MA, Liu X, Ahmad N. Plk1 inhibitors in cancer therapy: From laboratory to clinics. *Mol Cancer Ther*. 2016. 15:1427-35.
210. Rudolph D *et al*. BI 6727, a Polo-like kinase inhibitor with improved pharmacokinetic profile and broad antitumor activity. *Clin Cancer Res*. 2009. 15:3094-102.
211. Lin CC *et al*. A phase I study of two dosing schedules of volasertib (BI 6727), an intravenous polo-like kinase inhibitor, in patients with advanced solid malignancies. *Br J Cancer*. 2014. 110:2434-40.
212. Stadler WM *et al*. An open-label, single-arm, phase 2 trial of the Polo-like kinase inhibitor volasertib (BI 6727) in patients with locally advanced or metastatic urothelial cancer. *Cancer*. 2014. 120:976-82.
213. Döhner H *et al*. Randomized, phase 2 trial of low-dose cytarabine with or without volasertib in AML patients not suitable for induction therapy. *Blood*. 2014. 124:1426-33.
214. Van den Bossche J *et al*. Spotlight on volasertib: preclinical and clinical evaluation of a promising Plk1 inhibitor. *Med Res Rev*. 2016. 36:749-86.
215. Gumireddy K *et al*. ON01910, a non-ATP-competitive small molecule inhibitor of Plk1, is a potent anticancer agent. *Cancer Cell*. 2005. 7:275-86.

216. Bowles DW *et al*. Phase I study of oral rigosertib (ON 01910.Na), a dual inhibitor of the PI3K and Plk1 pathways, in adult patients with advanced solid malignancies. *Clin Cancer Res*. 2014. 20:1656-65.
217. Silverman LR *et al*. Clinical activity and safety of the dual pathway inhibitor rigosertib for higher risk myelodysplastic syndromes following DNA methyltransferase inhibitor therapy. *Hematol Oncol*. 2015. 33:57-66.
218. Shin SB, Woo SU, Yim H. Differential cellular effects of Plk1 inhibitors targeting the ATP-binding domain or polo-box domain. *J Cell Physiol*. 2015. 230:3057-67.
219. Reindl W, Yuan J, Krämer A, Strebhardt K, Berg T. Inhibition of polo-like kinase 1 by blocking polo-box domain-dependent protein-protein interactions. *Chem Biol*. 2008. 15:459-66.
220. Sharow A *et al*. Optimized Plk1 PBD inhibitors based on poloxin induce mitotic arrest and apoptosis in tumor cells. *ACS Chem Biol*. 2015. 10:2570-9.
221. Gascoigne KE, Taylor SS. How do anti-mitotic drugs kill cancer cells? *J Cell Sci*. 2009. 122:2579-85.
222. Gascoigne KE, Taylor SS. Cancer cells display profound intra- and interline variation following prolonged exposure to antimitotic drugs. *Cancer Cell*. 2008. 14:111-22.
223. Topham CH, Taylor SS. Mitosis and apoptosis: how is the balance set? *Curr Opin Cell Biol*. 2013. 25:780-5.
224. Maes *et al*. Proteomics in cancer research: Are we ready for clinical practice? *Crit Rev Oncol Hematol*. 2015. 96:437-48.
225. Boja E *et al*. Evolution of clinical proteomics and its role in medicine. *J Proteome Res*. 2011. 10:66-84.
226. Stelloo *et al*. Endogenous androgen receptor proteomic profiling reveals genomic subcomplex involved in prostate tumorigenesis. *Oncogene*. 2018. 37:313-322.
227. Shruthi BS, Vinodhkumar P, Selvamani. Proteomics: A new perspective for cancer. *Adv Biomed Res*. 2016. 5:67.
228. Srinivas PR, Srivastava S, Hanash S, Wright GL Jr. Proteomics in early detection of cancer. *Clin Chem*. 2001. 47:1901-11.
229. Flores-Morales A, Iglesias-Gato D. Quantitative mass spectrometry-based

proteomic profiling for precision medicine in prostate cancer. *Front Oncol*. 2017. 7:267.

230. Sallam RM. Proteomics in cancer biomarkers discovery: challenges and applications. *Dis Markers*. 2015. 2015:321370.
231. Cho WC. Mass spectrometry-based proteomics in cancer research. Expert Rev *Proteomics*. 2017. 14:725-727.
232. Zhang B *et al*. Proteogenomic characterization of human colon and rectal cancer. *Nature*. 2014. 513:382-7.
233. Mertins P *et al*. Proteogenomics connects somatic mutations to signaling in breast cancer. *Nature*. 2016. 534:55-62.
234. Wang H *et al*. Quantification of mutant SPOP proteins in prostate cancer using mass spectrometry-based targeted proteomics. *J Transl Med*. 2017. 15:175.
235. Stevens EV, Posadas EM, Davidson B, Kohn EC. Proteomics in cancer. *Ann Oncol*. 2004. 15 Suppl 4:iv167-71.
236. Tanase CP *et al*. Prostate cancer proteomics: Current trends and future perspectives for biomarker discovery. *Oncotarget*. 2017. 8:18497-18512.
237. Saraon P *et al*. Proteomic profiling of androgen-independent prostate cancer cell lines reveals a role for protein S during the development of high grade and castration-resistant prostate cancer. *J Biol Chem*. 2012. 287:34019-31.
238. Höti N, Shah P, Hu Y, Yang S, Zhang H. Proteomics analyses of prostate cancer cells reveals cellular pathways associated with androgen resistance. *Proteomics*. 2017. 17:pmic.201600228.
239. Ong SE *et al*. Stable Isotope Labeling by Amino acids in Cell culture, SILAC, as a simple and accurate approach to expression proteomics. *Mol Cell Proteomics*. 2002. 1:376-86.
240. Cifani P, Kentsis A. Towards comprehensive and quantitative proteomics for diagnosis and therapy of human disease. *Proteomics*. 2017. 17:pmic.201600079.
241. Chen X, Wei S, Ji Y, Guo X, Yang F. Quantitative proteomics using SILAC: Principles, applications and developments. Proteomics. 2015. 15:3175-92.
242. Ong SE. The expanding field of SILAC. *Anal Bioanal Chem*. 2012. 404:967-76.
243. Mann M. Functional and quantitative proteomics using SILAC. *Nat Rev Mol Cell Biol*. 2006. 7:952-8.

244. Doherty MK, Hammond DE, Clague MJ, Gaskell MJ, Beynon RJ. Turnover of the human proteome: determination of protein intracellular stability by dynamic SILAC. *J Proteome Res*. 2009. 8:104-12.
245. Saraon P *et al*. Quantitative proteomics reveals that enzymes of the ketogenic pathway are associated with prostate cancer progression. *Mol Cell Proteomics*. 2013. 12:1589-1601.
246. Iglesias-Gato D *et al*. The proteome of primary prostate cancer. *Eur Urol*. 2016. 69:942-52.
247. Geiger *et al*. Use of stable isotope labeling by amino acids in cell culture as a spike-in standard in quantitative proteomics. Nat Protoc. 2011. 6:147-57.
248. Geiger T, Cox J, Ostasiewicz P, Wisniewski JR, Mann M. Super-SILAC mix for quantitative proteomics of human tumor tissue. Nat Methods. 2010. 7:383-5.
249. Mann M, Jensen ON. Proteomic analysis of post-translational modifications. *Nat Biotechnol*. 2003. 21:255-61.
250. Macek B, Mann M, Olsen JV. Global and site-specific quantitative phosphoproteomics: principles and applications. *Annu Rev Pharmacol Toxicol*. 2009. 49:199-221.
251. Sharma K *et al*. Ultradeep human phosphoproteome reveals a distinct regulatory nature of Tyr and Ser/Thr-based signaling. *Cell Rep*. 2014. 8:1583-94.
252. Wirbel J, Cutillas P, Saez-Rodriguez J. Phosphoproteomics-based profiling of kinase activities in cancer cells. *Methods Mol Biol*. 2018. 1711:103-132.
253. Rodrigues DN *et al*. The molecular underpinning of prostate cancer: impacts on management and pathology practice. *J Pathol*. 2017. 241:173-182.
254. Knight ZA, Lin H, Shokat KM. Targeting the cancer kinome through polypharmacology. *Nat Rev Cancer*. 2010. 10:130-7.
255. Ferguson FM, Gray NS. Kinase inhibitors: the road ahead. *Nat Rev Drug Discov*. 2018. 17:353-377.
256. Olsen JV *et al*. Global, in vivo, and site-specific phosphorylation dynamics in signaling networks. *Cell*. 2006. 127:635-48.
257. Lemeer S, Heck AJ. The phosphoproteomics data explosion. *Curr Opin Chem Biol*. 2009. 13:414-20.
258. Nilsson CL. Advances in quantitative phosphoproteomics. *Anal Chem*. 2012.

84:735-46.

259. Giudice G, Petsalaki E. Proteomics and phosphoproteomics in precision medicine: applications and challenges. *Brief Bioinform*. 2019. 20:767-777.
260. Yang W, Freeman MR, Kyprianou N. Personalization of prostate cancer therapy through phosphoproteomics. *Nat Rev Urol*. 2018. 15:483-497.
261. Cheng LC, Tan VM, Ganesan S, Drake JM. Integrating phosphoproteomics into the clinical management of prostate cancer. *Clin Transl Med*. 2017. 6:9.
262. Drake JM *et al*. Phosphoproteome integration reveals patient-specific networks in prostate cancer. *Cell*. 2016. 166:1041-1054.
263. Drake JM *et al*. Oncogene-specific activation of tyrosine kinase networks during prostate cancer progression. *Proc Natl Acad Sci USA*. 2012. 109:1643-8.
264. Drake JM *et al*. Metastatic castration-resistant prostate cancer reveals intrapatient similarity and interpatient heterogeneity of therapeutic kinase targets. *Proc Natl Acad Sci USA*. 2013. 110:E4762-9.
265. Jiang N *et al*. In vivo quantitative phosphoproteomic profiling identifies novel regulators of castration-resistant prostate cancer growth. *Oncogene*. 2015. 34:2764-76.
266. Wang HQ *et al*. Differential phosphoprotein levels and pathway analysis identify the transition mechanism of LNCaP cells into androgen-independent cells. *Prostate*. 2010. 70:508-17.
267. Ino Y *et al*. Phosphoproteome analysis demonstrates the potential role of THRAP3 phosphorylation in androgen-independent prostate cancer cell growth. *Proteomics*. 2016. 16:1069-78.
268. Grasso CS *et al*. The mutational landscape of lethal castration-resistant prostate cancer. Nature. 2012. 487:239-43.
269. Robinson D *et al*. Integrative clinical genomics of advanced prostate cancer. Cell. 2015. 161:1215-1228.
270. Weinstein JN *et al*. The Cancer Genoma Atlas Pan-Cancer analysis project. *Nat Genet.* 2015. 45:1113-20.
271. Ong SE, Mann M. A practical recipe for stable isotope labeling by amino acids in cell culture (SILAC). *Nat Protoc*. 2006. 1:2650-60.
272. Lanucara F, Eyers CE. Mass spectrometric-based quantitative proteomics

using SILAC. *Methods Enzymol*. 2011. 500:133-50.

273. Cox J, Mann M. MaxQuant enables high peptides identification rates, individualized p.p.b.-range mass accuracies and proteome-wide protein quantification. *Nat Biotechnol*. 2008. 26:1367-72.
274. Cox J *et al*. A practical guide to the MaxQuant computational platform for SILAC-based quantitative proteomics. *Nat Protoc*. 2009. 4:698-705.
275. Huang da W, Sherman BT, Lempicki RA. Systematic and integrative analysis of large gene lists using DAVID bioinformatics resources, *Nat Protoc*. 2009. 4:44-57.
276. Vizcaino JA *et al*. 2016 update of the PRIDE database and its related tools. *Nucleic Acids Res*. 2016. 44:D447-56.
277. Aytes A *et al*. ETV4 promotes metastasis in response to activation of PI3-kinase and Ras signaling in a mouse model of advanced prostate cancer. *Proc Natl Acad Sci U S A*. 2013. 110:E3506-15.
278. Gao M, Ossowski L, Ferrari AC. Activation of Rb and decline in androgen receptor protein precede retinoic acid-induced apoptosis in androgen-dependent LNCaP cells and their androgen-independent derivative. *J Cell Physiol*. 1999. 179:336-46.
279. Martin P *et al*. Prostate epithelial Pten/TP53 loss leads to transformation of multipotential progenitors and epithelial to mesenchymal transition. *Am J Pathol*. 2011. 179:422-35.
280. Wang LG, Ossowski L, Ferrari AC. Androgen receptor level controlled by a suppressor complex lost in an androgen-independent prostate cancer cell line. *Oncogene*. 2004. 23:5175-84.
281. Wang LG, Ossowski L, Ferrari AC. Overexpressed androgen receptor linked to p21WAF1 silencing may be responsible for androgen independence and resistance to apoptosis of a prostate cancer cell line. *Cancer Res*. 2001. 61:7544-51.
282. Finn RS *et al*. PD 0332991, a selective cyclin D kinase 4/6 inhibitor, preferentially inhibits proliferation of luminal estrogen receptor-positive human breast cancer. *Breast Cancer Res*. 2009. 11:R77.
283. Patnaik A *et al*. Efficacy and safety of abemaciclib, an inhibitor of CDK4 and CDK6, for patients with breast cancer, non-small cell lung cancer, and other

solid tumors. *Cancer Discov*. 2016. 6:740-53.

284. Walker AJ *et al*. FDA approval of palbociclib in combination with fulvestrant for the treatment of hormone receptor-positive, HER2-negative metastatic breast cancer. *Clin Cancer Res*. 2016. 22:4968-4972.
285. Gelbert LM *et al*. Preclinical characterization of the CDK4/6 inhibitor LY2735219: in-vivo cell cycle-dependent/independent anti-tumor activities alone/in combination with gemcitabine. *Invest New Drugs*. 2014. 32:825-37.
286. Blangy A *et al*. Phosphorylation by p34cdc2 regulates spindle association of human Eg5, a kinesin-related motor essential for bipolar spindle formation in vivo. *Cell*. 1995. 83:1159-69.
287. Santamaria A *et al*. The Plk1-dependent phosphoproteome of the early mitotic spindle. *Mol Cell Proteomics*. 2011. 10:M110.004457.
288. Chen S, Xu Y, Yuan X, Bubley GJ, Balk SP. Androgen receptor phosphorylation and stabilization in prostate cancer by cyclin-dependent kinase 1. *Proc Natl Acad Sci U S A*. 2006. 103:15969-74.
289. Mortezavi A, *et al*. KPNA2 expression is an independent adverse predictor of biochemical recurrence after radical prostatectomy. *Clin Cancer Res*. 2001. 17:1111-21.
290. Søgaard CK, *et al*. APIM-peptide targeting PCNA improves the efficacy of docetaxel treatment in the TRAMP mouse model of prostate cancer. *Oncotarget*. 2018. 9:11752-11766.
291. Basu A, *et al*. Differential expression of peroxiredoxins in prostate cancer: consistent upregulation of PRDX3 and PRDX4. *Prostate*. 2011. 71:755-65.
292. Eales KL, Hollinshead KE, Tennant DA. Hypoxia and metabolic adaptation of cancer cells. *Oncogenesis*. 2016. 5:e190.
293. Hegedüs C *et al*. Redox control of cancer cell destruction. *Redox Biol*. 2018. 16:59-74.
294. Khandrika L, Kumar B, Koul S, Maroni P, Koul HK. Oxidative stress in prostate cancer. *Cancer Lett*. 2009. 282:125-136.
295. Kumar B, Koul S, Khandrika L, Meacham RB, Koul HK. Oxidative stress in inherent in prostate cancer cells and is required for aggressive phenotype. *Cancer Res*. 2008. 68:1777-1785.
296. Gupta-Elera G, Garrett AR, Robinson RA, O'Neill KL. The role of oxidative

stress in prostate cancer. *Eur J Cancer Prev*. 2012. 21:155-62.

297. Paschos A, Pandya R, Duivenvoorden WCM, Pinthus JH. Oxidative stress in prostate cancer: changing research concepts towards a novel paradigm for prevention and therapeutics. *Prostate Cancer Prostatic Dis*. 2013. 16:217-25.
298. Shiota M, Yokomizo A, Naito S. Oxidative stress and androgen receptor signaling in the development and progression of castration-resistant prostate cancer. *Free Radic Biol Med*. 2011. 51:1320-8.
299. Giunchi F, Fiorentino M, Loda M. The metabolic landscape of prostate cancer. *Eur Urol Oncol*. 2019. 1:28-36.
300. Tamura K *et al*. Molecular features of hormone-refractory prostate cancer cells y genome-wide gene expression. *Cancer Res*. 2007. 67:5117-25.
301. Chen S, Xu Y, Yuan X, Bubley GJ, Balk SP. Androgen receptor phosphorylation and stabilization in prostate cancer by cyclin-dependent kinase 1. *Proc Natl Acad Sci U S A*. 2006. 103:15969-74.
302. Sircar K *et al*. Integrative molecular profiling reveals asparagine synthetase is a target in castration-resistant prostate cancer. Am J Pathol. 2012. 180:895-903.
303. Shih MC *et al*. TOPK/PBK promotes cell migration via modulation of the PI3K/PTEN/AKT pathway and is associated with poor prognosis in lung cancer. *Oncogene*. 2012. 31:2389-400.
304. Warren AY *et al*. A reciprocal feedback between the PDZ binding kinase and androgen receptor drives prostate cancer. *Oncogene*. 2019. 38:1136-1150.
305. Joel M *et al*. Targeting PBK/TOPK decreases growth and survival of glioma initiating cells in vitro and attenuates tumor growth in vivo. *Mol Cancer*. 2015. 14:121.
306. Abe Y *et al*. A mitotic kinase TOPK enhances Cdk1/cyclin B1-dependent phosphorylation of PRC1 and promotes cytokinesis. *J Mol Biol*. 2007. 370:231-45.
307. Park JH, Nishidate T, Nakamura Y, Katagiri T. Critical roles of T-LAK cell-originated protein kinase in cytokinesis. *Cancer Sci*. 2010. 101:403-11.
308. Brown-Clay JD *et al*. PBK/TOPK enhances aggressive phenotype in prostate cancer via β-catenin-TCF/LEF-mediated matrix metalloproteinases production and invasion. *Oncotarget*. 2015. 6:15594-609.

309. Kim DJ *et al*. Novel TOPK inhibitor HI-TOPK-032 effectively suppresses colon cancer growth. *Cancer Res*, 2012. 72:3060-8.
310. Matsuo *et al*. TOPK inhibitor induces complete tumor regression in xenograft models of human cancer through inhibition of cytokinesis. *Sci Transl Med*. 2014. 6:259ra145.
311. Ishikawa C, Senba M, Mori N. Mitotic kinase PBK/TOPK as a therapeutic target for adult T-cell leukemia/lymphoma. Int J Oncol. 2018. 53:801-814.
312. Wang MY *et al*. PDZ binding kinase (PBK) is a theranostic target for nasopharyngeal carcinoma: driving tumor growth via ROS signaling and correlating with patient survival. *Oncotarget*. 2016. 7:26604-16.
313. Sun H *et al*. TOPK is highly expressed in circulating tumor cells, enabling metastasis of prostate cancer. *Oncotarget*. 2015. 6:12392-404.
314. Shiraishi T *et al*. Cancer/Testis antigens as potential predictors of biochemical recurrence of prostate cancer following radical prostatectomy. *J Transl Med*. 2011. 9:153.
315. Chen JH *et al*. Overexpression of PDZ-binding kinase confers malignant phenotype in prostate cancer via the regulation of E2F1. *Int J Biol Macromol*. 2015. 81:615-23.
316. Pirovano G *et al*. TOPK modulates tumour-specific radiosensitivity and correlates with recurrence after prostate radiotherapy. Br J Cancer. 2017. 117:503-512.
317. Li S, Hou J, Xu W. Screening and identification of key biomarkers in prostate cancer using bioinformatics. *Mol Med Rep*. 2020. 21:311-319.
318. Rizkallah R, Batsomboom P, Dudley GB, Hurt MM. Identification of the oncogenic kinase TOPK/PBK as a master mitotic regulator of C2H2 zinc finger proteins. *Oncotarget*. 2015. 6:1446-61.
319. Alachkar H *et al*. T-LAK cell-originated protein kinase represents a novel therapeutic target in FLT3-ITD mutated acute myeloid leukemia. *Oncotarget*. 2015. 6:33410-25.
320. Zou J, Kuang W, Hu J, Rao H. miR-216b promotes cell growth and enhances chemosensitivity of colorectal cancer by suppressing PDZ-binding kinase. *Biochem Biophys Res Commun*. 2017. 488:247-252.
321. Gao T *et al*. Novel selective TOPK inhibitor SKLB-CO5 inhibits colorectal

carcinoma growth and metastasis. *Cancer Lett*. 2019. 445:11-23.

322. Pirovano G, Roberts S, Reiner T. TOPKi-NBD: a fluorescent small molecule for tumor imaging. *Eur J Nucl Med Mol Imaging*. 2020. 47:1003-1010.
323. Jiang Y *et al*. TOPK promotes metastasis of esophageal squamous cell carcinoma by activating the Src/GSK3B/STAT3 signaling via y-catenin. *BMC Cancer*. 2019. 19:1264.
324. Pirovano G *et al*. [18F]FE-OTS964: A small molecule targeting TOPK for in vivo PET imaging in a glioblastoma xenograft model. *Mol Imaging Biol*. 2019. 21-705-712.
325. Mao P *et al*. PDZ-binding-kinase-dependent transcriptional regulation of CCNB2 promotes tumorigenesis and radio-resistance in glioblastoma. *Transl Oncol*. 2020. 13:287-294.
326. Yang YF *et al*. PDZ binding kinase, regulated by FOXM1, enhances malignant phenotype via activation of β-catening signaling in hepatocellular carcinoma. *Oncotarget*. 2017. 8:47205.
327. Yang QX *et al*. PBK overexpression promotes metastasis of hepatocellular carcinoma via activating ETV4-uPAR signaling pathway. *Cancer Lett*. 2019. 452:90-102.
328. Stefka AT *et al*. Potent anti-myeloa activity of the TOPK inhibitor OTS514 in pre-clinical models. *Cancer Med*. 2020. 9:324-334.
329. Ikeda *et al*. T-LAK cell-originated protein kinase (TOPK) as a prognostic factor and a potential therapeutic target in ovarian cancer. *Clin Cancer Res*. 2016. 22:6110-6117.
330. Ma H *et al*. PBK, targeted by EVI1, promotes metastasis and confers cisplatin resistance through inducing autophagy in high-grade serous ovarian carcinoma. *Cell Death Dis*. 2019. 10:166.
331. Aytes A *et al*. Cross-species regulatory network analysis identifies a synergistic interaction between FOXM1 and CENPF that drives prostate cancer malignancy. *Cancer Cell*. 2014. 25:638-651.
332. Shahryari V *et al*. Pre-clinical orthotopic murine model of human prostate cancer. *J Vis Exp*. 2016. 114-54125.
333. Borhani S, Gartel AL. FOXM1: a potential therapeutic target in human solid cancers. *Expert Opin Ther Targets*. 2020. 24:205-217.

334. Liu Y *et al*. FOXM1 promotes the progression of prostate cancer by regulating PSA gene transcription. *Oncotarget*. 2017. 8:17027-17037.
335. Kim MY *et al*. High FOXM1 expression is a prognostic marker for poor clinical outcomes in prostate cancer. *J Cancer*. 2019. 10:749-756.
336. Pan H, Zhu Y, Wei W, Shao S, Rui X. Transcription factor FOXM1 is the downstream target of c-Myc and contributes to the development of prostate cancer. *World J Surg Oncol*. 2018. 16:59.
337. Davis JN *et al*. Elevated E2F1 inhibits transcription of the androgen receptor in metastatic hormone-resistant prostate cancer. *Cancer Res*. 2006. 66:11897-906.
338. Cheeseman I, MacLeod I, Yates JR, Oegema K, Desai A. The CENP-F-like proteins HCP-1 and HCP-2 target CLASP to kinetochores to mediate chromosome segregation. *Curr Biol*. 2005. 15:8:771-7.
339. Ma L, Zhao X, Zhu X. Mitosin/CENPF in mitosis, transcriptional control, and differentiation. *J Biomed Sci*. 2006. 13:205-13.
340. Lin SC *et al*. Dysregulation of miRNAs-COUP-TFII-FOXM1-CENPF axis contributes to the metastasis of prostate cancer. *Nat Commun*. 2016. 7:11418.
341. Mateo J *et al*. Olaparib in patients with metastatic castration-resistant prostate cancer with DNA repair gene aberrations (TOPARP-B): a multicenter, open-label, randomised, phase 2 trial. *Lancet Oncol*. 2019. (published online Dec 2).
342. Hussain M *et al*. PROfound: Phase 3 study of olaparib versus enzalutamide or abiraterone for metastatic castration-resistant prostate cancer (mCRPC) with homologous recombination repair (HRR) gene alterations. *Ann Oncol*. 2019. 30:v851-v934.
343. Van Dessel LF *et al*. The genomic landscape of metastatic castration-resistant prostate cancers reveals multiple distinct genotypes with potential clinical impact. *Nat Commun*. 2019. 10:5251.
344. Mitchell S, Abel P, Ware M, Stamp G, Lalani EN. Phenotypic and genotypic characterization of commonly used human prostatic cell lines. *BJU Int*. 2000. 85:932-44.
345. Chlenski A, Nakashiro K, Ketels KV, Korovaitseva GI, Oyasu R. Androgen receptor expression in androgen-independent prostate cancer cell lines. *Prostate*. 2001. 47:66-75.

346. Hewit K *et al*. A functional genomic screen reveals a strong synergistic effect between docetaxel and the mitotic gene DLGAP5 that is mediated by the androgen receptor. *Cell Death Dis*. 2018 9:1069.
347. Fu X *et al*. Overexpression of BUB1 contributes to progression of prostate cancer and predicts poor outcome in patients with prostate cancer. *Onco Targets Ther*. 2016. 9:2211-20.
348. Chieffi P *et al*. Aurora B expression directly correlates with prostate cancer malignancy and influence prostate cell proliferation. *Prostate*. 2006. 66:326-33.
349. Zeng YR *et al*. Overexpression of NIMA-related kinase 2 is associated with progression and poor prognosis of prostate cancer. *BMC Urol*. 2015. 15:90.
350. Liu P, Kao TP, Huang H. CDK1 promotes cell proliferation ad survival via phosphorylation and inhibition of FOXO1 transcription factor. *Oncogene*. 2008. 27:4733-44.
351. Lee EC, Frolov A, Li R, Atala G, Greenberg NM. Targeting Aurora kinases for the treatment of prostate cancer. *Cancer Res*. 2006. 66:4996-5002.
352. Wissing MD *et al*. Nuclear Eg5 (kinesin spindle protein) expression predicts docetaxel response and prostate cancer aggressiveness. *Oncotarget*. 2014. 5:7357-67.
353. Gleixner KV *et al*. Polo-like kinase 1 (Plk1) as a novel drug target in chronic myeloid leukemia: overriding imatinib resistance with the Plk1 inhibitor BI 2536. *Cancer Res*. 2010. 70:1513-23.
354. Shah KN *et al*. Aurora kinase A drives the evolution of resistance to third generation EGFR inhibitors in lung cancer. *Nat Med*. 2019. 25:111-118.
355. De S, Cipriano R, Jackson MW, Stark GR. Overexpression of kinesins mediates docetaxel resistance in breast cancer cells. Cancer Res. 2009. 69:8035-42.
356. Zhou B *et al*. Quantitative proteomic analysis of prostate tissue specimens identifies deregulated protein complexes in primary prostate cancer. *Clin Proteomics*. 2019. 16:15.
357. Sinha A *et al*. The proteogenomic landscape of curable prostate cancer. *Cancer Cell*. 2019. 35:414-427.
358. Gao H, Chen X, Cai Q, Shang Z, Niu Y. Increased KIF4A expression is a potential prognostic factor in prostate cancer. *Oncol Lett*. 2018. 15:7941-7947.

359. Hu F *et al*. c-Myc and E2F1 drive PBK/TOPK expression in high-grade malignant lymphomas. *Leuk Res*. 2013. 37:447-54.
360. Tang C *et al*. Transcriptional regulation of FOXM1 by HIF-1α mediated hypoxia-induced EMT in prostate cancer. *Oncol Rep*. 2019. 42:1307-1318.
361. Kar A *et al*. Targeting PDZ-binding kinase is anti-tumorigenic in novel preclinical models of ACC. *Endocr Relat Cancer*. 2019. 26:765-778.